Aus der III. Medizinischen Klinik und Poliklinik

der Universitätsmedizin der Johannes Gutenberg-Universität Mainz

Investigation of cellular senescence and its regulation by two defined p53 isoforms: Implication for T-cell-based cancer immunotherapy

Untersuchung zellulärer Seneszenz und deren Regulation durch zwei p53 Isoformen im Kontext T-Zell-basierter Krebsimmuntherapie

Inauguraldissertation

zur Erlangung des Doktorgrades der

Medizin

der Universitätsmedizin

der Johannes Gutenberg-Universität Mainz

Vorgelegt von

Kevin Jan Legscha

aus Darmstadt

Mainz, 2022

~~Wissenschaftlicher Vorstand: Name~~

1. Gutachter:	Univ.-Prof. Dr. Matthias Theobald
2. Gutachter:	Univ.-Prof. Dr. Tobias Bopp
3. Gutachterin:	Prof. Dr. Annkristin Heine
Tag der Promotion:	06. Dezember 2022

Affidavit

Hereby, I declare that I wrote my doctoral thesis entitled “Investigation of cellular senescence and its regulation by two defined p53 isoforms: Implication for T-cell-based cancer immunotherapy” independently and with no other sources or aids than quoted. The presented experiments were designed, planned, and analyzed by me under direct supervision from Hakim Echchannaoui and Matthias Theobald (both Principal Investigators). If not otherwise indicated, experiments were performed by me after initial training/help by Edite Antunes (Lab Technician). Animal experiments and transduction of patient-derived T cells were mainly performed by Edite Antunes, supported by me.

Mainz, July 2022

_____

(Signature)

Table of Content

List of Figures

List of Tables

List of Abbreviations

ACT	Adoptive T cell therapy/transfer
AML	Acute myeloid leukemia
APC	Antigen-presenting cell
Aqua dest.	Double distilled water
CAR	Chimeric antigen receptor
CD	Cluster of differentiation
CD155/PVR	Cluster of differentiation 155/Poliovirus Receptor
CFSE	Carboxyfluorescein succinimidyl ester
CRS	Cytokine release syndrome
CTL	Cytotoxic T lymphocytes
CTLA-4	Cytotoxic T-lymphocyte-associated protein-4
CDKI	cyclin-dependent kinase inhibitor
DC	Dendritic cell
DMEM	Dulbecco’s Modified Eagle Medium
DMSO	Dimethyl sulfoxide
ECM	Extracellular matrix
E:T	Effector to target ratio
FCS	Fetal Calf Serum
FL	Full length
GAPDH	Glyceraldehyde 3-phosphate dehydrogenase
GvHD	Graft versus Host Disease
HLA	Human leukocyte antigen
HD	Healthy donor
IL-2	Interleukin-2
IPSC	Induced pluripotent stem cells
LAG-3	Lymphocyte-activation gene 3
LB medium	Lysogeny Broth medium
mAb	Monoclonal antibody
MDSC	Myeloid-derived suppressor cell
gMFI	geometric Mean fluorescence intensity

MHC	Major histocompatibility complex
MM	Multiple myeloma
NK cells	Natural killer cells
OD	Optical density
OKT3	Muromonab (Orthoclone Okt-3®), anti-CD3 antibody
PBMCs	Peripheral blood mononuclear cells
PBS	Phosphate-buffered saline
PCR	Polymerase chain reaction
PDL	Population doubling level
PD-L1	Programmed cell death 1 ligand 1
PD-1	Programmed cell death protein-1
PFA	Paraformaldehyde
rpm	Rounds per minute
RPMI medium	RPMI 1640 Roswell Park Memorial Institute medium
RT	Room temperature
SASP	Senescence associated secretory phenotype
SDS	Sodium dodecyl sulfate
SOB-medium	Super Optimal Broth-medium
TAA	Tumor-associated antigen
TAE buffer	Tris-acetate EDTA buffer
TCR	T cell receptor
Tfb I	Transformation buffer I
Tfb II	Transformation buffer II
TIGIT	T cell immunoreceptor with Ig and ITIM domains
TIL	Tumor infiltrating lymphocyte
TIM-3	T cell immunoglobulin and mucin-domain containing-3
TME	Tumor microenvironment
T_{reg}	Regulatory T cell

T_{EMRA}	Effector memory T cells re-expressing CD45RA

1 Zusammenfassung

Maligne Neoplasien sind auch heutzutage noch eine der weltweit häufigsten Todesursachen mit allein 19,3 Millionen neuen Fällen und 10 Millionen Todesfällen im Jahr 2020 (1). Gerade in fortgeschrittenen Stadien bleibt die Chance auf eine Heilung durch bisher etablierte Therapieverfahren (chirurgische Entfernung, Strahlen- und Chemotherapie) für viele Entitäten gering. Das zunehmende Verständnis der Tumorbiologie und der Interaktion mit dem Immunsystem, führte jedoch in den letzten Jahrzehnten zur Entwicklung neuer, vielversprechender Therapien. Prinzipiell verfügt das menschliche Immunsystem über die Fähigkeit körperfremde sowie entartete Zellen zu erkennen und zu beseitigen. Diese Fähigkeit wird beim adoptiven T-Zelltransfer genutzt. Hierfür werden T-Zellen der Tumorpatienten entnommen und genetisch mit tumorantigenspezifischen T-Zell-Rezeptoren (TZR) oder chimären Antigen-Rezeptoren (CAR) ausgestattet. Hiermit können die modifizierten T-Zellen Tumorzellen spezifisch erkennen und diese gezielt beseitigen. Nach Modifikation und Expansion *in vitro* werden die T-Zellen daher den Patienten wieder infundiert. Diese Art der Therapie erzielte vor allem mit CAR-T-Zellen hervorragende Ansprechraten und teilweise langfristige Remissionen bei hämatologischen Neoplasien (2). Häufig ist die Effektivität und Persistenz der transferierten T-Zellen durch die Interaktion mit dem inhibitorisch wirkenden Tumormikromilieu jedoch stark reduziert (3). Ein entscheidender Faktor für den Erfolg der Therapie scheint daher eine ausreichende T-Zellzahl bzw. deren Proliferation zu sein. So konnte gezeigt werden, dass vor allem naive- , wenig differenzierte T-Zellen mit hoher Proliferationskapazität effektive Immunantworten gegen Tumore induzieren (4). In T-Zellen wurden bisher verschiedene dysfunktionale Stadien beschrieben, welche durch einen Proliferationsarrest gekennzeichnet sind (5). In der hier zusammengefassten Arbeit lag der Fokus auf der Seneszenz von T-Zellen. Seneszenz kann am Ende des normalen Alterungs- bzw. Differenzierungsprozesses der Zellen entstehen, kann jedoch auch durch externe Faktoren wie DNA-Schäden oder oxidativen Stress hervorgerufen werden (6, 7). Dieser Zustand ist durch einen vollständigen Zellzyklusarrest definiert, der die Proliferation der Zellen verhindert. Einer der zentralen Transkriptionsfaktoren der diesen Vorgang kontrolliert ist der Tumorsuppressor p53 (8). Die Tatsache, dass das TP53-Gen mehrere Isoformen kodiert, erhöht die Komplexität bei der Regulation des Zellzyklus. Andererseits könnte dies auch die Möglichkeit bieten, die Zellzykluskontrolle zu beeinflussen. Die

Änderung der Expression einer oder weniger Isoformen könnte hierfür ausreichen, ohne die Expression des wichtigen Tumorsuppressors p53α (p53FL) zu manipulieren. Eine Studie identifizierte bereits zwei p53 Isoformen (p53β und Δ133p53α), die an der Regulation von Seneszenz in $CD8^+$ T-Zellen beteiligt zu sein scheinen (9). Die Expression der längeren, C-terminal modifizierten Isoform p53β förderte das Auftreten von Seneszenz, wohingegen die N-terminal verkürzte Isoform Δ133p53α Seneszenz teilweise rückgängig machen bzw. verzögern konnte (9). Ob eine Modifikation der Expression dieser beiden Isoformen in tumorantigenspezifischen T-Zellen auch zu einer verbesserten anti-Tumorantwort der T-Zellen führt, ist jedoch bisher ungeklärt. In der hier beschriebenen Arbeit wurden daher T-Zellen gesunder Spender mit einem tumorantigenspezifischen TZR ausgestattet und gleichzeitig jeweils eine der beiden p53 Isoformen mittels retroviraler Transduktion überexprimiert. Die erfolgreiche (Über-)Expression des T-Zell-Rezeptors sowie der jeweiligen p53 Isoform wurde zunächst per Durchflusszytometrie bzw. Western Blot bestätigt. Hierbei zeigte sich keine Beeinflussung der TZR-Expression durch die Isoformen. Auch das Verhältnis der CD4- und CD8-positiven Zellen blieb unverändert. Als nächstes wurden die T-Zellen bezüglich ihres zellulären Phänotyps charakterisiert. Hierbei zeigte sich, dass die Überexpression der p53β-Isoform zu einer Verringerung der eher naiven bzw. gering differenzierten $CD8^+CD28^+CD57^-$ T-Zellen führte, wobei die Anzahl der spät-differenzierten $CD8^+CD28^-CD57^+$ T-Zellen leicht erhöht war. Im Einklang mit diesen Ergebnissen zeigte sich zudem, dass die Proliferation der p53β-transduzierten T-Zellpopulation verfrüht (nach wenigen Wochen *in vitro* Kultur) abnahm und schließlich sistierte, während die Kontrollpopulation weiter expandiert werden konnte. Auch die Fähigkeit Tumorzellen zu eliminieren war vermindert. So zeigte sich eine geringere Lyse von Tumorzellen im entsprechenden (*in vitro*) Tumormodell. Diese Ergebnisse deuten auf eine seneszenz-fördernde Funktion von p53β hin.

Als nächstes wurden der zelluläre Phänotyp sowie die Funktion der Δ133p53α-überexprimierenden T-Zellen untersucht. Auch hier zeigte sich eine Veränderung bezüglich der Expression verschiedener Oberflächenmoleküle. Ko-stimulatorische und Adhäsions-Rezeptoren, die eher mit naiven bzw. wenig differenzierten T-Zellen assoziiert sind, wie CD28, CD27 und CD62L, waren nach Transduktion mit Δ133p53α leicht erhöht. Inhibitorische Oberflächenrezeptoren (sogenannte Immuncheckpoints) wie TIGIT und CD160 waren jedoch leicht erniedrigt. Auch der

Anteil spät differenzierter/seneszenter $CD8^+CD28^-CD57^+$ T-Zellen war leicht verringert. Während der mehrwöchigen *in vitro* Kultur zeigte sich zudem eine gesteigerte Proliferationsrate. Die im Vergleich zu Kontrollzellen erhöhte Zellteilungsrate konnte in der Durchflusszytometrie mittels CFSE-Markierung bestätigt werden. *In vitro* zeigten Δ133p53α-überexprimierende T-Zellen ebenfalls eine erhöhte Sekretion verschiedener Zytokine wie IL-2, GM-CSF und IFN-γ nach antigenspezifischer Stimulation. Auch die Degranulation, d.h. die Sekretion von Effektormolekülen wie Granzym-B und Perforin, war entsprechend höher als in Kontrollzellen. Im Einklang mit diesen Ergebnissen, konnte auch eine effizientere Lyse von Tumorzellen *in vitro* beobachtet werden. Ob die *in vitro* beobachteten Effekte der Δ133p53α-Isoform auch die Tumorkontrolle der T-Zellen *in vivo* verbessern kann, wurde schließlich in einem Xenograft-Tumormodell untersucht. Hierfür wurde die bereits *in vitro* verwendete Osteosarkom-Zelllinie als Zieltumor verwendet. Nach Anwachsen des Tumors in den immunsupprimierten Mäusen erfolgte die Infusion der tumorantigenspezifischen T-Zellen. Mäuse, die T-Zellen mit Δ133p53α-Überexpression erhielten, zeigten dabei eine etwas verbesserte Tumorkontrolle und somit eine leichte Verlängerung des durchschnittlichen Überlebens im Vergleich zu den Mäusen der Kontrollgruppe. Wenige dieser Mäuse zeigten hierbei jedoch Nebenwirkungen, welche am ehesten auf eine Überproduktion und Sekretion von (inflammatorischen) Zytokinen zurückzuführen waren.

Als letztes wurden T-Zellen von Patienten mit neudiagnostiziertem Multiplen Myelom isoliert und auf Veränderungen bezüglich des zellulären Phänotyps und der Δ133p53α-Expression untersucht. Hierbei konnte ein - im Vergleich zu gesunden Spendern - vermehrtes Vorkommen von spätdifferenzierten $CD8^+CD28^-CD57^+$ T-Zellen beobachtet werden. T-Zellen gesunder Spender wiesen auch eine meist deutliche Expression von Δ133p53α auf, während die Isoform in T-Zellen der Patienten kaum oder gar nicht nachweisbar war. Auch die spezifische Lyse von Tumorzellen war in von Patienten stammenden T-Zellen vermindert. Dies konnte durch Überexpression von Δ133p53α gesteigert werden.

Die hier beschriebenen Ergebnisse deuten darauf hin, dass die Proliferation und Tumorkontrolle antigenspezifischer T-Zellen durch die Expression von p53 Isoformen beeinflusst werden kann. Die Überexpression der Δ133p53α-Isoform scheint mit dem verzögerten Einsetzen von zellulärer Seneszenz assoziiert zu sein, bzw. scheint die Funktion spät-differenzierter T-Zellen teilweise zu verbessern. Dies könnte

therapeutisch genutzt werden, um die für den adoptiven T-Zell-Transfer verwendeten T-Zellen vor verfrühtem Auftreten von Seneszenz zu schützen bzw. um die Effektivität bereits differenzierter T-Zellen zu steigern. Zur Verbesserung der Evidenz dieser Hypothese könnten weitere Experimente bezüglich des zugrundeliegenden Wirkmechanismus beitragen. Die Wirkweise der p53 Isoformen ist, insbesondere in T-Zellen, bisher nur unvollständig verstanden. Evidenz limitierend ist zudem die geringe Anzahl an biologischen Replikaten in einzelnen Experimenten. Ein Risiko zur malignen Transformation der T-Zellen durch Manipulation von p53-Isoformen konnte in dieser und anderen Studien nicht beobachtet werden, sollte jedoch in zukünftigen Experimenten erneut berücksichtigt werden. Das potenzielle Risiko einer unkontrollierten Proliferation sowie die *in vivo* beobachteten Nebenwirkungen könnten durch ein Zelltod-induzierendes Sicherheitssystem kontrolliert werden (10).

Zusammenfassend liefert die hier beschriebene Arbeit erste Hinweise zur möglichen Verbesserung der anti-tumoralen Aktivität von T-Zellen durch Überexpression von Δ133p53α. Die Modifikation von p53 Isoformen könnte eine neue und effektive Möglichkeit zur Kontrolle von Seneszenz in T-Zellen darstellen. Dies hätte ein breites Anwendungsspektrum zur Verbesserung T-Zell-basierter Krebs-Immuntherapien und darüber hinaus im Bereich der chronischen Infektions- und Autoimmunkrankheiten.

2 Introduction

Malignant tumors form a heterogenous group of diseases with increasing incidence. It was estimated that 19.3 million new cases and 10.0 million deaths occurred only in 2020 (1). For most cancers, surgery, radiation and chemotherapy were the only treatment options available for decades. But they frequently fail in treating cancer in advanced stages and often cause severe adverse effects (11). These limitations highlight the requirement of novel and more powerful tumor-specific treatment options. Over years, intensive research on the underlying biology, development and features of malignant cells has offered many new therapeutic approaches including immunotherapy (12). Among today's available therapies which proved to be effective in cancer patients, immunotherapy appears to be one of the most promising approaches. Among these, the transfer of genetically modified T cells that specifically target malignant cells has proven great potential and has induced complete and even durable remissions in some patients (2). However, in many patients the overall benefit is still limited due to various mechanisms impeding T cell anti-tumor responses (3). One aspect contributing to impaired T cell functions is the "natural" differentiation process of tumor reactive T cells that is associated with major metabolic and functional changes in T cells. For example, $CD8^+$ T cells continuously differentiate from naïve into effector memory, central memory and eventually into terminally differentiated senescent cells. Despite the acquisition of effector functions during the differentiation process, it has been shown that naïve T cells are associated with better clinical outcomes in adoptive cell therapy (ACT) compared to memory T cells (2, 13, 14). T cells that already reached the stage of senescence including cell cycle arrest do not proliferate or expand upon transfer and finally fail to elicit effective and durable anti-tumor responses (15, 16). Preventing senescence or modulating the differentiation to favor a naïve T cell population may therefore increase response rates in ACT. One major regulator of cell cycle control, proliferation and apoptosis is the transcription factor p53. However, the human p53 gene encodes not only for the full-length protein, but for at least 12 different protein isoforms (17). One study has identified two isoforms of p53, namely p53β and Δ133p53α, as regulators of senescence in human $CD8^+$ T cells. Senescent T cells exhibited a dysregulated protein expression of these two isoforms compared to non-senescent control cells and genetic overexpression of Δ133p53α increased proliferation of $CD8^+$ T cells (9).

Therefore, modulating p53 isoform expression for adoptive T cell therapy might further increase the efficiency of anti-tumor T cells.

Aim of the study

Adoptive transfer of T cells genetically engineered to express tumor antigen-specific T cell receptors (TCRs) has definitely become a powerful treatment option in cancer immunotherapy. However, different obstacles such as the naturally occurring or tumor-induced T cell dysfunction, are still limiting its wide clinical application. Therefore, novel strategies that ensure sustained T cell proliferation leading to robust anti-tumor responses are needed. Age- or stress-related processes can induce cellular senescence which heavily impedes T cell expansion and their effective anti-tumor response. Prevention of T cell senescence by modulation of transcriptional regulators of senescence like p53 isoforms may enhance the efficacy of adoptive T cell therapy. Previous studies suggested that p53β promotes, while Δ133p53α prevents or repressess the onset of senescence in human polyclonal $CD8^+$ T cells (9). Therefore, this study aims to investigate the effects of these two p53 isoforms in human tumor antigen-specific T cells with a focus on the Δ133p53α isoform. T cells genetically equipped with a tumor-antigen specific TCR were retrovirally co-transduced with either isoform. *In vitro* experiments first examined any relevant changes in phenotype and differentiation profiles of the T cells upon modification. Next, we determined if the cellular phenotype correlates with the proliferation potential of the T cells and if functional properties including cytokine secretion, degranulation of effector cytotoxic molecules and cytolysis of tumor target cells are altered. The therapeutic efficacy and potential adverse effects of the engineered T cells was further assessed in *in vivo* xenograft tumor model. The clinical relevance of p53 isoforms for T cell senescence was also investigated by determining the expression pattern of Δ133p53α in T cells from patients with multiple myeloma (MM). Reprograming of late-stage differentiated, cancer patient-derived T cells with Δ133p53α will allow us to evaluate the feasibility of this approach to “revert” senescence-associated T cell dysfunction.

The present study aims to first characterize the specific effects of p53 isoforms p53β and Δ133p53α on the cellular functions in human tumor antigen-specific T cells. Secondly, it should investigate if T cell anti-tumor immunity *in vitro* and *in vivo* is

enhanced by modulating p53 isoform expression, which could offer a new way to improve T cell-based immunotherapy.

3 Literature discussion

3.1 Cancer immunotherapy

In general, immunotherapy refers to the idea of harnessing the immune system to treat malignant disease (18). In 1909, Paul Ehrlich already proposed the concept of immunological tumor control (19) and Thomas and Burnet developed the hypothesis of “cancer immunosurveillance”, stating that the immune system can detect and eliminate malignant/transformed cells, before the tumor becomes clinically observable (20, 21). Burnet even called immunosurveillance an “evolutionary necessity” in order to remove potential dangerous mutated cells that probably arise quite frequently during the life of multicellular organisms (20, 22, 23). Both considered lymphocytes being crucial for this natural protection against cancer (22). Studies revealed that immunocompromised mice are prone to the spontaneous development of malignant intraepithelial tumors, as well as sarcomas, compared to control mice (24, 25). Additionally, a broad spectrum of epidemiological data from different countries supports these results, showing that transplant patients and patients with immunodeficient disorders have a higher risk of developing all kinds of cancer, as compared to the general population (20, 26). Dunn et al. later refined the concept of immunosurveillance by including the mechanisms of cancer immunoediting. They noted that the immune system not only eliminates tumors – but in cases where it fails to elicit a protective immune response, it can exert a rather “tumor-sculpting” effect on the developing tumor (20). These findings were supported by the observation that many tumors, most notably melanomas, were infiltrated by lymphocytes. Importantly, the presence of tumor-infiltrating lymphocytes (TILs) has been shown to positively correlate with prolonged patient survival (27-29). Furthermore, the improved understanding of tumor-immunology and the progress made in the fields of molecular biology and genetics, has contributed to the development of various new approaches added to the spectrum of immunotherapy. These are mainly cytokine-, antibody- or cell-based approaches. By now, different cell-based approaches utilizing either lymphocytes, such as T cells and natural killer cells (NK cells), or antigen-presenting cells (APCs) like dendritic cells (DCs) have reached clinical trials and some have been approved for the treatment of different tumor entities (30).

3.2 Adoptive T cell therapy

Beside observations that the presence of TILs correlates with improved patient survival, it was further demonstrated that the endogenous immune system is capable of eliminating growing tumors (27, 29). In the 1980s, Rosenberg and his colleagues were one of the pioneers who tested TILs for cancer treatment (31, 32). The T cells that infiltrated tumors could specifically recognize antigens expressed on the malignant cells via their endogenous TCR, however, the tumor was not completely eradicated upon recognition. In order to harness the specificity of these T cells, Rosenberg and others isolated the TILs, expanded them ex-vivo and transferred them back to the patients (31-33). Patients were additionally pre-conditioned with different regimens of lymphodepleting chemotherapies (32). This adoptive transfer of TILs achieved response rates of up to 50 % for example in melanoma patients (31). Despite the encouraging results, only few patients experienced long-term benefits, while most patients had short-term responses or did not response (32). Clinical studies in melanoma could show that TIL numbers decreased in patients already within few weeks after infusion (34). Except melanomas, solid tumors frequently had lower mutational rates (35) and a lower immunogenicity with poor expression of tumor-specific antigens (32). Therefore, these “cold” tumors were poorly infiltrated and hardly recognized by T cells, making it very challenging to obtain enough cells *ex-vivo*. To overcome these obstacles, researchers started to genetically modify autologous T cells, which can be easily obtained from the peripheral blood in high numbers (32). New methods, e.g. immunization of transgenic mice, made it possible to generate high-affinity TCRs specific for human tumor antigens (36-39). The genes encoding for these αβ-TCRs were introduced via transduction with viral vectors into T cells collected from the peripheral blood to generate tumor-reactive T cells ex-vivo. After these modifications, the redirected T cells were transferred back to the patients (32) (Figure 1). First clinical trials tested the transfer of genetically modified T cells in patients with metastatic melanoma (40, 41). Although only a small fraction of patients responded, these trials proved the efficacy and feasibility of genetically engineered T cells for cancer therapy.

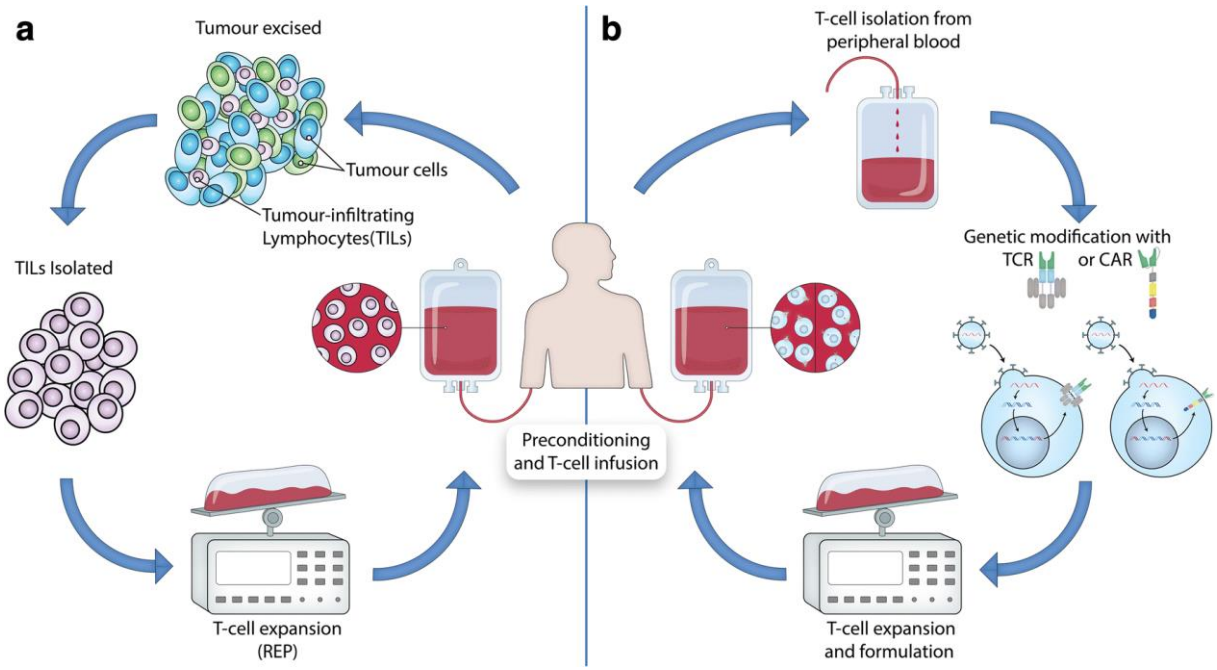

Figure 1: Principles of adoptive T cell therapy

Schematic presentation of the principle of adoptive T cell therapy. T cells isolated from resected tumors (TILs) are expanded ex-vivo and transferred back to the patient (a). Another approach is the expansion and infusion of genetically modified T cells, typically obtained from the peripheral blood (b). TCR or CAR constructs are designed to redirect these T cells to specific tumor antigens. Both approaches generate therapeutic numbers of T cells capable of recognizing malignant cells and eliciting an anti-tumor response (42, 43). Reprinted with permission from the European Society for Medical Oncology; © 2018.

In summary, the modified T cells could have the ability to specifically sense and target the malignant cells through the whole body and establish an anti-tumor immune memory response. This makes adoptive T cell therapy a powerful approach, virtually applicable for any type of tumor, even in metastatic stages and with few serious adverse effects. Practically, however, there are several barriers limiting the application of this treatment. On-target/off-tumor toxicity (40) and autoimmunity due to mispairing of endogenous and transgenic TCR (44) are sources of potential side effects. Furthermore, the downregulation of major histocompatibility complex (MHC) molecules and thus antigen presentation in some tumors is another major limitation (45). Therefore, T cells lose the ability of recognizing the mutated cells via the TCR, which can contribute to cancer cells escaping the anti-tumor immune response. This escape mechanism can be bypassed using chimeric antigen receptors (CARs) instead of TCRs (46). CARs are generated by linking an extracellular single chain fragment variable (scFv) antibody-derived domain to an intracellular signaling domain of a TCR. The antibody-derived scFv is specific for an antigen and provides the ability of tumor recognition without the requirement of peptide presentation via the

MHC (46). Upon recognition, the signaling domain transmits an activation signal and ensures T cell stimulation. As a signaling domain, the first CAR constructs possessed only the CD3ζ-chain (47), which is part of the TCR-CD3-complex (48). Effective T cell activation via the TCR, however, also requires co-stimulatory signals via receptors like CD28, OX40 or CD137 (49). The development of second and third generation CARs overcomes this limitation of TCR T cells by including one or two co-stimulatory domains (46). Therefore, CARs endow T cells to target cell surface proteins, carbohydrates, and glycolipids independent of MHC expression, human leukocyte antigen (HLA) restriction or co-stimulation. Clinical trials with CAR T cells targeting the CD19 molecule, which is exclusively and highly expressed on normal and malignant B cells, revealed the great potential of this treatment (50-52). For non-solid, hematologic B cell malignancies, CAR therapy achieved impressive complete response rates e.g., 66.7 % in acute lymphoblastic leukemia (53, 54) with in part durable responses. Unfortunately, some patients still relapse due to loss of target antigen or do not respond because the CAR-T cells fail to proliferate after infusion (46). Another limitation of CAR-based immunotherapy is the dependence on antigens presented on the cell surface, while TCRs are capable of recognizing intracellular epitopes presented by the MHC (2). Additionally, some patients relapsed or even failed to respond to treatment of T cell transfer due to so-called tumor escape mechanism (55). Taken together, for many patients the overall benefit of adoptive T cell transfer is still limited. Understanding the mechanisms leading to tumor escape and developing strategies to overcome these barriers is therefore of paramount importance to further improve the efficacy of this treatment approach.

3.3 T cell dysfunction in the tumor microenvironment

Tumor escape mechanisms enable malignant cells to evade the elimination by the immune system and hence contribute to treatment failure (55). In their well-established concept, Hanahan and Weinberg described the “hallmarks of cancer” as underlying principles for the extraordinary diversity and complexity of malignant diseases, including the ability of evading the immune system (12). A key factor contributing to the immune escape is the so-called tumor microenvironment (TME), which is formed by the interaction of cancer cells with the extracellular matrix (ECM), stromal and immune cells (56). Myeloid-derived suppressor cells (MDSCs), regulatory T cells (T_{regs}), and type 2-polarized macrophages (M2) for example are

often recruited to the TME and impede immune-responses via direct cell-cell interaction or by the release of soluble factors like cytokines (3, 57). Moreover, T cells rely on the availability of nutrients for proliferation and effector functions to maintain an effective immune response. For proper activation and cytolytic functions, T cells have to adapt their metabolism to their functional needs (58). Within the TME, however, the high energetic demands of proliferating cancer cells can lead to a nutrient depletion, as well as an increase of immunosuppressive metabolites (59). In this glucose-, oxygen- and amino-acid-depleted milieu with low pH, cancer and T cells compete for nutrients. This competition can lead to a severely impaired T cell metabolism resulting in proliferation arrest and late-stage differentiation (59-62). Therefore, the TME promotes T cell differentiation associated with poor proliferative capacity and persistence (63). This highlights that effective ACT must meet multiple functional requirements to overcome obstacles such as the immunosuppressive TME. These needs may differ not only between cancer types, but also between individual patients. Therefore, Lim and June named “five major challenges for a therapeutic T cell”. Besides trafficking, tumor recognition/killing, counteracting the microenvironment and control, they refer to proliferation/persistence (64). It seems obvious that proliferation and persistence of T cells is determinant for an effective tumor eradication, as well as anti-tumor memory response. Interestingly, proliferation and persistence of CAR T cells seems to be one of the best predictors of clinical efficacy (64, 65). While engineered TCRs and first-generation CARs do not have additional co-stimulatory domains, they often show only short-term persistence. CARs including intracellular co-stimulatory domains (such as CD28 or 4-1BB) induced long-term remission in patients with ALL and showed increased proliferation plus effector functions in pre-clinical studies (64). Nevertheless, incorporation of co-stimulatory domains may not be enough to ensure proliferation in some cancers and TCR engineered T cells may be in a greater extend dependent on co-stimulatory signals (46). Additionally, the hostile TME conditions alter the phenotype, proliferative capacity, and functions of (effector) T cells, and force T cells towards dysfunctional states (3, 59, 63). According to phenotypic and functional features, dysfunctional T cells can be classified into three different categories, defined as (I) anergy, (II) exhaustion and (III) senescence (Figure 2) (5).

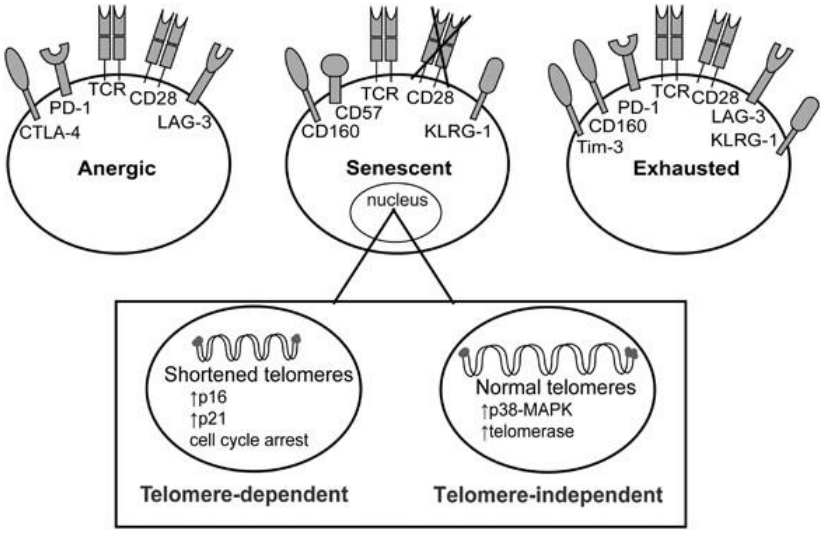

Figure 2: Phenotypes of dysfunctional T cell states

Schematic model illustrating the phenotype of dysfunctional T cell states: (I) anergy, (II) senescence and (III) exhaustion. Depending on the causing mechanism, the dysfunctional T cells differ in expression of inhibitory, co-stimulatory and other cell surface markers. Reprinted with permission from Springer Nature © (5).

T cell anergy is a state of functional inactivity due to deficient co-stimulation or co-inhibitory signaling (66). While anergy occurs during T cell priming, T cell exhaustion (III) is thought to be caused during chronic antigen (over)stimulation, like in cancer or chronic infections. Exhausted T cells have poor effector functions and a high expression of inhibitory receptors including T-cell immunoglobulin and mucin-domain containing-3 (TIM-3), Lymphocyte-activation gene 3 (LAG-3), Programmed cell death protein-1 (PD-1) and Cytotoxic T-lymphocyte-associated protein-4 (CTLA-4) (5, 67, 68). Monoclonal antibodies targeting these receptors have already been approved in the clinic, aiming at overcoming T cell exhaustion (69). Another inhibitory receptor called T cell immunoreceptor with Ig and ITIM domains (TIGIT) is not exclusively upregulated in exhausted T cells but is expressed at high levels in senescent T cells as well (70). Antibodies that block TIGIT to boost T cell anti-tumor immunity in myeloma, lung cancer and other entities are currently under evaluation in several clinical trials (71-74). However, in some cancers T cell senescence (II), rather than exhaustion or anergy, may be the key mechanism leading to deficient T cell responses. For example, in patients with multiple myeloma, a study reported potentially protective clonal T cells that failed to proliferate *in vitro* and were hypo-responsive, compared to non-clonal T cells from the same patients. These T cells exhibited phenotypic features of senescent T cells, while “exhaustion markers” like PD-1 or CTLA-4 were expressed at low levels (5). Moreover, it has been reported

that tumor cells are able to induce T cell senescence *in vitro* (75). Accordingly, several studies reported an accumulation of senescent T cells in certain types of cancer (76, 77). A study of TIL therapy in melanoma patients, has even correlated the telomere length of transferred T cells to *in vivo* persistence and tumor regression (15). It is also known that the number of less-differentiated (naïve) $CD8^+$ T cells in the peripheral blood declines with age, most likely due to thymic involution and differentiation to memory cells (78). Taken together, T cell senescence contributes to a weakened immune response in different subtypes of cancer, like multiple myeloma. To improve immunotherapeutic approaches, an improved understanding of causative mechanisms and therapeutic options to prevent or circumvent T cell senescence are required.

3.4 Immunosenescence and cellular senescence in T cells

Immunosenescence refers to the observable decline in protective immune responses as a function of age. The innate, as well as the adaptive immunity show changes in many elderly individuals. For example, responses to vaccination are reduced in older individuals and they are more susceptible to infections (79). Immunosenescence is observed in various long- and short-living species (80) and is thought to be a major contributor to many age-related diseases. The enormous complexity and the interplay between the components of the immune system, however, still hamper a complete understanding of immunosenescence. Increasing numbers of studies provide evidence that immunosenescence also impedes anti-tumor immunity (81, 82). Especially, cellular senescence of different immune cells seems to contribute to impaired immune responses. For example, T cells used for ACT can become dysfunctional due to cellular senescence (83).

In contrast to immunosenescence, cellular senescence is defined as a state of (irreversible) cell cycle arrest resulting in a stop of proliferation. In 1961, Hayflick and Moorhead published their observations of normal human fibroblasts reaching cellular growth arrest after several rounds of division *in vitro* (84). The limited number of cellular divisions restricts the proliferation and lifespan of normal cells, is often called the “Hayflick Limit”, and was considered to be aging at the cellular level (85). This state of cell cycle arrest due to telomere shortening is called replicative senescence and prevents permanent growth of human cells (9, 86). It contributes to the protection against the formation of cancer cells and is also involved in organismal aging (87).

Independent of the number of divisions, reactive oxygen species (ROS), oncogene activation and other stressors increase DNA damage signaling and can induce cellular (stress-induced) senescence (9, 88, 89). Stress-induced senescence therefore represents a potential mechanism that promotes the immune escape of tumor cells.

In T cells, senescence is characterized by a reduced proliferative activity, low telomerase activity and the so-called senescence associated secretory phenotype (SASP) (83). These cells are also characterized by a loss of co-stimulatory receptors such as CD27 and CD28 and express high levels of CD57 and KLRG1 on the cell surface (Figure 2). It has also been shown that the late differentiated T_{EMRA} (Effector memory T cells re-expressing CD45RA) subset ($CD27^{-}CD45RA^{+}$) exhibit many features of senescent cells (90). Mechanistically, different proteins such as p16 and p38 are involved in the regulation of cellular senescence in T cells (83). Among these, p53 is one of the central molecules and has been linked to e. g. cell cycle control, senescence, apoptosis and metabolism (17).

3.5 p53 isoforms and cellular senescence

The transcription factor p53 is a key molecule in stress-response signaling pathways. Under physiological conditions, p53 is a transiently expressed protein, which is ubiquitinated by Mouse double minute 2 homolog (MDM2) and continuously degraded by the proteasome (91). Additionally, its activity is strictly regulated by several other processes such as transcriptional control and posttranslational modifications (PTMs) (92, 93). Under stress conditions like DNA damage, p53 is stabilized via phosphorylation by kinases such as the ataxia telangiectasia and Rad3-related protein (ATR) (93, 94). Besides its role in stress response pathways, p53 primarily regulates cell cycle control and induces cell cycle arrest and apoptosis (95). Therefore, it is a powerful tumor suppressor and was described as “the guardian of the genome” (96). A major pathway of replicative senescence is the p53-mediated upregulation of its target gene CDKN1A/p21, which in turn leads to the inhibition of CDK4,6/cyclin-D and ultimately to cell cycle arrest in G1-phase (97). Additionally, a multitude of other pathways have been identified, linking p53 to senescence, cell cycle control (98), apoptosis (99), metabolism (100), reproduction (101) and development (17). For a long time, it was unclear how a single protein could be involved in the regulation of many diverse cell signals, regulating thousands of

genes, modulated by several extracellular and intracellular signals (102). However, the discovery of 12 different isoforms encoded by the p53 gene (TP53) could, at least partially, explain its manifold functions and further increased the complexity of this exceedingly intricate network of p53 pathways (Figure 3) (102, 103).

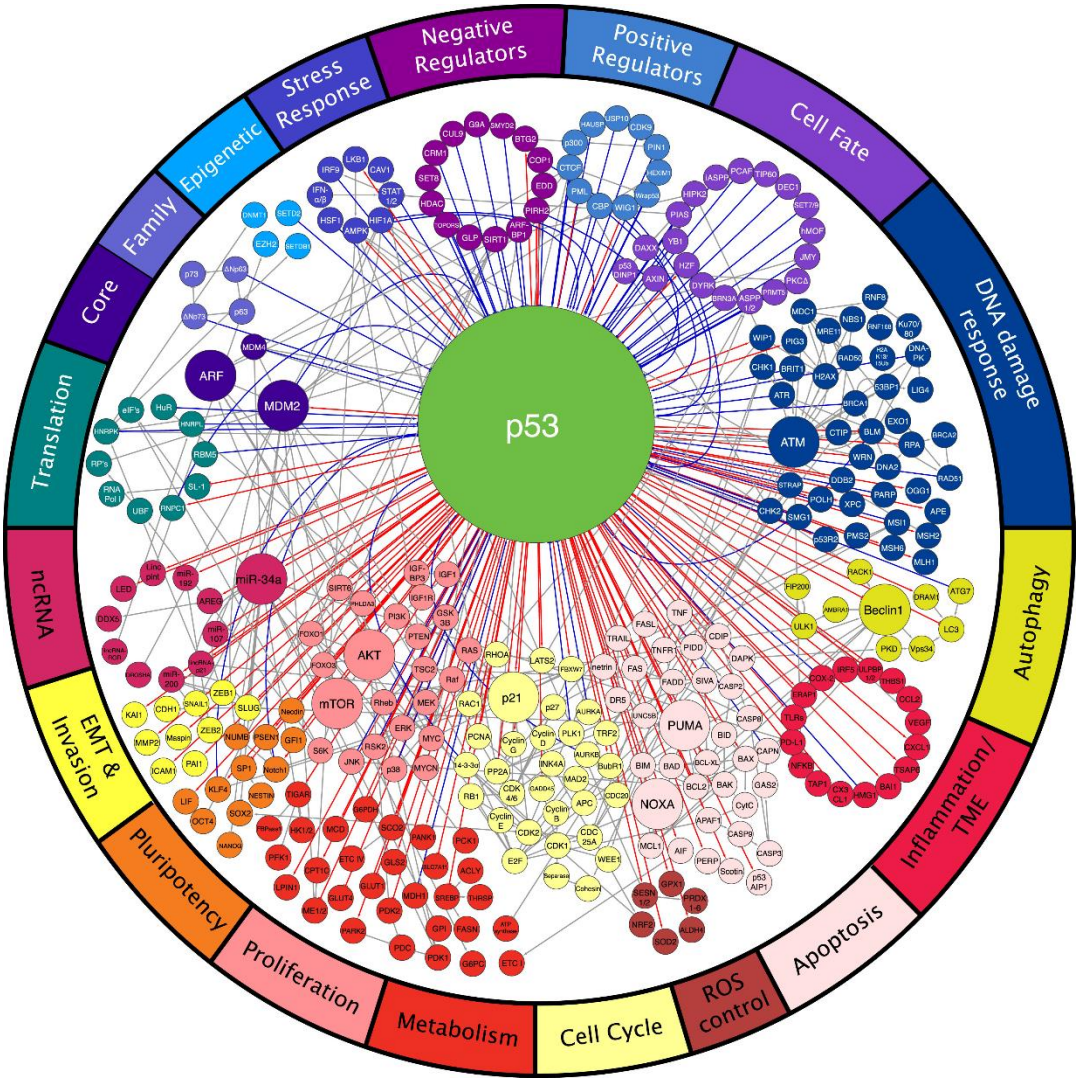

Figure 3: The network of p53 pathways
The figure depicts the various pathways and transcription factors modulated by p53. Blue lines indicated p53 inputs, red lines indicate p53 outputs. The outer circle names the corresponding processes. Reprinted with permission from Elsevier © (104).

The human p53 gene (TP53), located on chromosome 17p13.1, contains 13 exons of which two are cryptic exons (9b and 9g). Minimum nine different mRNAs are differentially transcribed from TP53 by the usage of two alternative promotors (P1 and P2) and by alternative splicing of intron-2 and -9 (102, 103). These nine mRNAs encode for at least 12 different protein isoforms (Figure 4). Alternative splicing of exon-9 leads to retention of exon-9β or exon-9γ, which contain stop codons.

Therefore, exon-10 and -11 are noncoding in mRNA splice variants β and γ (102). Additionally, translation of mRNA transcripts from P1 can be initiated at codons 1 and/or 40, transcripts from P2 at codons 133 and/or 160 (102).

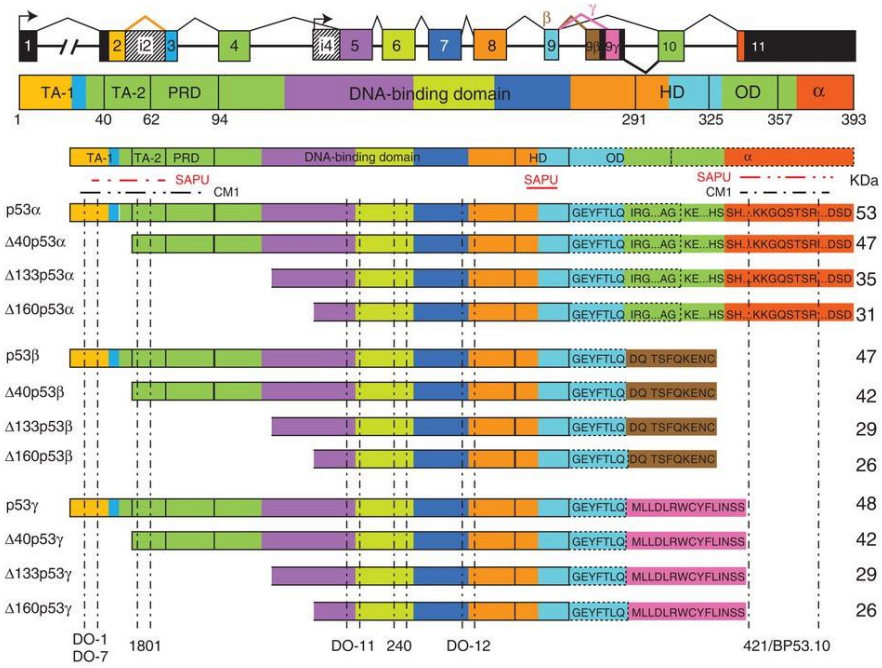

Figure 4: Overview of the different isoforms encoded by the human p53 gene
The exons of TP53 are illustrated at the top. The protein domains are labeled in different colors and match the corresponding exons. Depending on the initiation of transcription, isoforms differ on the N-terminal part. Other isoforms (β and γ) are altered on the carboxy-terminal part due to alternative splicing of intron-9. Reprinted with permission from Cold Spring Habor Laboratory Press © (102).

Over the years, most studies have primarily analyzed ("abnormal") expression of p53 isoforms in several cancer entities including e.g. acute myeloid leukemia (AML) (105), multiple myeloma (106), colon carcinoma (107), breast cancer (108) and glioblastoma (102, 109) and linked it to patient prognosis (110, 111), partially in combination with TP53 mutation status (112, 113). However, only few studies have investigated the physiological expression and functions of p53 isoforms. Two of them, namely p53β and Δ133p53α, have been linked to the regulation of senescence in fibroblasts (107). In the C-terminally truncated isoform p53β, the α-carboxy-terminal protein domain is replaced by the β-carboxy-terminal domain, which is composed of 10 amino acids (DQTSFQKENC) (102, 107). It modulates p53 transcriptional activity (114) and facilitates cellular senescence via the p53-dependent induction of p21 expression (107). In contrast to p53β, the N-terminally truncated Δ133p53α isoform, which lacks the first 132 amino acids of p53 full length (FL), inhibits p53 transcriptional activity and cellular senescence (107, 114).

Interestingly, a recent study could confirm the role of these two isoforms in the regulation of senescence in human $CD8^+$ T cells. Senescent $CD28^-/CD57^+$ T cells exhibited an upregulation of p53β, while the expression of Δ133p53α was diminished. Further, it could be shown that restoring Δ133p53α expression in $CD28^-$ cells delays replicative senescence, increases proliferative capacity, and changes the phenotype of these T cells (9). Modulation of p53 isoform expression could therefore be a novel approach to overcome T cell senescence in different immunotherapeutic strategies.

In summary, adoptive cellular immunotherapy has proven to be a powerful treatment option for hematological malignancies. To further improve its efficacy and to broaden its application to solid tumors, ensuring T cell proliferation and overcoming natural and tumor-induced T cell senescence is a major issue for adoptive T cell therapy. First findings provided evidence, that senescence and terminal differentiation could be delayed or even reverted by reprogramming T cells with physiologically expressed isoforms, without major risks for malignant transformation (9). Nevertheless, the expression pattern of p53 isoforms in tumor-antigen specific T cells and their effect on T cell functionality remain unexplored and require further investigation.

4 Material and Methods

4.1 Devices

Table 1: Devices used for cell culture and molecular biology

Device	Manufacturer
Balance L2200S	Sartorius, Göttingen, Germany
Cell irradiating machine Gammacell 2000	Mølsgaard Medical, Ganløse, Denmark
Centrifuge 5417R	Eppendorf, Hamburg, Germany
Centrifuge Biofuge fresco	Heraeus, Hanau, Germany
Centrifuge Megafuge 1.0R	Heraeus, Hanau, Germany
Centrifuge Megafuge 3.0R	Heraeus, Hanau, Germany
Centrifuge Megafuge 4.0R	Thermo Scientific, Langenselbold, Germany
Centrifuge Omnifuge 2.0RS	Heraeus, Hanau, Germany
CO_2 Incubator Heracell	Heraeus, Hanau, Germany
CO_2 Incubator Function line	Heraeus, Hanau, Germany
Electrophoresis EPS600 power supply	Pharmacia Biotech, München, Germany
Flow Cytometer FACS Canto II	BD Bioscience, Heidelberg, Germany
Gamma counter Cobra II	Canberra Packard, Schwadorf, Austria
Heating block Thermo Stat plus	Eppendorf, Hamburg, Germany
Hemocytometer (Neubauer improved)	Brand GMBH + CO KG, Wertheim, Germany
Laminar Flow S2020 1.8	Thermo Scientific, Langenselbold Germany
Luminex MAGPIX System	Thermo Fischer Scientific, Waltham, USA
MACS-Systems MidiMACS and QuadroMACS Seperators	Miltenyi Biotec, Bergisch Gladbach, Germany
Microvolume UV-Vis Spectrophotometer (NanoDrop One)	Thermo Fischer Scientific, Waltham, USA
Microscope Wilovert	Hund, Wetzlar, Germany
Microscope Axiostar	Zeiss, Jena, Germany
MRXII Mircoplate reader	Dynex Technologies Inc., Chantilly, USA
PCR Cycler MasterCycler Gradient	Eppendorf, Hamburg, Germany
PCR Cycler Gene Touch	Biozym, Hessisch Oldendorf, Germany
PCR-System Quantstudio3	Applied Biosystem, Waltham, USATB
Knick pH-meter 766	Calimatic, Zweibrücken, Germany
Photometer Ultrospec 1000	Pharmacia Biotech, Munich, Germany
Photometer Gene Quant II	Pharmacia Biotech, Munich, Germany
Scanner Epson Perfection 2400 Photo	Epson, Suwa, Japan
Shaker ORS aero r	Infors AG, Bottmingen, Switzerland
UV documentation Transilluminator	Biostep GmbH, Jahnsdorf, Germany
Water bath 1003	Gesellschaft für Labortechnik, Burgwedel, Germany
Water bath F12	Julabo Labortechnik GmbH, Seelbach, Germany
iBlot 2 Dry Blotting System	Thermo Fischer Scientific, Waltham, USA

iBright CL1500 Imaging System	Thermo Fischer Scientific, Waltham, USA

4.2 Chemicals and reagents

Table 2: Chemicals and reagents used for cell culture and molecular biology

Reagent	Manufacturer
Cell culture	
AB-Serum (human)	Obtained from the Blood Transfusion Center of the University Medical Center of the Johannes Gutenberg-University Mainz
Anti-PE MicroBeads	Miltenyi Biotec, Bergisch Gladbach, Germany
Bovine serum albumin (BSA)	Sigma-Aldrich, St. Louis, USA
CD4 MicroBeads	Miltenyi Biotec, Bergisch Gladbach, Germany
CD8 MicroBeads	Miltenyi Biotec, Bergisch Gladbach, Germany
CellTrace™ CFSE Cell Proliferation Kit	Invitrogen, Carlsbad, USA
Chromium-51 ($Na_2{}^{51}CrO_4$)	Perkin Elmer, Waltham, USA
Dimethyl sulfoxide (DMSO)	Sigma-Aldrich, St. Louis, USA
Dulbecco's Modified Eagle Medium (DMEM)	Lonza, Basel, Switzerland
Grams Crystal violet solution	Merck KGaA, Darmstadt, Germany
Fetal Calf Serum (FCS)	PAA, Linz, Austria
Ficoll-Paque	STEMCELL Technologies Inc., Vancouver, Canada
FuGENE® 6	Promega, Madison, USA
Gibco™ Dynabeads™ Human T-Activator CD3/CD28	Fisher Scientific, Pittsburgh, USA
Geneticin (G418)	Gibco, Eggensheim, Germany
HEPES buffer	Lonza, Basel, Switzerland
Human IL-2 (Proleukin® S)	Novartis, Basel, Switzerland
Ionomycin	Cayman Chemical Company, Ann Arbor, USA
L-Glutamine	Sigma-Aldrich, St. Louis, USA
Monensin	eBioscience Inc., San Diego, USA
OKT3 (Orthoclone Okt-3®)	Janssen-Cilag GmbH, Frankfurt/Main, Germany
Phorbol-12-myristat-13-acetat (PMA)	Sigma-Aldrich, St. Louis, USA
Phosphate-buffered saline (PBS)	Sigma-Aldrich, St. Louis, USA
Polybrene	Sigma-Aldrich, St. Louis, USA
Puromycin	Sigma-Aldrich, St. Louis, USA
RPMI 1640	Sigma-Aldrich, St. Louis, USA
Sodium dodecyl sulfate (SDS)	Carl Roth GmbH & Co. KG, Karlsruhe, Germany
Sodium-Penicillin/Streptomycin	Sigma-Aldrich, St. Louis, USA
Trypan Blue solution 0.4 %	Sigma-Aldrich, St. Louis, USA

Trypsin-EDTA (0.25 %)	Sigma-Aldrich, St. Louis, USA
Molecular biology	
Ampicillin	Sigma-Aldrich, St. Louis, USA
Bolt MES SDS Running buffer (20x)	Invitrogen, Carlsbad, USA
DNA ladder (1 kb)	New England Biolabs, Frankfurt/Main, Germany
EndoFree Plasmid Maxi Kit	QIAGEN, Venlo, Netherlands
High-Capacity cDNA Reverse Transcription Kit	Thermo Fischer Scientific, Waltham, USA
LB medium	Roth, Karlsruhe, Germany
Enhanced chemiluminescent (ECL) HRP SuperSignal™ West Femto Maximum Sensitivity Substrate	Thermo Fischer Scientific, Waltham, USA
Laemmli Sample Buffer 2x	Bio-Rad Laboratories Inc., Hercules, USA
pegGREEN	PEQLAB GmbH, Erlangen, Germany
Pfx PCR Buffer (10X)	Invitrogen, Carlsbad, USA
Pfx50 Polymerase	Invitrogen, Carlsbad, USA
PowerUp SYBR Green Master Mix	Applied Biosystem, Waltham, USA
Precision Plus Protein WesternC Blotting Standard	Bio-Rad Laboratories Inc., Hercules, USA
Protein Assay Reagent A, B and S	Bio-Rad Laboratories Inc., Hercules, USA
Precision Protein™ StrepTactin-HRP Conjugate	Bio-Rad Laboratories Inc., Hercules, USA
QIAprep Spin Miniprep Kit	QIAGEN, Venlo, Netherlands
QIAquick Gel Extraction Kit	QIAGEN, Venlo, Netherlands
Restriction enzyme BamHI HF	New England Biolabs, Frankfurt/Main, Germany
Restriction enzyme NotI HF	New England Biolabs, Frankfurt/Main, Germany
RNeasy Mini Kit	QIAGEN, Venlo, Netherlands
Skimmed milk powder	Carl Roth GmbH & Co. KG, Karlsruhe, Germany
Tetracycline	Sigma-Aldrich, St. Louis, USA
T4 DNA Ligase	New England Biolabs, Frankfurt/Main, Germany
T4 DNA Ligase Reaction Buffer	New England Biolabs, Frankfurt/Main, Germany

4.3 Consumables, buffer, and cell culture media

Table 3: Consumables

Item	Manufacturer
Cell Culture Dish, 100/20 mm	Greiner Bio-One GmbH, Frickenhausen, Germany
Cell Culture Flask, 50 ml, 25 cm^2	Greiner Bio-One GmbH, Frickenhausen, Germany
Cell Culture Flask, 250 ml, 75 cm^2	Greiner Bio-One GmbH, Frickenhausen, Germany
Centrifuge Tube 15 ml	Greiner Bio-One GmbH, Frickenhausen,

	Germany
Centrifuge Tube 50 ml	Greiner Bio-One GmbH, Frickenhausen, Germany
Cover Slip	Glaswarenfabrik Karl Hecht GmbH & Co. KG, Sondheim vor der Rhön, Germany
Freezing Tube, 2 ml	Greiner Bio-One GmbH, Frickenhausen, Germany
Mini Protein Gels Bolt™ 10%, Bis-Tris, 1.0 mm	Invitrogen, Carlsbad, USA
Multiwell Cell Culture Plate, 6 well	Greiner Bio-One GmbH, Frickenhausen, Germany
Multiwell Cell Culture Plate, 12 well	Greiner Bio-One GmbH, Frickenhausen, Germany
Multiwell Cell Culture Plate, 24 well	Greiner Bio-One GmbH, Frickenhausen, Germany
Multiwell Cell Culture Plate, 96 well, f-bottom	Greiner Bio-One GmbH, Frickenhausen, Germany
Multiwell Cell Culture Plate, 96 well, u-bottom	Greiner Bio-One GmbH, Frickenhausen, Germany
PCR Reaction Tube, 0.2 ml	Thermo Fischer Scientific, Waltham, USA
Pipette Tip, 1000 µl (blue)	Sarstedt, Nümbrecht, Germany
Pipette Tip, 200 µl (yellow)	Sarstedt, Nümbrecht, Germany
Pipette Tip, 10 µl (transparent)	Sarstedt, Nümbrecht, Germany
Polystyrene Test Tube, 5 ml (Flow Cytometry)	Falcon, Corning, USA
Reaction Tube 1.5 ml	Greiner Bio-One GmbH, Frickenhausen, Germany
Reaction Tube 5 ml	Greiner Bio-One GmbH, Frickenhausen, Germany
Syringe (2-Piece Design), 10 ml	BD Bioscience, Heidelberg, Germany
Syringe (2-Piece Design), 20 ml	BD Bioscience, Heidelberg, Germany
TransWell Inserts (24-well, 0.4 µm)	Falcon, Corning, USA

Table 4: Buffers and media used for cell culture and molecular biology and the corresponding supplements

Buffer / medium	**Supplements**
DMEM complete (Gibco)	10 % heat inactivated FCS 1 % L-glutamine 1 % penicillin-streptomycin 2.5 % HEPES filtered sterile, added to 500 ml DMEM
DMEM only (Gibco)	DMEM without supplements
Freezing medium	10 % DMSO (filtered sterile) in heat inactivated FCS
Erythrocyte lysis buffer	174 mM NH_4Cl 10 mM $KHCO_3$ 0.1 mM Na_2EDTA

	added to 500 ml aqua dest. adjusted to pH 7.3
LB ampicillin agar plates	1 l LB medium + 20 g agar
MACS buffer	PBS 1 mM EDTA 2 % heat inactivated Fetal Calf Serum (FCS)
RPMI	10 % heat inactivated FCS 1 % L-glutamine 1 % penicillin-streptomycin 2.5 % HEPES filtered sterile and added to 500 ml RPMI 1640
huRPMI	10 % heat inactivated human AB-serum 1 % L-glutamine 1 % penicillin-streptomycin 2.5 % HEPES filtered sterile and added to 500 ml RPMI 1640
Running buffer 1x	20 ml 20x Bolt MES SDS Running buffer 380 ml deionized water
SOB-medium	0.5 g NaCl 20 g bactotryptone 5 g yeast extract 10 ml 250 mM KCl 5 ml 2 M $MgCl_2$ added to 1 l aqua dest. adjusted pH to 7.0
TAE buffer (50x)	242 g Tris base 100 ml 0.5 M Na2EDTA pH 8.0 57.1 ml acetic acid adjusted to 1 l with aqua dest.
TBST	Tris-buffered saline with Tween20
Tfb I	30 mM Cobaltacetate 50 mM $MnCl_2$ 100 mM KCl 10 mM $CaCl_2$ 15 % Glycerin pH adjusted to 5.8 filtered sterile
Tfb II	10 mM NaMOPS (pH = 7.0) 75 mM $CaCl_2$ 10 mM KCl 15 % Glycerin filtered sterile

4.4 Peptides

Human $p53_{264-272}$ (9-mer) LLGRNSFEV from Biosynthan, Berlin, Germany dissolved in sterile DMSO at a concentration of 10 mg/ml

4.5 Primers for PCR

Table 5: Primer sequences for PCR and qPCR

Target	Forward	Reverse
p53β	5'-CAGCCAAGTCTGTGACTTGCA-3'	5'-TCATAGAACCATTTTCATGCTCTCTT-3'
Δ133p53α	5'-ACTCTGTCTCCTTCCTCTTCCTACAG-3'	5'-CTCACGCCCACGGATCTGA-3'
TIGIT	5'-TGCCAGGTTCCAGATTCCA-3'	5'-ACGATGACTGCTGTGCAGATG-3'
Glyceraldehyde 3-phosphate dehydrogenase (GAPDH)	5'-GTTTACATGTTCCAATATGATTCCAC-3'	5'-TCATATTTGGCAGGTTTTTCTAGAC-3'
Sequencing primer (SE-206)	5'-TTACACAGTCCTGCTGACCACC-3'	-

4.6 Cell lines and bacterial strains

4.6.1 Bacterial strains

Bacterial E. coli strains XL-1 Blue or JM-109 were used for transformation. Details regarding handling and storage see 4.7.1.7.

JM-109 stock solution — New England Biolabs, Frankfurt/Main, Germany

XL-1 Blue stock solution — Agilent Technologies, Santa Clara, USA

4.6.2 Cell lines

For culturing cell lines, RPMI medium was used. Only Phoenix-AMPHO cells were cultured in DMEM complete.

Phoenix-AMPHO: The packaging cell line Phoenix-AMPHO was purchased from the Nolan Laboratory, Stanford University, USA.

K562_A2_CD80^{+}: The human chronic myelogenous leukaemia cell line K562 has a very poor MHC class I and II expression. To function as APCs the cells were transfected with an HLA_A*0201 encoding vector. These K562_A2 cells were again transfected with a vector encoding for the costimulatory human CD80 to facilitate T cell activation.

SAOS 2 p53^{null} and SAOS 2/143: The SAOS 2 cell lines are human HLA_A*0201 osteosarcoma-derived cell lines. SAOS 2 are p53-

deficient, while SAOS 2/143 are transfected with the human p53 gene harbouring the mutation V143A (115).

4.7 Methods

4.7.1 Cloning of p53 isoforms p53β and Δ133p53α in retroviral expression vectors

Cloning was performed as described earlier in the doctoral thesis of ~~Name~~ (AG Theobald, III. Med. Dep. University Medical Center Mainz) (116). Details for the cloning performed in this thesis are described below.

p53β

pcDNA3.1 p53β TOPO GFP, encoding for p53β, was kindly provided by ~~Name~~ (Group Leader Neurooncology, Mainz, Germany). Briefly, the p53β insert was amplified out of the cDNA by PCR (see 4.7.1.3). The obtained DNA was purified with the QIAquick PCR Purification Kit (QIAGEN, Venlo, Netherlands) according to the manufacturer's protocol and digested as described below (see 4.7.1.2). The digestion products were separated by agarose gel electrophoresis (see 4.7.1.4). Bands with the expected size (insert 1225 bps and vector 5846 bps) were cut out and DNA was extracted using the PCR Purification Kit (QIAGEN, Venlo, Netherlands, see 4.7.1.5). Ligation of the isolated DNA was performed overnight (see 4.7.1.6). Correct ligation was checked again by digestion and agarose gel electrophoresis. Finally, DNA was amplified by transformation with XL-1 Blue bacteria (see 4.7.1.7) and purified by maxipreparation (see 4.7.1.9).

Δ133p53α

'cmvd133s' vector encoding for Δ133p53α was provided (as dried DNA on filter paper) by ~~Name~~ (University of Dundee, United Kingdom). First, filter paper carrying the Δ133p53α DNA was inserted into a 1.5 ml reaction tube. To recovered DNA from the filter paper, 100 µl of TE buffer (TRIS/EDTA buffer from QIAGEN's Endofree Plasmid Kit) was added. After 5 minutes incubation at RT, the tube was centrifuged for 15 seconds at 13'000 rpm (≙ 16'200 g). Then 10 µl of the supernatant containing DNA was used to perform a transformation with JM-109 bacteria (see 4.7.1.7) and subsequent minipreparation of DNA (see 4.7.1.9). The DNA was digested as

described below and insert and vector were used to perform ligation overnight (see 4.7.1.6). Next, ligation products were checked by digestion and agarose gel electrophoresis and finally used to perform another transformation and maxipreparation (see 4.7.1.9).

4.7.1.1 Vectors

DNA encoding for the p53 isoforms were cloned in the following retroviral plasmids: pMx_IRES_puro (RTV-014), pMx_IRES_neo or pBu_IRES_puro.

All vector maps are listed in the supplement.

4.7.1.2 Digestion of DNA

p53β for cloning into pMx_IRES_puro

p53β (DNA template)	20 µl	DNA
	1 µl	cut smart buffer
	1 µl	BamHI HF
	1 µl	NotI HF

Add 2 aqua dest. (double distilled water) up to a total volume of 25 µl. Incubate for 60 minutes at 37 °C.

pMx_IRES_puro (Vector)	1 µl ≙ 1 µg	
	1 µl	cut smart buffer
	1 µl	BamHI HF
	1 µl	NotI HF

Add 6 µl aqua dest. up to a total volume of 10 µl. Incubate for 60 minutes at 37 °C.

Δ133p53α for cloning into pMx_IRES_puro

Δ133p53α (DNA template)	3 µl	DNA
	1 µl	cut smart buffer
	1 µl	BamHI HF
	1 µl	NotI HF

Add 4 µl aqua dest. up to a total volume of 10 µl. Incubate for 60 minutes at 37 °C.

pMx_IRES_puro (Vector)	1 µl ≙ 1 µg	
	1 µl	cut smart buffer
	1 µl	BamHI HF
	1 µl	NotI HF

Add 6 µl aqua dest. up to a total volume of 10 µl. Incubate for 60 minutes at 37 °C.

Δ133p53α for cloning into pMx_IRES_neo

Δ133p53α_pMx_IRES_puro (DNA template)	10 µl DNA
	1 µl cut smart buffer
	1 µl BamHI HF
	1 µl NotI HF

Add 7 µl aqua dest. up to a total volume of 20 µl. Incubate for 60 minutes at 37 °C.

pMx_IRES_neo (Vector)	10 µl ≙ 1 µg
	1 µl cut smart buffer
	1 µl BamHI HF
	1 µl NotI HF

Add 7 µl aqua dest. up to a total volume of 20 µl. Incubate for 60 minutes at 37 °C.

Δ133p53α for cloning into pBu_IRES_puro

Δ133p53α_pMx_IRES_puro (DNA template)	5 µl DNA
	1 µl cut smart buffer
	1 µl BamHI HF
	1 µl NotI HF

Add 2 µl aqua dest. up to a total volume of 10 µl. Incubate for 60 minutes at 37 °C.

pBu_IRES_puro (Vector)	5 µl ≙ 1 µg
	1 µl cut smart buffer
	1 µl BamHI HF
	1 µl NotI HF

Add 2 µl aqua dest. up to a total volume of 10 µl. Incubate for 60 minutes at 37 °C.

4.7.1.3 PCR to amplify insert of interest

Using specific primers (Table 5) listed above, p53β was amplified out of pcDNA3.1 Topo GFP. In a PCR tube 200 ng (0.2 µl) of cDNA, 100 µM (0.5 µl) of forward and reverse primers were mixed with 25 mM (0.8 µl) dNTPs, 5 µl 10X Pfx PCR buffer, 0.25 µl Pfx 50 Polymerase and 50 mM (1 µl) $MgSO_4$. The mixture was filled up to a volume of 50 µl with H_2O. The PCR was performed with the following program:

Reaction	Temperature	Duration	Cycles
Initial denaturation	94 °C	4 minutes	1
Denaturation	94 °C	30 seconds	34
Annealing	58.6 °C	30 seconds	
Elongation	72 °C	30 seconds	
Final elongation	72 °C	5 minutes	1
Hold	14 °C	-	-

4.7.1.4 Agarose gel electrophoresis

Using 1x TAE buffer, a 1 % (weight/volume) agarose gel was prepared. 1 µl/ml peqGREEN was added, allowing visualization of DNA under UV light. The gel was kept at room temperature (RT) until polymerization. The digested DNA was mixed with 1:6 diluted 6x loading dye. As DNA size marker, a 1 kb DNA ladder was diluted 1:10 with aqua dest. and mixed with 1x loading dye. Subsequently, the gel was loaded with 10 µl of the DNA ladder and 25 µl of digestion products. To separate digested DNA, agarose gel electrophoresis was performed at 100 V and 400 mA for 40 minutes in 1x TAE buffer. Afterwards, the samples were visualized under UV-light and corresponding DNA bands (inserts and vectors) were cut out with a scalpel and purified as described below.

4.7.1.5 Purification of DNA

DNA extracted from 1 % agarose gel was purified according to the manufacturer protocol (QIAquick Spin Handbook: QIAquick Gel Extraction Kit Protocol, QIAGEN, Venlo, The Netherlands). After purification, the DNA was eluted in 30 µl EB-buffer, provided with the kit.

4.7.1.6 Ligation

To insert DNA of interest into the destination expression vector, an overnight ligation was performed. In a total volume of 10 µl, including 1 µl 10x T4 DNA

Ligase Reaction Buffer and 1 ml of T4 DNA Ligase, insert and vector were mixed at a 2:1, 3:1 or 5:1 ratio. The mixture was incubated overnight (16 hours) at 16 °C in a water bath.

The ligation products were immediately used for transformation (4.7.1.7) or stored in the fridge until use.

4.7.1.7 Transformation with chemocompetent bacteria

The E. coli strains XL-1 Blue or JM-109 were used for transformation. Stock solution of bacteria were aliquoted as described earlier (116). 1 µl bacteria stock solution and 100 µg/ml tetracycline for XL-1 Blue or 100 µg/ml ampicillin for JM-109 were added to 3 ml LB (Lysogeny Broth) medium and incubated overnight in a shaking incubator (ORS Aero r, Infors AG) at 250 rpm and 37 °C. Following incubation, the culture was diluted with SOB-medium (Super Optimal Broth-medium) until measured OD_{550} = 0.05. Then bacteria were again incubated at 250 rpm and 37 °C until OD_{550} = 0.5. Afterwards, the bacterial culture was harvested and centrifuged in 50 ml falcon tubes (1363 g, 4 °C, 8 minutes). Bacterial pellet was resuspended in 30 ml Tfb I (Transformation buffer I) and incubated for 50 minutes on ice. Afterwards, the cells were again centrifuged (872 g, 4 °C, 6 minutes) and resuspended in 4 ml Tfb II (Transformation buffer II). The bacteria were aliquoted in 100 µl samples and stored at -80 °C.

For transformation, 10 µl of DNA was incubated with 100 µl of chemocompetent XL-1 Blue or JM-109 bacteria on ice for 30 minutes. After incubation, a heat shock at 42 °C was performed for 90 seconds, to allow the uptake of the DNA plasmids. The cells were then cooled down on ice for 3 minutes and transferred to 15 ml centrifuge tubes. LB medium was added up to a volume of 1 ml and the cells were incubated at 37 °C and 250 rpm for 60 minutes. Finally, the bacteria were plated on LB ampicillin (100 µg/ml) agar plates (800 µl/plate) and incubated overnight at 37 °C.

4.7.1.8 Overnight culture

For bacterial mini-culture, a single colony was selected from the LB ampicillin agar plate and transferred into 15 ml centrifuge tube, containing 3.5 ml LB medium and 100 µg/ml ampicillin. Bacterial mini-cultures incubated overnight at 37°C and 250 rpm for 16 hours. For bacterial maxi-cultures, single colonies picked from

corresponding plates were cultured in 100 ml LB medium with 100 µg/ml ampicillin and incubated for 16 hours at 37 °C and 280 rpm.

4.7.1.9 Plasmid DNA preparation

Miniprep: From the 3.5 ml bacterial mini-culture, 3 ml were used for plasmid DNA preparation. The preparation was done as described in the manufacturer protocol (QIAprep Miniprep Handbook: QIAprep Spin Miniprep Kit, QIAGEN, Venlo, The Netherlands) and DNA was eluted in 50 µl of EB buffer (provided with the kit).

Maxiprep: The 100 ml overnight culture was prepared according to the manufacturer protocol (EndoFree Plasmid Purification Handbook: EndoFree Plasmid Maxi Kit, QIAGEN, Venlo, The Netherlands). The plasmid DNA was eluted in 200 µl endotoxin-free TE buffer (provided with the kit). Then DNA concentration was measured as described below and adjusted to 1 mg/ml by adding the appropriate volume of TE buffer.

4.7.1.10 Measuring DNA concentration

The DNA concentration and purity were quantified by measuring the absorption in ultraviolet-visible spectrophotometry. Therefore, the samples were diluted 1:50 in aqua dest. DNA concentration was determined by measuring the absorption at a wavelength of 260 nm, sample purity was assessed by using the 260 nm:280 nm ratio.

4.7.1.11 Sequencing

To exclude any spontaneous mutations during bacterial DNA replication, the inserted DNA was sequenced. In a mini reaction tube 1 µl ≙ 1 µg of the construct and 1 µl of a specific sequencing primer of the expression vector was added to 3 µl of aqua dest. The sequencing was carried out by GENterprise GENOMICS (StarSEQ GmbH, Mainz, Germany) according to the ‘Homerun’ program. The primers used for each construct are listed in table 5.

4.7.2 Western Blot

For detection of p53 isoform overexpression via western blot (iBlot Dry Blotting System from Thermo Fisher, provided by AG Kühn), proteins were extracted from 5 million T cells. First, T cells were washed two times with PBS and centrifuged at 300 × g. Supernatant was discarded, and cell pellets were frozen at - 20 °C or used

immediately. Western blot was performed with the help of Edite Antunes (lab technician).

Protein extraction: To extract proteins, cell pellets were resuspended in 50 µl lysis buffer (Pepstatin, PMSF 100 mM, Sodium fluoride 1M, Sodium orthovanadate, Leup, 1% Brij 96 V solution) vortexed and incubate on ice for 10 minutes. Vortex and incubation procedure of suspension was repeated for three times and finally centrifuged at 16000 × g and 4 °C for 10 minutes. Supernatant was transferred into new 1.5 ml reaction tubes.

Measurement of protein concentration: Protein concentrations were measured by performing a DC Protein Assay (BioRad) according to the manufacturer's recommendations. Briefly, 1 ml of reagent A and 20 µl of reagent S were mixed and 25 µl of this mixture was pipetted to each well of a flat-bottom 96-well plate. Protein standard (4000 µg/ml) was diluted with lysis buffer at seven different concentrations: 4000, 2000, 1000, 500, 250, 125 and 62.5 µg/ml. Lysis buffer served as blank control. 5 µl of each sample and of each protein standard dilution was added to the wells. Finally, 200 µl of reagent B was added to each well. After 10 minutes of incubation in darkness, protein concentrations were measured at 690 nm.

Western blot: First, gel (Bolt 10 % Bis-Tris Plus, Invitrogen) and chamber were prepared for gel electrophoresis. The chamber was filled with 1x running buffer until it reached the marker and gel cassette was inserted. After removing the gel comb, wells were rinsed with running buffer. Up to 40 µl of each sample was loaded to the corresponding wells. Prior to the loading, protein samples were diluted 1:2 with 1x Laemmli Buffer. For detection of p53 isoforms in transduced T cells, up to 60 µg of protein was used. For detection of p53 isoforms in primary T cells from healthy donors or myeloma patients as much protein as possible was used (see lists below). This mixture was boiled at 95 °C for 5 minutes and shortly centrifuged. 5 µl of Precision Plus Protein WesternC Blotting Standard (Bio-Rad) was used as protein marker. Next, the gel was run at 120 V for 10 minutes and 150 V for approximately 1 hour. Then, the gel was removed from the cassette and the stacking gel was cut out. Protein samples were transferred to a nitrocellulose membrane (iBlot 2 Transfer Stacks) using the iBlot 2 Dry Blotting System (Invitrogen) at 20 V for 7 minutes. Next, the membrane was washed with TBST (Tris-buffered saline with Tween20). After 1 hour incubation in 10 ml TBST + 5 % skim milk, the membrane was washed again three times for 10 minutes in TBST. Primary antibodies (see table 6) dissolved in

TBST + 5 % skim milk were added and incubated overnight at 4 °C. After three additional washing steps, the secondary antibodies (see table 7) were added together with 2 µl of Precision Protein™ StrepTactin-HRP Conjugate (1:5000) and incubated for 1 hour at RT. Finally, the membrane was washed three times in TBST and chemiluminescence was detected with iBright Western Blot Imaging System after 5min incubation with SuperSignal West Femto substrate (ThermoFisher Scientific) and approximately 1 minute exposure time.

Table 6 Primary antibodies used for western blot

Name	Antigen	Clone	Species	Reactivity	Company/Provider	Dilution
KJC12	p53	-	Sheep	Anti-human	Gift from ~~Name~~ (University of Dundee)	1:1000
HR231	p53	HR231	Mouse	Anti-human	Invitrogen, Carlsbad, USA	1:2000
DO-2	p53	sc-53394	Mouse	Anti-human	Santa Cruz Biotechnology, Dallas, USA	1:500
GAPDH	GAPDH	14C10	Rabbit	Anti-human	Cell Signaling Technology, Cambridge United Kingdom	1:2000

Table 7 Secondary antibodies (IgG-HRP conjugates) used for western blot

Clone	Species	Reactivity	Company/Provider	Dilution
sc-2005	Goat	Anti-mouse	Santa Cruz, Biotechnology, Dallas, USA	1:2000
ab7111	Rabbit	Anti-sheep	Abcam, Cambridge United Kingdom	1:5000
#7074	Goat	Anti-rabbit	Cell Signaling Technology, Cambridge United Kingdom	1:2000

4.7.3 qPCR

Extraction of RNA from cell pellets was performed with RNeasy Mini Kit (Qiagen) according to the manufacturer's protocol. RNA was diluted in RNase-free water. Concentration and purity were determined using a Microvolume UV-Vis Spectrophotometer (NanoDrop One, ThermoFischer Scientific).

Reverse Transcription: Complementary DNA (cDNA) was generated from 0.5 µg RNA by reverse transcription using the High-Capacity cDNA Reverse Transcription Kit (ThermoFischer Scientific). Briefly, mix 2 µl 10X RT Buffer, 0.8 µl 25X dNTP Mix (100 nM), 2 µl 10X Random Primers, 1 µl MultiScribe Reverse Transcriptase and 4.7 µl Nuclease-free water in a reaction tube and add 10 µl nuclease-free water containing 0.5 µg RNA. Reverse transcription was performed using the GeneTouch Thermal Cycler (Biozym Scientific GmbH) with the following conditions: 10 minutes at 25 °C, 60 minutes at 37 °C and 5 minutes at 85 °C.

Quantitative real-time PCR: For quantification of cDNA, the PowerUp SYBR Green Master Mix (Applied Biosystems) was used. In each well of a 96-well PCR plate, 1 µl of Forward TIGIT Primer and 1 µl of Reverse TIGIT Primer (see table 5) were mixed with 1 µl cDNA template, 7 µl nuclease-free water and 10 µl of the SYBR Green Master Mix. The same was performed for GAPDH as a reference gene, using 1 µl Forward GAPDH and 1 µl Reverse GAPDH Primers. For each samples duplicates were used as technical replicates. Finally, qPCR was performed using the Standard Curve program from the Quantstudio3 Real-Time-PCR-System (Applied Biosystems) with an annealing temperature of 60 °C.

For determining the fold difference in mRNA expression, the $\Delta\Delta C_t$ method was used according to the manufacturer's protocol (Real-time PCR handbook, Applied Biosystems). Expression levels were normalized to the reference gene GAPDH.

4.7.4 Isolation of peripheral blood mononuclear cells (PBMCs)

Peripheral blood mononuclear cells (PBMCs) were isolated from buffy coats obtained from HLA.A2$^-$ healthy donors and were provided by the Transfusion Center of the University Medical Center Mainz. First, 15 ml Ficoll-Paque (STEMCELL Technologies Inc., Vancouver, Canada) was placed at the bottom of a 50 ml conical tube. The buffy coat was diluted 1:1 with PBS and carefully added on top of the Ficoll-Paque and centrifuged for 10 minutes at 2200 rpm (≙ 700 g) at RT. The PBMCs, located at the

interphase, were harvested and washed three times with PBS. To remove residual erythrocytes, the cells were additionally incubated in 5 ml erythrocyte lysis buffer for 3 minutes at 37 °C. Erythrocyte-free PBMCs were then washed with PBS and either used immediately for retroviral transduction or frozen. To freeze PBMCs, the cells were transferred into fetal calf serum (FCS), containing 10 % Dimethyl sulfoxide (DMSO), at a concentration of 50 million cells/ml. Aliquots of 1 ml per tube were stored at -80 °C for at least 24 hours and subsequently transferred to a liquid nitrogen storage. PBMCs from patients with newly diagnosed multiple myeloma were isolated the same way as healthy donor PBMCs. Patient samples were provided by the III. Medical Department of the University Medical Center Mainz and from the Department of Hematology of the Heidelberg University Hospital (117, 118). Peripheral blood of patients was obtained after informed consent, in accordance with the Declaration of Helsinki and authorization by the Ethical Review Committee of the Ruprecht-Karls-University Heidelberg (approval numbers 837.119.10 (7128) and 2014-003079-40).

4.7.5 Retroviral transduction of freshly isolated human T cells

Delivery of Δ133p53α or p53β DNA, in combination with DNA encoding for a single-chain T cell receptor (scTCR) recognizing HLA.A2-restricted $p53_{264\text{-}272}$ epitope (119), into human T cells was realized by retroviral transduction. As a packaging cell line, Phoenix-AMPHO cells were used. The cells were cultured in T75 flasks (1×10^6 cells/flask) for three days at 37 °C and 5 % CO_2, using Dulbecco's Modified Eagle Medium (DMEM) containing 10 % FCS, 1 % Penicillin/Streptomycin, 1 % L-glutamine and 2.5 % HEPES buffer (DMEM complete). Afterwards, the cells were detached by using Trypsin-EDTA, counted and transferred to 10 cm petri dishes with 1.2×10^6 cells in 8 ml DMEM complete per petri dish. The next day, transfection of the Phoenix-AMPHO cells was prepared by pipetting 35 µl transfection reagent (FuGENE® 6) into a 1.5 ml reaction tube filled with 800 µl of serum free DMEM. This mixture was incubated for 5 minutes at RT, followed by adding 10 µg of the respective plasmid DNA and 5 µg of each helper plasmid (pHIT60 and pColt-Galv (120, 121)). After 15 minutes of incubation at RT, this mixture was dropwise pipetted on the prepared Phoenix-AMPHO cells. Four hours in advance, the medium of the cells was exchanged with 6 ml DMEM complete. The Phoenix-AMPHO cells were then cultured, as described before. To isolate T cells, freshly isolated or frozen

PBCMs from healthy donors (see 4.6.2) were seeded in 24-well plates at a density of 2×10^6 cells/well in 2 ml RPMI 1640 supplemented with 10 % human AB-serum, 1 % Penicillin/Streptomycin, 1 % L-glutamine and 2.5 % HEPES buffer (huRPMI). For T cell stimulation, 30 ng/ml of an anti-CD3 antibody (OKT3) and 600 U/ml of Proleukin (IL-2) were added to the huRPMI. The PBMCs were kept at 37 °C and 5 % CO_2 until the transduction. The transduction of isolated T cells was performed two days after the transfection. Culture medium of the Phoenix-AMPHO cells was replaced with 8 ml fresh huRPMI the day before. This medium was then collected and centrifuged at 2000 rpm (≙ 600 g) for 10 minutes at 32 °C to separate residual detached cells and the retroviral supernatant. Simultaneously, the T cells were collected, and the medium was removed after centrifugation (1500 rpm ≙ 300 g, 5 minutes, RT). Then, 2×10^6 T cells were resuspended in 0.5 ml retroviral supernatant. For co-transductions, 0.25 ml retroviral supernatant of each construct was used for the same number of T cells. To increase transduction efficacy, hexadimethrine bromide (Polybrene) was added at a concentration of 5 µg/ml. The cells were transferred to a 24-well plate (0.5 ml/well) and centrifuged for 90 minutes, at 2000 rpm (≙ 600 g) and 32 °C, without brake. After centrifugation, the cells were stored in an incubator at 37 °C and 5 % CO_2. Finally, the T cells were restimulated (4.6.4) 16 hours after transduction. After selection (4.6.3.1), the transduction efficiency was determined by western blot for the expression of p53 isoforms, and by flow cytometry for the expression of the introduced TCR.

Selection after transduction: To select successfully transduced T cells, pMx vectors, containing a puromycin or neomycin-geniticin selection cassette downstream an internal ribosome entry site (IRES), were used. Neomycin selection was carried out by adding 800 µg/ml geniticin (G418) on the day of the first restimulation. For puromycin selection, 5 µg/ml puromycin was added one day before the second restimulation (= 6 days after transduction).

4.7.6 Restimulation and culture of human T cells

Human T cells were cultured and expanded by stimulation (weekly or twice a week) with either anti-CD3/anti-CD28 microbeads (polyclonal/non-specific) or with peptide-pulsed antigen-presenting cells (antigen-specific).

Polyclonal/non-specific: T cells were collected in conical 50 ml tubes. Before each stimulation, microbeads were magnetically removed. Three minutes of incubation allowed the magnetic microbeads to adhere to the tube wall. For separation, the cells were carefully transferred to a new conical tube, while the beads remained at the wall. After centrifugation at 1500 rpm (≙ 300 g) for 5 minutes, the medium was removed, and the cells were resuspended in fresh huRPMI. For non-specific stimulation, 600 U/ml human IL-2 and 5 µl anti-CD3/anti-CD28 microbeads were added per 1×10^6 T cells.

Antigen-specific: To stimulate T cells via antigen recognition, K562_A2_CD80$^+$ cells served as antigen-presenting cells (APCs). These HLA_A2.1 and CD80 expressing, chronic myelogenous leukaemia derived cells were loaded with 1 µl $p53_{264\text{-}272}$ peptide (stock solution: 10 mg/ml) in 100 µl RPMI 1640 containing 10 % FCS, 1 % Penicillin/Streptomycin and 1 % L-glutamine (RPMI). After incubation for 2 hours at 37 °C and 5 % CO_2, 10 ml medium was added, and cells were irradiated with a dose of 100 Gy. After irradiation, the medium was replaced by fresh huRPMI, adjusting a concentration of 0.3×10^6 cells/ml. Total cell numbers varied, depending on the number of T cells. T cells were collected, and medium was discarded after centrifugation. T cells were resuspended in fresh huRPMI at a concentration of 1×10^6 cells/ml. Finally, 600 U/ml IL-2 and 0.3×10^6 K562_A2_CD80$^+$ cells were added per 1×10^6 T cells.

Non-specific and antigen-specific stimulated T cells were both culture in 24-well plates with 2 ml per well, at a density of 0.5×10^6 cells/ml. The cells were incubated at 37 °C and 5 % CO_2.

4.7.7 Flow cytometry

The flow cytometer FACS Canto II from BD Bioscience was used to analyse and measure the expression of different cell surface markers. For the measurements, the cells were labeled with fluorophore-conjugated antibodies. The cells were transferred to FACS tubes, with 0.2 - 0.4 × 10^6 cells per tube. To wash out residual medium, the cells were centrifuged and the supernatant was discarded. This was repeated two times using PBS. Then, the fluorochrome-coupled antibodies (see table 5 below) were added to the corresponding samples. Before, the cells were resuspended in the remaining PBS (≈ 50 µl). After 15 minutes of incubation in the dark and at RT, the

antibodies were washed out with PBS, which was removed again after centrifugation. For fixation, fresh PBS containing 1 % of paraformaldehyde (PFA) (200 µl/tube) was used to resuspend the cells before the measurement.

Table 8: Antibodies used for flow cytometry

Antigen	Conjugate	Clone	Reactivity	Company	Dilution
CCR7	FITC	3D12	Human	BD Biosciences, Franklin Lakes, USA	1:50
CD3	APC	UCHT1	Human	BD Biosciences, Franklin Lakes, USA	1:50
CD4	FITC	RPA-T4	Human	BD Biosciences, Franklin Lakes, USA	1:50
CD4	APC	RPA-T4	Human	BD Biosciences, Franklin Lakes, USA	1:50
CD8	FITC	HIT8a	Human	BD Biosciences, Franklin Lakes, USA	1:50
CD8	PE-Cy7	RPA-T8	Human	BD Biosciences, Franklin Lakes, USA	1:50
CD8	APC	RPA-T8	Human	BD Biosciences, Franklin Lakes, USA	1:50
CD27	PE	M-T271	Human	BD Biosciences, Franklin Lakes, USA	1:10
CD27	APC	M-T271	Human	BD Biosciences, Franklin Lakes, USA	1:25

CD28	FITC	CD28.2	Human	BD Biosciences, Franklin Lakes, USA	1:50
CD28	PE	CD28.2	Human	BD Biosciences, Franklin Lakes, USA	1:50
CD45RA	PE	HI100	Human	BD Biosciences, Franklin Lakes, USA	1:25
CD45RA	V450	HI100	Human	BD Biosciences, Franklin Lakes, USA	1:50
CD57	APC	NK-1	Human	BD Biosciences, Franklin Lakes, USA	1:50
CD62L	PE-Cy5	DREG56	Human	Beckman Coulter, Brea, USA	1:25
CD107a	PE-Cy5	H4A3	Human	BD Biosciences, Franklin Lakes, USA	1:50
CD155	PE	SKII.4	Human	BD Biosciences, Franklin Lakes, USA	1:50
CD160	PE	BY55	Human	BD Biosciences, Franklin Lakes, USA	1:50
TIGIT	PE	REA1004	Human	Miltenyi Biotec, Bergisch Gladbach, Germany	1:50
TIGIT	APC	REA1004	Human	Miltenyi Biotec, Bergisch Gladbach,	1:50

				Germany	
PD-1	FITC	MIH4	Human	BD Biosciences, Franklin Lakes, USA	1:50
PD-1	APC	EH12.2.H7	Human	BD Biosciences, Franklin Lakes, USA	1:50
PD-L1	APC	MIH1	Human	BD Biosciences, Franklin Lakes, USA	1:50
Vβ3	PE	REA646	Mouse	Miltenyi Biotec, Bergisch Gladbach, Germany	1:50
Beta Mark TCR Vbeta Repertoire Kit	FITC and PE	For complete list see supplier's homepage (Product No: IM3497)	Human	Beckman Coulter, Brea, USA	1:50

4.7.8 CFSE Proliferation Assay

For monitoring T cell proliferation *in vitro*, carboxyfluorescein succinimidyl ester (CFSE) dye was used. The fluorescent CFSE dye can penetrate the cell membrane and binds covalently to intracellular molecules. With each cell division CFSE fluorescence is equally distributed in daughter cells, which allows differentiation between the generations of T cells by flow cytometric analysis.

T cells were collected, washed two times with 5 ml PBS by centrifugation and resuspended in 450 µl PBS. CFSE stock solution (10 mM) was diluted 1:200 with PBS to get a working solution of 50 µM. T cells were labeled with 50 µl of 50 µM CFSE solution for 5 minutes at RT. Then, 5 ml PBS 5 % Bovine serum albumin (BSA) was added, and the cells were centrifuged and washed again two times with 5 ml PBS. A fraction of T cells was immediately used to measure the initial

fluorescence intensity at “day 0” using the flow cytometer FACS Canto II (BD Biosciences). The rest of the cells was restimulated as described in 4.6.4. At different time points e.g., 3, 5 and 7 days after restimulation, the cells were washed two times with PBS and analysed by flow cytometry and compared to the initial measurement (day 0).

4.7.9 Cell counting and Population Doubling Levels

At the day of restimulation, the number of viable cells was determined by trypan blue exclusion test. Briefly, 50 µl of the cell suspension was mixed with 50 µl trypan blue to exclude dead cells, and the cells were transferred to a counting chamber and counted under the microscope. Population doubling levels (PDLs) were calculated with the following formula:

$$\frac{\log_{10}(\text{number of cells after expansion}) - \log_{10}(\text{number of cells seeded})}{\log_{10}(2)}$$

Cumulative population doubling levels were obtained by adding the values from each round of stimulation.

4.7.10 Magnetic cell separation

T cells were divided into $CD4^+$ and $CD8^+$ or $TIGIT^{high}$ and $TIGIT^{low}$ populations by magnetic cell separation. For CD4/CD8 separation, T cells were labelled with CD4 or CD8 MicroBeads and selected according to manufacturer’s protocol. Shortly, T cells were suspended in 5 ml MACS buffer and centrifuged at 300 × g for 5 minutes. This washing procedure was performed two times. Afterwards, supernatant was discarded, and T cells were resuspended in 80 µl MACS buffer per 10^7 cells. 20 µl of CD4 or CD8 MicroBeads were added to 80 µl MACS buffer and incubated at 4 °C for 15 minutes. For TIGIT separation, T cells were first labelled with anti-TIGIT mAb for 15 minutes and secondly with anti-PE MicroBeads for 30 minutes at 4 °C. Then, cells were washed again by adding 5 ml MACS buffer. After centrifugation, supernatant was discarded, and labelled T cells were resuspended in 500 µl MACS buffer. LS columns were placed in a MidiMACS separator and washed one time with 2 ml

MACS buffer. MACS buffer including T cells were then applied to the column. Unlabeled cells passing the filter were collected in a 50 ml tube. After three washing steps with 3 × 3 ml MACS buffer, columns were removed from the separator, placed into a 15 ml tube and filled with 5 ml MACS buffer. Labeled cells were then removed by pushing the plunger into the column.

4.7.11 Chromium-51 release assay

Short-term killing capacity of T cells was determined by chromium release assays (38). T cells equipped with the p53 scTCR were co-cultured with the SAOS 2/143 target tumor cells at 37 °C and 5 % CO_2 at different effector:target (E:T) ratios. For E:T = 1:1, 0.5×10^6 tumor and T cells were plated in 200 µl huRPMI. Before co-culture, tumor cells were labeled with 100 µCi radioactive sodium ^{51}chromate ($Na_2{}^{51}CrO_4$) for 90 minutes at 37 °C. Then tumor cells were washed two times with huRPMI and added to the T cells. After five hours of co-culture, lysis of target cells was quantified by measuring the ^{51}chromium release in 100 µl supernatant using a gamma counter. Maximum release was examined by measuring gamma rays from medium with labeled tumor cells. Spontaneous lysis was assessed by using supernatant from tumor cells without T cell co-culture. Supernatant was harvested after 10 minutes of centrifugation at 368 g.

The following formula was used to determine specific lysis of T cells in percent:

$$\frac{\text{experimental chromium release} - \text{spontaneous chromium release}}{\text{maximum chromium release} - \text{spontaneous chromium release}} \times 100 = \text{specific lysis}\ (\%)$$

4.7.12 Long-term colony-forming assay

To examine the long-term killing capacity of TCR-engineered T cells, T cells were co-cultured with their target cells (SAOS 2/143) for at least 24 hours and the target cell viability was determined by a staining with crystal violet dye and expressed in percent.

4.7.12.1 Co-culture of human T cells and tumor cells

SAOS 2/143 cells were transferred to 6- or 12-well plates, seeding 0.1 – 0.3 × 10^6 cells per well, suspended in 0.5 or 1 ml medium (RPMI). After the cells attached to the plate (latest after 24 h), the medium was removed and T cells in fresh huRPMI

were added at an E:T ratio of 1:1. For 24 hours, the co-culture was incubated at 37 °C and 5 % CO_2. Additionally, T cells were co-incubated with SAOS-2 null cells as negative controls. If all target tumor cells were killed within 24 hours, the T cells were transferred to another well with freshly seeded target cells for a second round. After co-culturing the cells, the medium including T cells and dead target cells was removed and the wells were washed carefully with 1 ml PBS. The remaining adherent/live target cells were fixed by adding 1 ml of 4 % PBS/PFA for 10 minutes at RT and counterstained with a crystal violet dye (see below). The PBS/PFA was removed, and the wells were washed again with 1 ml PBS. For blocking CD155/TIGIT interaction, an unlabeled, monoclonal anti-TIGIT antibody (blocking-antibody) was used with a dilution of 1:500 (MBSA43, eBioscience, San Diego, USA). For co-culture experiments, the antibody was added together with the effector T cells.

4.7.12.2 Crystal violet assay

To visualize the remaining viable target cells, 600 µl of 1 % crystal violet dye was added to each well. After 15 minutes of incubation at RT, the dye was removed, followed by another washing step with 1 ml PBS. The staining results were documented by scanning the plates. For quantification, the incorporated dye was dissolved by adding 400 µl of 5 % PBS/SDS. After 5 minutes, the recovered dye was transferred to a 96-well flat-bottom plate, using 200 µl per well using technical duplicates. To determine the optical density, the absorbance was measured at 570 nm by an ELISA reader. Blank wells contained 200 µl 5 % PBS/SDS.

4.7.13 Co-culture in Transwell-system

To test the effects of supernatant from target tumor cells on the T cell population, T cells were seeded in a 24-well plate with 1×10^6 cells/ml in 1 ml per well. Tumor cells 1×10^6 cells/ml were seeded in 0.3 ml in a transwell insert. The transwell insert was transferred to the 24-well plate containing T cells and incubated at 37 °C for 24 hours.

4.7.14 Multiplex Immunoassay

The cytokine production of the modified human T cells was analysed by performing Luminex Multiplex Assays. T cells and target cells were co-cultured in 12-well plates

for 24 or 48 hours as describe in 4.7.12.1. Cytokine concentrations were measured in the culture medium using Human Cytokine & Chemokine Panel 1A (34 plex) kit (eBioscience, San Diego, USA) according to the manufacturer protocol and with the help of AG Bosmann from the Center for Thrombosis and Hemostasis (CTH) Mainz.

4.7.15 Degranulation assay

As an important T cell function, the capacity of T cells to secrete major effector molecules like perforin and granzymes was determined by degranulation assays. These molecules are stored in cytoplasmic vesicles, the so-called granules. The lysosomal-associated membrane protein 1 (LAMP1/CD107a) is found on the membranes of these granules and can be detected on the cell surface of T cells upon degranulation. Thus, LAMP1 expression was used as a marker of degranulation and was analyzed by flow cytometry. First, 0.5×10^6 T cells were collected and washed two times with PBS. After centrifugation, supernatant was discarded and 5 µl of anti-CD107a antibody was added for 15 minutes. Then, 500 µl of huRPMI was added to the cells containing 1X Monensin (2 µM) and either phorbol 12-myristate 13-acetate (PMA) + Ionomycin or 0.5×10^6 SAOS 2/143 tumor cells. Medium alone served as a negative control. As a resting condition, T cells were used seven days after restimulation. Stimulation with PMA + Ionomycin was used as a positive control. After 12 – 24 hours, T cells were washed two times with PBS and CD107a expression was measured by flow cytometry.

4.7.16 Murine xenograft model

All mice procedures were performed according to the German federal and state regulations and approved by the responsible national authority (National Investigation Office Rhineland-Palatinate, Approval ID: 23 177-07/G16-1-016). Immunodeficient NOD.Cg-Prkdc^{scid}IL2rg^{tm1Wjl}/SzJ (NSG) mice were used to engraft human cells including the human osteosarcoma cell line SAOS 2/143 and T cells. Mice were obtained from the central animal facility of the Johannes Gutenberg University Mainz, Germany. Mice were kept according to the guidelines for animal care of the Johannes Gutenberg University Mainz and treated as described previously (116, 119). All animal experiments were performed by or under active supervision from Edite Antunes (Lab Technician) or Hakim Echchannaoui (Principal Investigator).

To test adoptive T cell transfer *in vivo*, 3 × 10^6 target tumor cells were injected subcutaneously in the left flank on day 0. One mouse from the control group (without TCR^+ T cells) showed engraftment failure and was omitted from the experiment. The transfer of T cells was performed on day 7, by injecting 5 × 10^6 $CD3^+V\beta3^+$ T cells co-expressing a specific p53 isoform suspended in 200 µl PBS intravenously. For transduction of T cells, different retroviral expression vectors for the p53 scTCR and Δ133p53α isoform were tested. As puromycin was more efficient than neomycin selection, we decided to only use vectors including puromycin resistance cassette for Δ133p53α in order to ensure its sufficient expression. For p53 scTCR, vectors without any selection or with neomycin selection were used. After T cell transfer IL-2 was administered intraperitoneally at the same day. Tumor volume was measured with a digital caliper twice a week. Tumor volume was calculated by the following formula: length × $width^2$. Mice were sacrificed when the tumor volume reached 1 cm^3. T cells isolated from freshly extracted spleens and tumors (for TILs) were analyzed by flow cytometry. Serum was obtained from the peripheral blood at the indicated time after T cell transfer.

4.7.17 Software and programs

DNA sequencing results were verified with FinchTV Windows Version 1.4.0 (Geospiza Inc.). Flow cytometric data was analyzed with FlowJo_V10 Windows software (Tree Star). Metabolic flux experiments were designed and analyzed with the Seahorse Wave Desktop software, Windows Version V2.6.3.5 (Agilent). Graphs and statistics were generated with the GraphPad Prism, Windows version 6.07 (Dotmatics).

4.7.18 Statistical analysis

Statistical analysis of differences between groups was determined by two-tailed Student's *t* test. Normal (Gaussian) distribution was tested with D'Agostino & Pearson normality test. For multiple testing, ANOVA was performed followed by Tukey's multiple comparison test, adjusted p values are reported there. For mouse studies, Log-rank (Mantel-Cox) test was used to compare survival curves from three different groups. All tests were computed using GraphPad Prism 6.07. If not

otherwise indicated significance level were defined as: $p<0.05$ (*), $p<0.01$ (**), $p<0.001$ (***).

5 Results

5.1 Overexpression of p53β and Δ133p53α in human antigen-specific T cells

It has been shown that changes in expression of p53β and Δ133p53α are associated with senescence in $CD8^+$ T cells (9), however the role of p53 isoforms in tumor antigen-specific T cells is still unexplored. To investigate the effects of p53 isoforms on effector functions of antigen-specific T cells, human T cells were equipped with a tumor antigen-specific TCR (TCR). The applied TCR is an optimized single-chain TCR specific for the HLA-A2.1-restricted (non-mutated) p53 (264-272) peptide (119). T cells were isolated from the peripheral blood of healthy $HLA.A2^-$ donors and retrovirally co-transduced with vectors encoding the TCR and p53β or Δ133p53α. As retroviral vectors included antibiotic resistance genes, successfully transduced T cells were selected by neomycin and puromycin treatment. Additionally, the overexpression of the respective isoform was confirmed by western blot (Figure 5). Expected protein size for p53β is 46 kDa and 35 kDa for Δ133p53α (103).

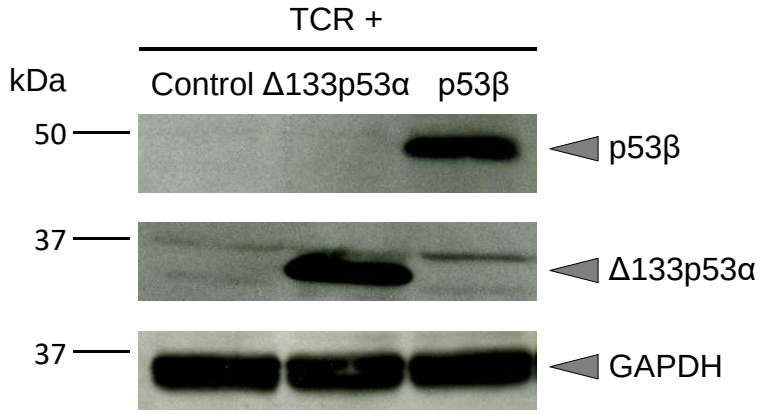

Figure 5: Overexpression of p53β and Δ133p53α in human antigen-specific T cells
Representative section of a western blot showing protein expression of p53β and Δ133p53α in retrovirally transduced bulk T cells. The housekeeping protein GAPDH served as loading control.

5.1.1 Overexpression of p53β facilitates the onset of premature senescence

To characterize first the phenotype of transduced cells, the expression of several cell surface markers was determined by flow cytometry. First, T cells were genetically modified with a TCR and the p53β isoform. As many surface molecules are differently expressed in $CD4^+$ and $CD8^+$ T cells, the CD4/CD8 ratio was examined shortly after transduction. Despite differences in individual donors, the overexpression of the

senescence-associated p53β did not modify the frequency of $CD4^+$ (p=0.3136) nor $CD8^+$ (p=0.299) T cells (Figure 6).

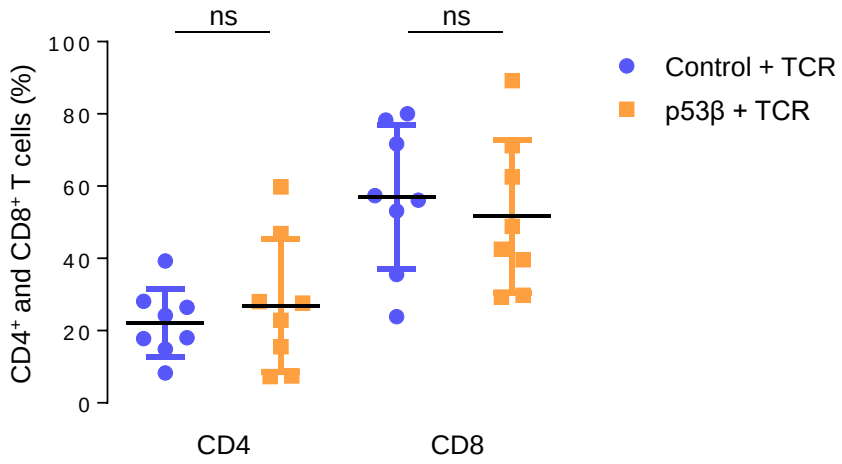

Figure 6: CD4/CD8 ratio is not altered by p53β overexpression
Fraction of $CD4^+$ and $CD8^+$ T cells early after transduction with p53β or empty control vector. The percentage of CD8 vs. CD4 subsets after transduction was analyzed by flow cytometry between day 3 and 6 after stimulation. Plots show mean and standard deviation from n=8 individual donors. *p < 0.05, **p < 0.01, ***p < 0.001, ns (not significant).

Surface expression of the co-stimulatory CD28 and the senescence-associated CD57 molecule can be used to differentiate between 'naïve'-like ($CD28^+CD57^-$) and late differentiated/'senescent' ($CD28^-CD57^+$) T cells (9). Early after transduction, T cells were co-stained for CD8, CD28 and CD57 for flow cytometric analysis. Overexpression of p53β in $CD8^+$ T cells leads to a slight reduction in 'naïve'-like $CD28^+CD57^-$ cells (mean control: 40.71 % vs. mean p53β: 35.93 %, p=0.0447, Figure 7, A). These results suggest that p53β induces a more differentiated cellular phenotype. Concomitantly, the number of senescent $CD28^-CD57^+$ cells was slightly increased in most donors (mean control 14.73 % vs. mean p53β: 17.67 %), however, it did not reach statistical significance (p=0.0841, Figure 7, B).

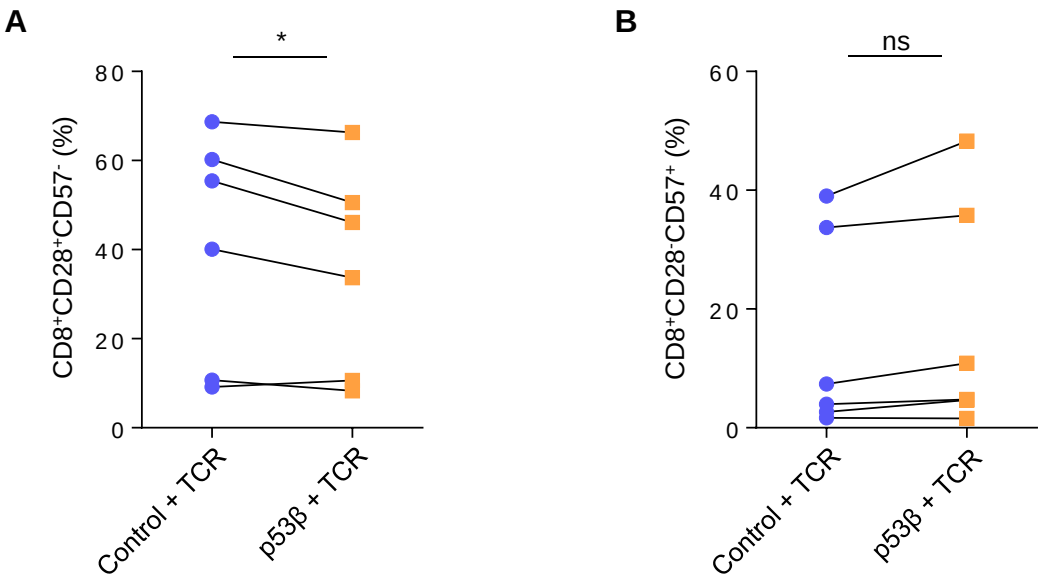

Figure 7: T cells overexpressing p53β reveal changes in cellular phenotype
Flow cytometric measurement of CD28 and CD57 expression on $CD8^+$ T cells shortly after transduction (week 2-3, day 3 or 4 after restimulation). Plots show the frequencies of (**A**) $CD28^+CD57^-$ and (**B**) $CD28^-CD57^+$ subsets in p53β-transduced and control T cells from n=6 individual donors (paired samples). *$p < 0.05$, **$p < 0.01$, ***$p < 0.001$, ns (not significant).

Naïve T cells have in general a high proliferative capacity while senescent cells exhibit cell cycle arrest. The decreased frequency of $CD28^+/CD57^-$ T cells in p53β-transduced cells therefore suggested a decline in the proliferative potential. To assess the proliferative capacity of transduced T cells, population doubling levels (PDL) were calculated based on the cell numbers counted on the day of restimulation. Stimulation was repeated every 7 days (+/- 1 day) with anti-CD3/anti-CD28 beads until proliferation began to decrease. Then, T cells were stimulated peptide specific by co-culture with $p53_{264\text{-}272}$ peptide-pulsed $K562\_A2\_CD80^+$. As indicated by the cumulative PDL values, p53β-modified T cells stopped proliferating during *in vitro* culture earlier than control cells. In the donor presented in Figure 8, p53β-transduced T cells reached cell cycle arrest between week 12 and 13, while control cells kept proliferating until week 18 (Figure 8). The maximum PDL in the representative donor was equivalently higher in control cells: 16.38 (control) vs. 7.96 (p53β, Figure 8).

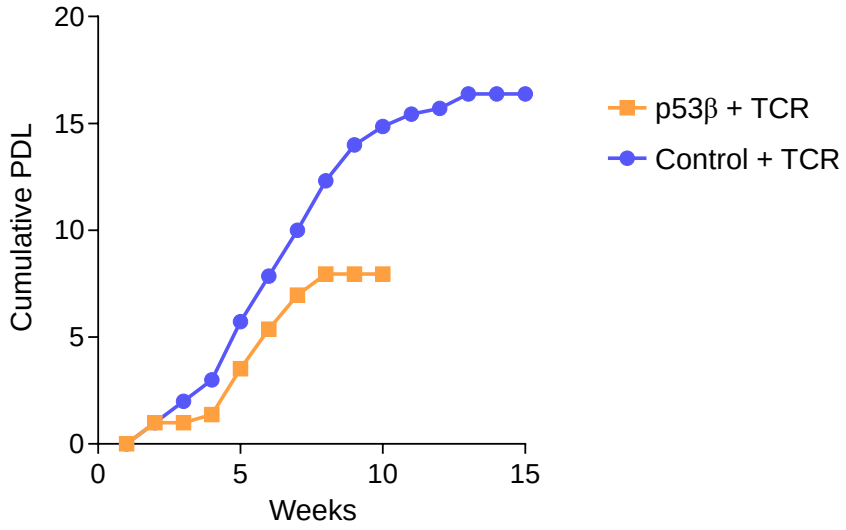

Figure 8: p53β-overexpressing cells undergo rapid proliferation arrest
Cumulative population doubling levels (PDL) of p53β-transduced and control cells as a function of time during *in vitro* cell culture. Representative data from one donor of n≥3 biological replicates.

5.1.2 Δ133p53α-overexpression promotes features of naïve T cells

In order to prevent or delay the onset of senescence in T cells, we transduced cells with a vector encoding for Δ133p53α. The ratio of CD4 and CD8 T cells was determined to exclude differences based on an imbalance of $CD4^+$ and $CD8^+$ T cells. Although, values differed between individual donors, the overall CD4/CD8 ratios remained unchanged ($CD4^+$ T cells p=0.1181, $CD8^+$ T cells p=0.7208, Figure 9). These results indicate that Δ133p53α-overexpression did not favor the expansion of CD4 or CD8 T cells.

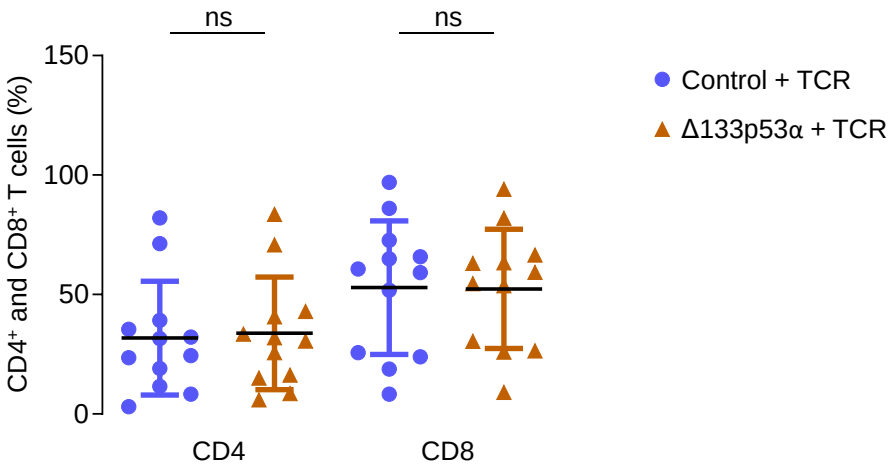

Figure 9: CD4/CD8 ratio is not affected by Δ133p53α overexpression
Plots demonstrating the frequencies and mean with standard deviation of $CD4^+$ and $CD8^+$ T cells in Δ133p53α-modified and control cells of n=12 individual donors. Analysis of CD4 and CD8 expression

was performed within the first 3 weeks after isolation between day 3 and 5 after restimulation. *$p < 0.05$, **$p < 0.01$, ***$p < 0.001$, ns (not significant).

Next, the cell surface expression of differentiation markers CD28 and CD57 were analyzed early after transduction. In contrast to p53β-transduced cells, overexpression of Δ133p53α resulted in a slight increase of $CD8^+CD28^+CD57^-$ "naïve-like" T cells (mean: 34.2 %) compared to empty vector transduced control T cells (mean: 30.13 %, p=0.0096). The subset of $CD8^+CD28^-CD57^+$ T cells was conversely reduced in Δ133p53α-modified cells (mean Δ133p53α: 12.41 % vs. mean control: 14.56 %, p=0.0108, Figure 10).

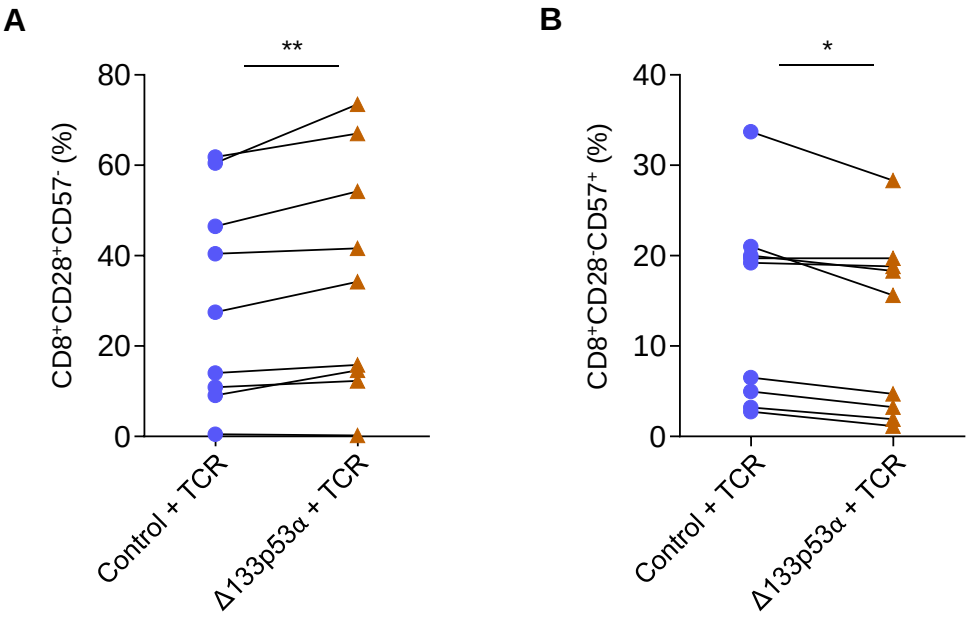

Figure 10: Δ133p53α overexpression is associated with an increase in 'naïve' $CD8^+CD28^+CD57^-$ T cells

Paired samples of Δ133p53α-transduced and control $CD8^+$ T cells showing the frequencies of (**A**) $CD28^+CD57^-$ and (**B**) $CD28^-CD57^+$ subsets. Surface expression was measured by flow cytometry within 5 weeks after transduction, between day 1 and 5 after restimulation. *$p < 0.05$, **$p < 0.01$, ***$p < 0.001$, ns (not significant).

To confirm the increase of less differentiated T cells after transduction with Δ133p53α, expression of the co-stimulatory receptor CD27 and the homing receptors CD62L and CCR7 were determined. These receptors are mainly expressed in naïve and central memory T cells (122). After transduction with Δ133p53α, CD27 was slightly but statistical significantly upregulated in $CD8^+$ T cells (mean control: 52.97 % vs. mean Δ133p53α: 57.54 %, p=0.0457). Additionally, the number of $CD62L^+CCR7^+$ double positive T cells also increased (mean control: 7.24 % vs. mean Δ133p53α: 10.55 %, p=0.0103, Figure 11).

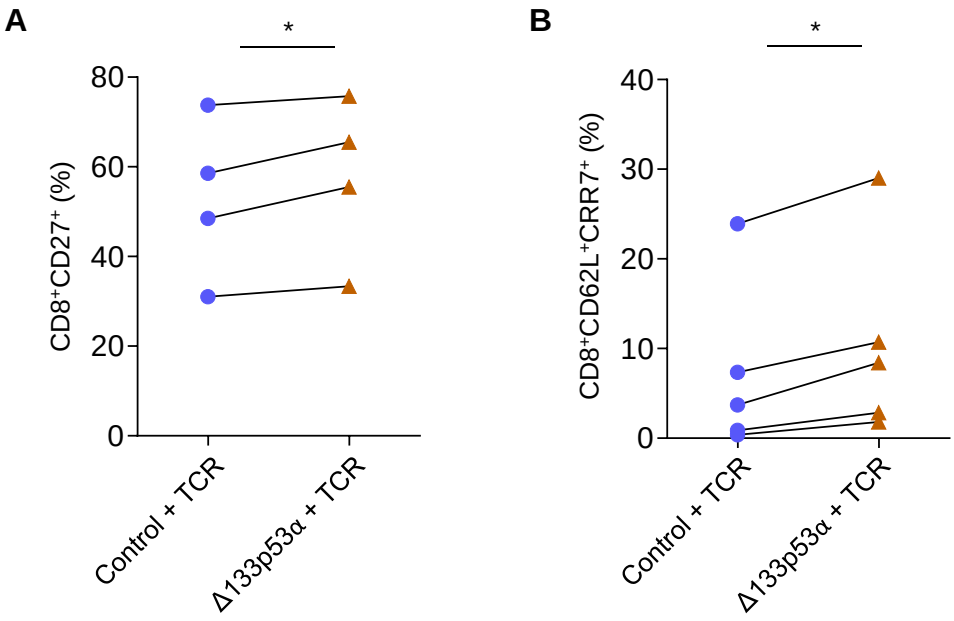

Figure 11: Upregulation of cell surface receptors CD27, CD62L and CCR7 in CD8⁺ Δ133p53α-modified T cells
Frequencies of (**A**) $CD27^+$ and (**B**) $CD62L^+CCR7^+$ in $CD8^+$ T cells early after transduction with Δ133p53α compared to control T cells. Expression was measured by flow cytometry. Graphs show different donors as paired samples (n=4 and 5 biological replicates). **p* < 0.05, ***p* < 0.01, ****p* < 0.001, ns (not significant).

Despite the increased number of less differentiated T cells, no significant differences in proliferation were observed during the early phase of *in vitro* culture. However, after several rounds of restimulation (as performed with p53β-transduced T cells, compare Figure 8), proliferation of control cells declined (around week 10 for representative donor shown in Figure 12) until the cells reached a complete cell cycle arrest (around week 12, Figure 12). In contrast, Δ133p53α-transduced T cells remained proliferative until week 14 (Figure 12) and reached higher PDL values (maximum PDL of control T cells: 21.07 vs. Δ133p53α-transduced T cells: 26.68, representative donor, Figure 12). After several weeks of *in vitro* culture, the higher cellular division observed in Δ133p53α-transduced T cells was confirmed by CFSE-labeling (a fluorescent dye). The decline of fluorescence was measured by flow cytometry at different time points (Figure 12). Importantly, the increased proliferative potential of Δ133p53α-overexpressing cells was not associated with infinite replication and cells ultimately reached cell cycle arrest.

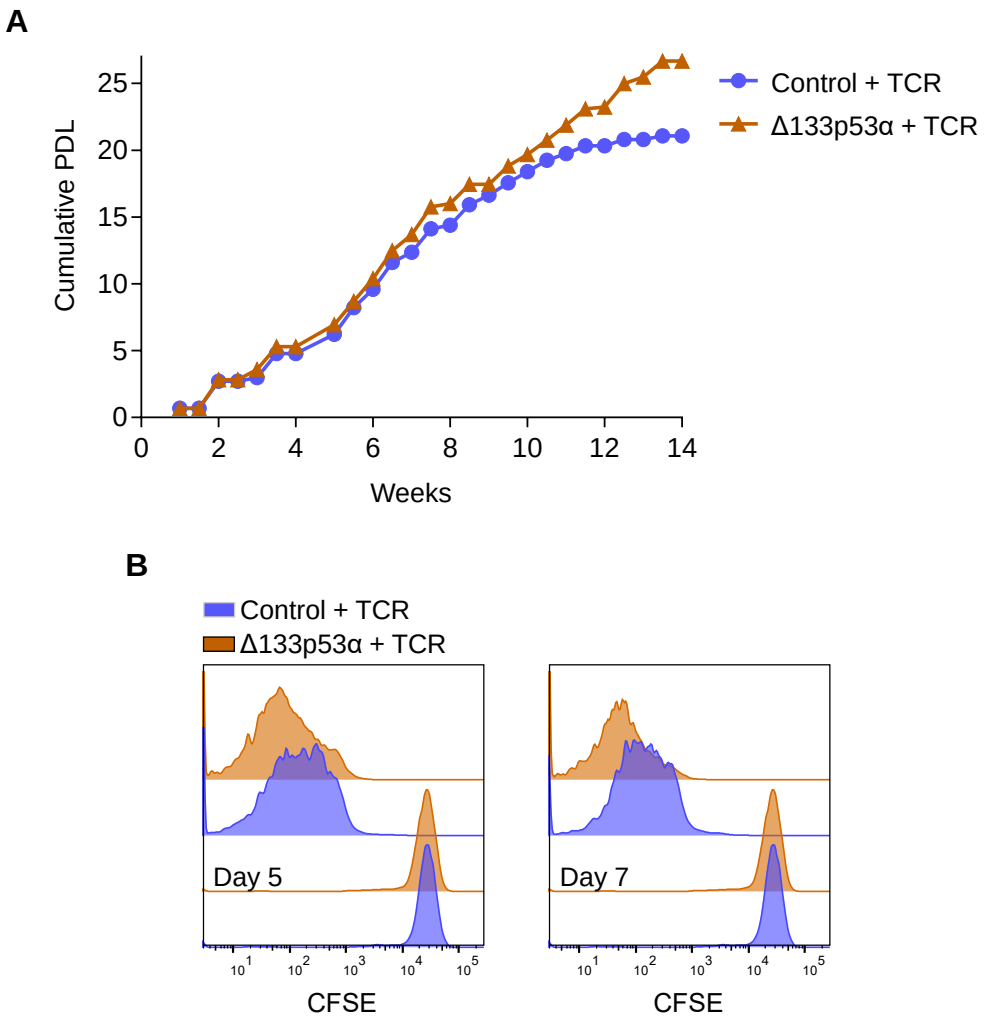

Figure 12: Δ133p53α overexpression promotes long-term proliferative capacity of T cells
(**A**) Cumulative PDL from Δ133p53α-transduced and control cells over time (representative of n=9 biological replicates). (**B**) Representative CFSE Proliferation Assay after repetitive stimulations. Δ133p53α and control T cells were labeled with CFSE at day 0. Proliferation-dependent reduction of CFSE signals were measured by flow cytometry at day 5 and 7 (n=3 biological replicates).

5.1.3 Overexpression of p53 isoforms affects anti-tumor responses in antigen-specific T cells

In addition to the modulation of differentiation markers and proliferation, potential effects of p53 isoform overexpression on anti-tumor responses were tested. Therefore, long-term tumor colony-forming assays were performed. The osteosarcoma cell line SAOS 2/143 was used as target cells. These tumor cells express the tumor-associated antigen $p53_{264\text{-}272}$ which is recognized by the provided specific scTCR. Prior to the assay, scTCR expression levels of transduced T cells were determined by flow cytometry to exclude potential differences. Usually, p53β-, as well as Δ133p53α-modified T cells showed similar TCR expression levels

compared to control cells (> 95 % scTCR expression in all groups, Figure 13, A and B).

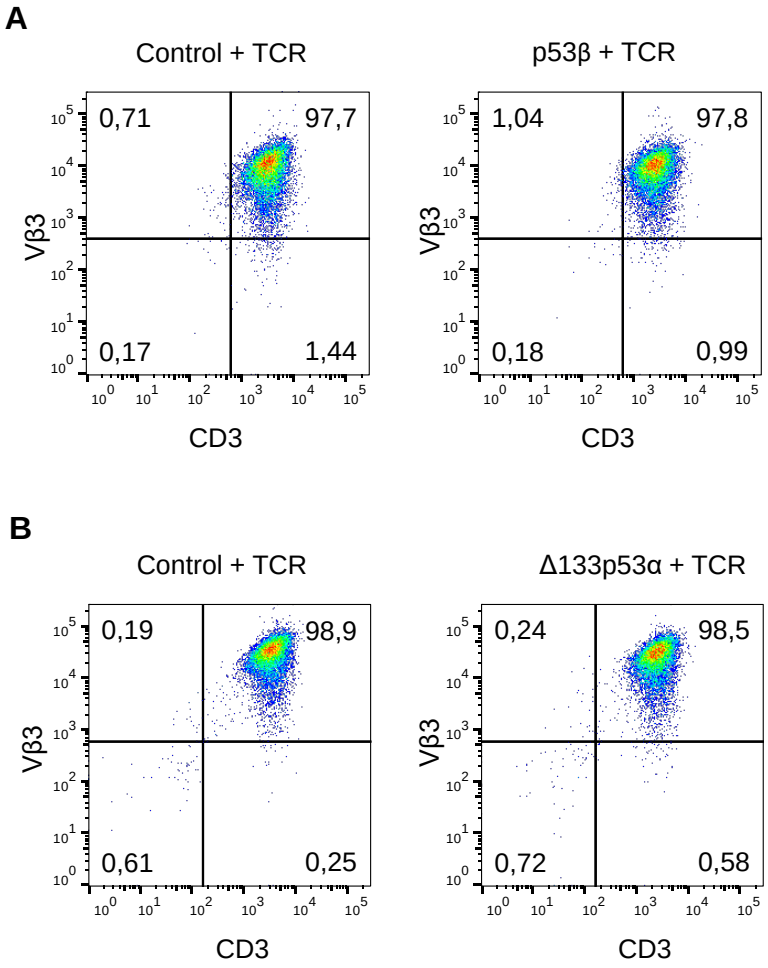

Figure 13: TCR expression of p53β-, Δ133p53α-transduced and corresponding control cells
Representative flow cytometric measurements of CD3 and TCR Vβ3 surface expression after antigen-specific stimulation of two independent experiments. (**A**) T cells transduced with p53β compared to control T cells. (**B**) Δ133p53α-overexpressing T cells and control T cells. Staining for the variable TCRβ3 (Vβ3) subfamily is used as direct measurement of the scTCR expression.

Tumor cells were seeded and co-cultured with T cells over 24 hours with an E:T ratio of 1:1. Remaining viable tumor cells (after washing out T cells and lysed tumor cells) were visualized by crystal violet staining. The optical density of crystal violet dye taken up by living tumor cells was measured to quantify the cytolytic activity of T cells. Early after transduction, T cells overexpressing p53β exhibited an impaired anti-tumor response (59.79 % viability of tumor cells) compared to control cells (7.77 % viability of tumor cells, Figure 14, A). The same experiments were performed for Δ133p53α-transduced T cells at later time points of *in vitro* culture when proliferation of control cells declined. Here an impaired lysis of tumor cells was

observed in the control T cell group (tumor cell viability: 39.73 %, Figure 14 B). In contrast, Δ133p53α-transduced T cells still efficiently eradicated the target tumor cells (tumor cell viability: 7.74 %, Figure 14, B).

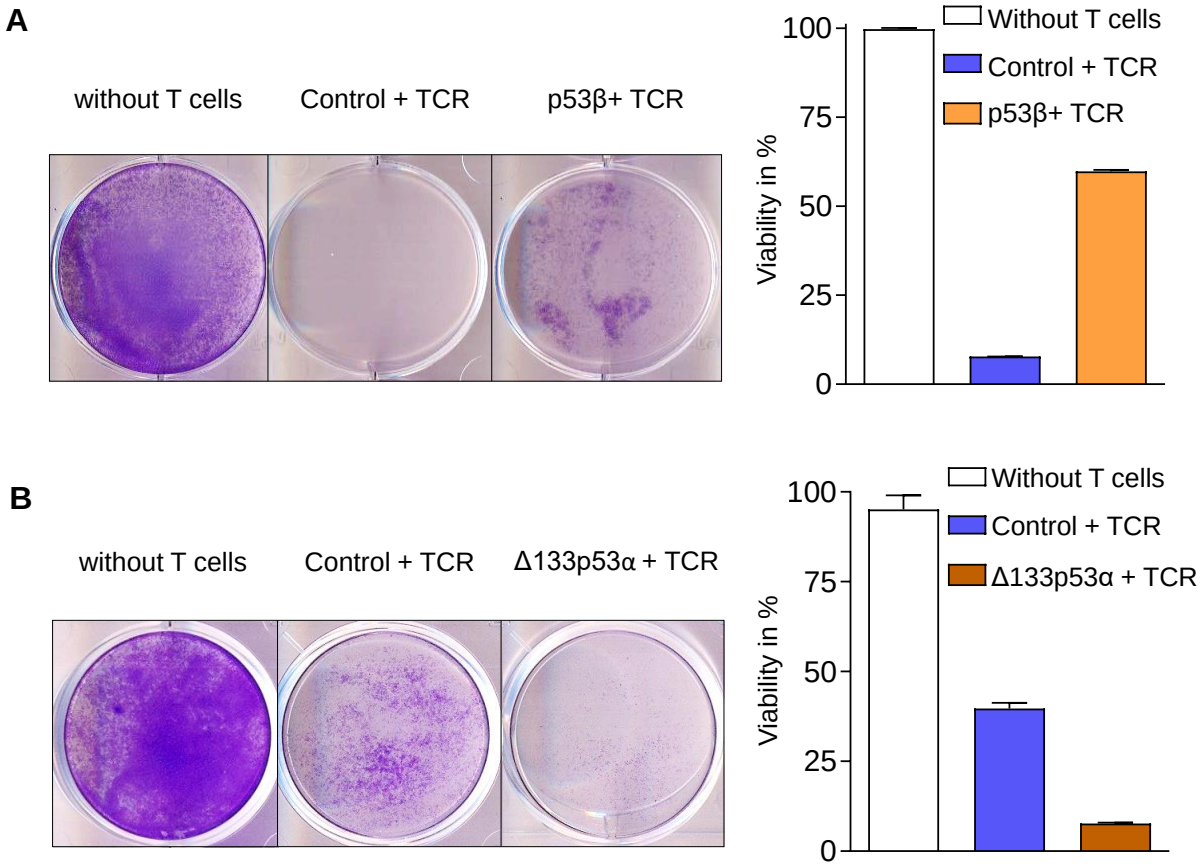

Figure 14: Overexpression of p53 isoforms affects anti-tumor responses in antigen-specific T cells *in vitro*
Tumor colony-forming assay over 24h and quantified data from crystal violet assays of (**A**) p53β-transduced T cells compared to control cells (representative example of n≥3 biological replicates), as well as (**B**) Δ133p53α-transduced T cells compared to control cells (representative example of n≥3 biological replicates). The latter was performed at late phase of *in vitro* culture. SAOS 2/143 served as target tumor cells. Y-axis indicates the viability of tumor cells in percent. Viability of tumor cells was determined by measuring optical density of crystal violet dye taken up by remaining tumor cells. Normalization was performed using values from tumor cells alone.

5.2 Δ133p53α preserves T cell effector functions

The enhanced anti-tumor response of Δ133p53α-modified T cells may offer new approaches to improve T cell-based immunotherapies. Therefore, the effect of Δ133p53α overexpression in $CD8^+$ T cells was further investigated. First, the phenotype of transduced T cells was characterized in more details. As Δ133p53α was associated with a higher frequency of less differentiated $CD28^+CD57^-$ cells, with increased expression of CD27, CD62L and CCR7, other cell surface molecules were

analyzed. In particular, immune checkpoints, such as PD-1 and TIGIT, which function as key inhibitory receptors and critical regulators of T cell immune response (123). These inhibitory receptors are associated with late-stage differentiation and impaired cytotoxicity. Among these molecules TIGIT (mean: 39.95 % vs. 34.62 %, p=0.0164) and CD160 (mean: 16.64 % vs. 13.80 %, p=0.0431) were slightly downregulated in Δ133p53α-modified CD8$^+$ cells (Figure 15, A and C). PD-1 also showed a moderate reduction, however differences did not reach statistical significance (mean: 16.01 % vs. 12.05 %, p=0.1168, Figure 15, B).

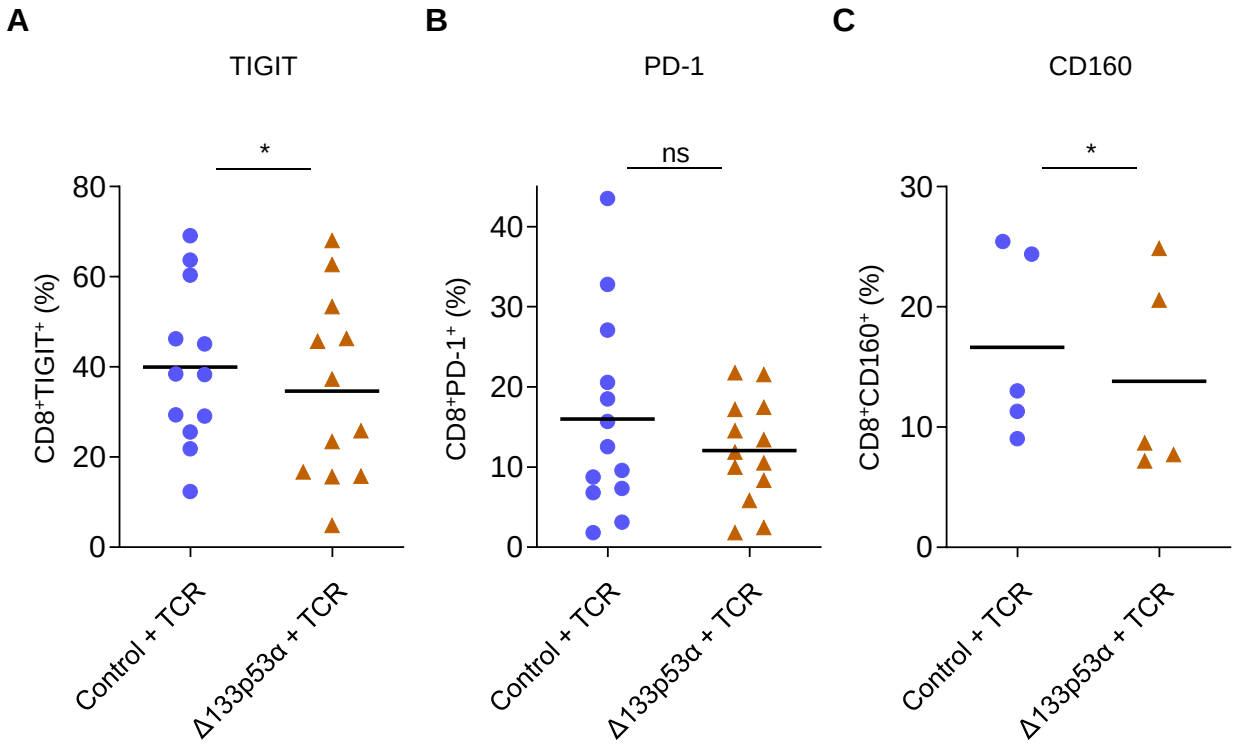

Figure 15: Δ133p53α overexpression leads to reduced surface expression of inhibitory receptors in CD8$^+$ T cells
Scatter blots showing single measurements and mean of surface expression for (**A**) TIGIT, (**B**) PD-1 and (**C**) CD160 in CD8$^+$ T cells. Expression was analyzed by flow cytometry at different time points of *in vitro* culture (between day 3 and 5 after restimulation). Samples include n=12, n=13 and n=5 individual donors. *p < 0.05, **p < 0.01, ***p < 0.001, ns (not significant).

Along with an impaired cytotoxicity, T cells might show differences in other important effector functions, such as secretion of cytokines and cytolytic granules. At advanced time points of *in vitro* culture when control T cells showed reduced anti-tumor responses, the secretion of important cytokines was examined under resting conditions (without antigen stimulation), as well as after antigen-specific stimulation with target tumor cells. After stimulation, Δ133p53α-modified T cells secreted higher amounts of cytokines like IFN-γ, TNF-α and GM-CSF compared to control T cells

(Figure 16, A). Under the same conditions, the secretion of lytic molecules like perforin and granzyme B by degranulation was examined. The granule membrane located molecule LAMP-1 (CD107a) is exposed to the cell surface of T cells upon degranulation. Therefore, the analysis of CD107a is an indirect measure of cytotoxicity. Compared to control cells, Δ133p53α-transduced cells reached higher levels of LAMP-1 expression in terms of geometric mean fluorescence intensity (gMFI) (332 vs. 522) and percent of CD107a^{+} T cells (33.6 % vs. 54.3 %) after antigen-specific stimulation (Figure 16, B).

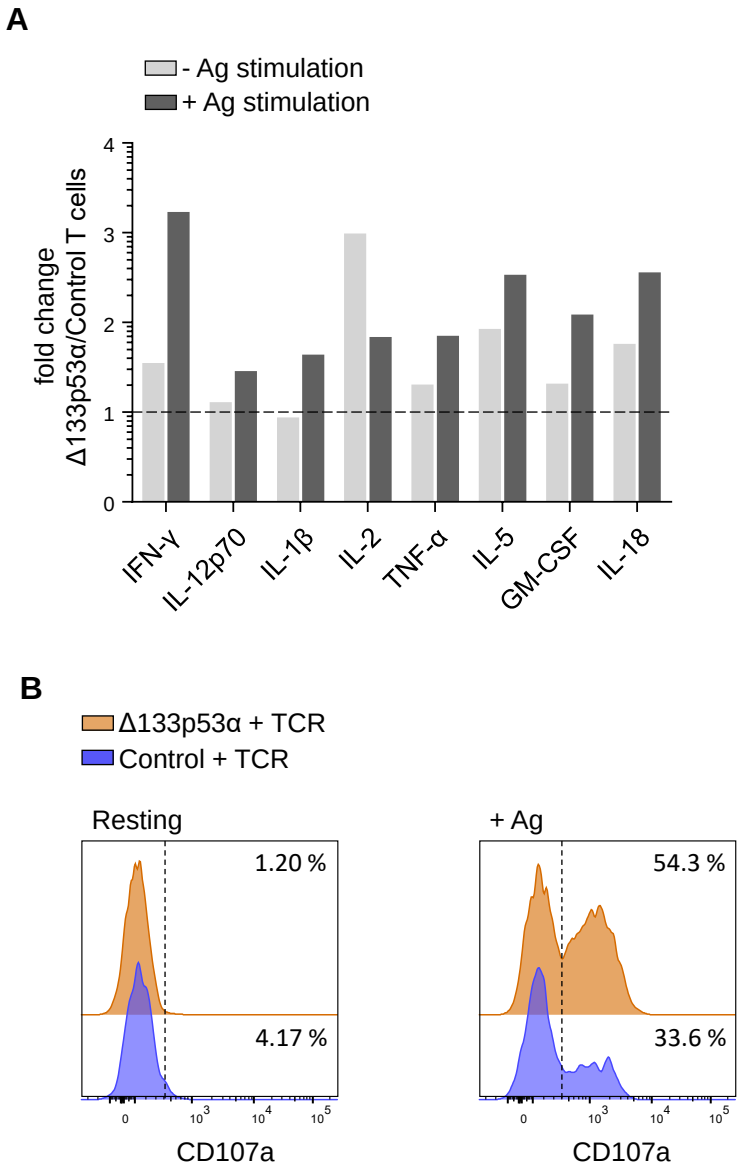

Figure 16: Δ133p53α overexpression enhances the secretion of different cytokines and increases the capacity of degranulation

(**A**) Cytokine secretion of Δ133p53α-transduced and control T cells over 24h. Cytokine concentrations were measured by Luminex Assay before and after antigen-specific stimulation. Y-axis indicates the difference between both groups represented as fold change. (n=1 biological replicate). (**B**) Degranulation Assay of Δ133p53α-modified and control T cells (CD8^{+}) upon antigen-specific

stimulation with SAOS 2/143 over 24h. Degranulation is indicated by surface expression of LAMP-1 (CD107a). T cells without stimulation (resting) served as control. (Representative of n=3 biological replicates).

5.3 TIGIT affects TCR-mediated anti-tumor immunity

To further identify mechanisms that contribute to the improved killing capacity of Δ133p53α-transduced T cells, the role of inhibitory receptors downregulated in these cells like TIGIT and PD-1 were investigated in a tumor cell-T cell contact model to mimic a TME-like condition. First, expression levels of the corresponding ligands CD155 (also known as Poliovirus Receptor, PVR) and PD-L1 on the target tumor cell line SAOS 2/143 were determined. As both ligands were strongly expressed (Figure 17, A) and Δ133p53α overexpression showed a pronounced downregulation of TIGIT, the interaction of TIGIT and CD155 was examined in more detail. TIGIT levels under resting conditions (without tumor cell exposure) were moderate in both groups. Here, control T cells showed TIGIT expression of up to 50 %, while Δ133p53α-modified T cells exhibited lower values of up to 35 % (Figure 17, B). Upon co-culture with the target tumor cells, in both control and Δ133p53α-modified T cells the frequency of $CD8^+TIGIT^+$ T cells increased and reached comparable levels around 70 % (Figure 17, B). However, the MFI remained lower in T cells with Δ133p53α-overexpression (Δ133p53α: 708 vs. control: 943).

A

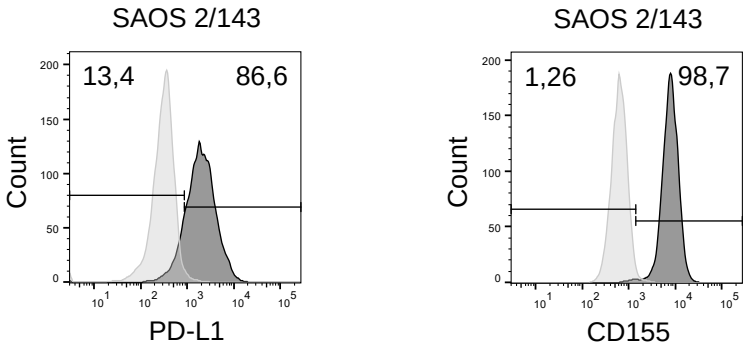

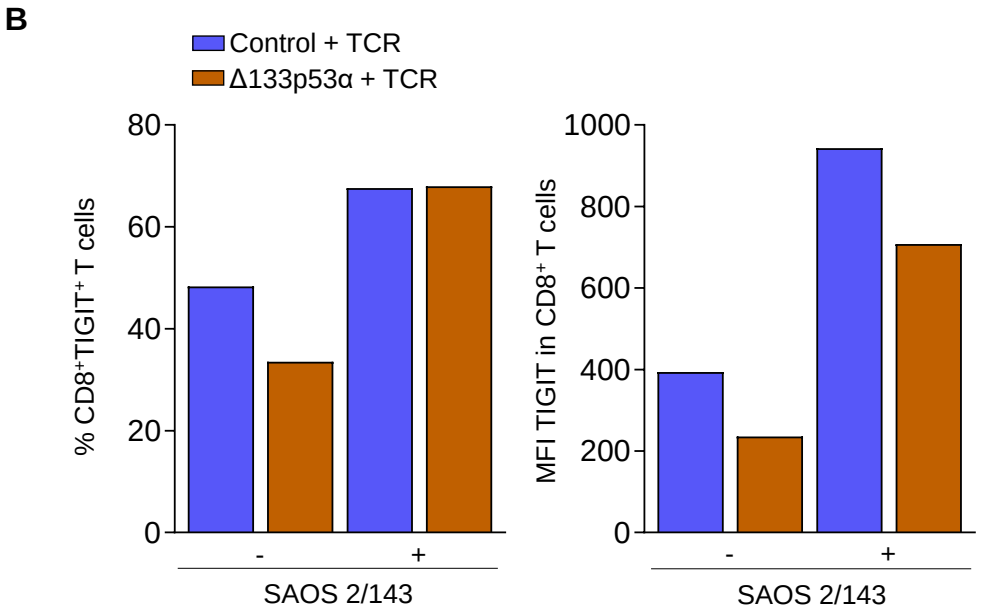

Figure 17: T cells upregulated TIGIT expression after encountering target tumor cells
(**A**) Cell surface expression of PD-L1 and CD155 in SAOS 2/143 measured by flow cytometry. (**B**) Representative data of n=3 biological replicates showing the frequency and MFI of TIGIT in $CD8^+$ T cells. Control and Δ133p53α-transduced cells were co-culture (E:T ratio: 1:1, over 24 h) with (+) or without (-) SAOS 2/143 and analyzed by flow cytometry.

Co-culture experiments with the p53-deficient SAOS 2 cells, that do express CD155 to similar levels as SAOS 2/143 (data not shown) but lack the p53 target antigen, did not result in increased TIGIT levels on T cells (mean T cells alone: 8.24 % vs. mean T cells + SAOS 2 null: 8.81 %, adjusted p>0.99, Figure 18, A). These results suggested an antigen dependent upregulation of TIGIT. Culturing T cells with supernatant from SAOS 2/143 (mean T cells alone: 8.24 % vs. T cells + SAOS 2/143 supernatant: 7.82 %, adjusted p>0.999) did not increase TIGIT expression. Also, co-culture of T cells and SAOS 2/143 in a transwell-system did not significantly increase TIGIT expression (mean T cells alone: 8.24 % vs. mean T cells + SAOS 2/143 in transwell: 10.14 %, adjusted p=0.9995, Figure 18, A), further confirming the cell-cell-contact dependency. Only T cells co-cultured with p53 antigen-presenting, $CD155^+$ tumor cells showed a significant upregulation of TIGIT (T cells alone mean: 8.24 % vs. T cells + SAOS 2/143 mean: 18.81 %, adjusted p=0.0479, Figure 18, A). Furthermore, SAOS 2 null cells pulsed with titrated concentrations of target antigen ($p53_{264\text{-}272}$) and subsequent co-culture with T cells, demonstrated the antigen dependent modulation of TIGIT on T cells (Figure 18, B).

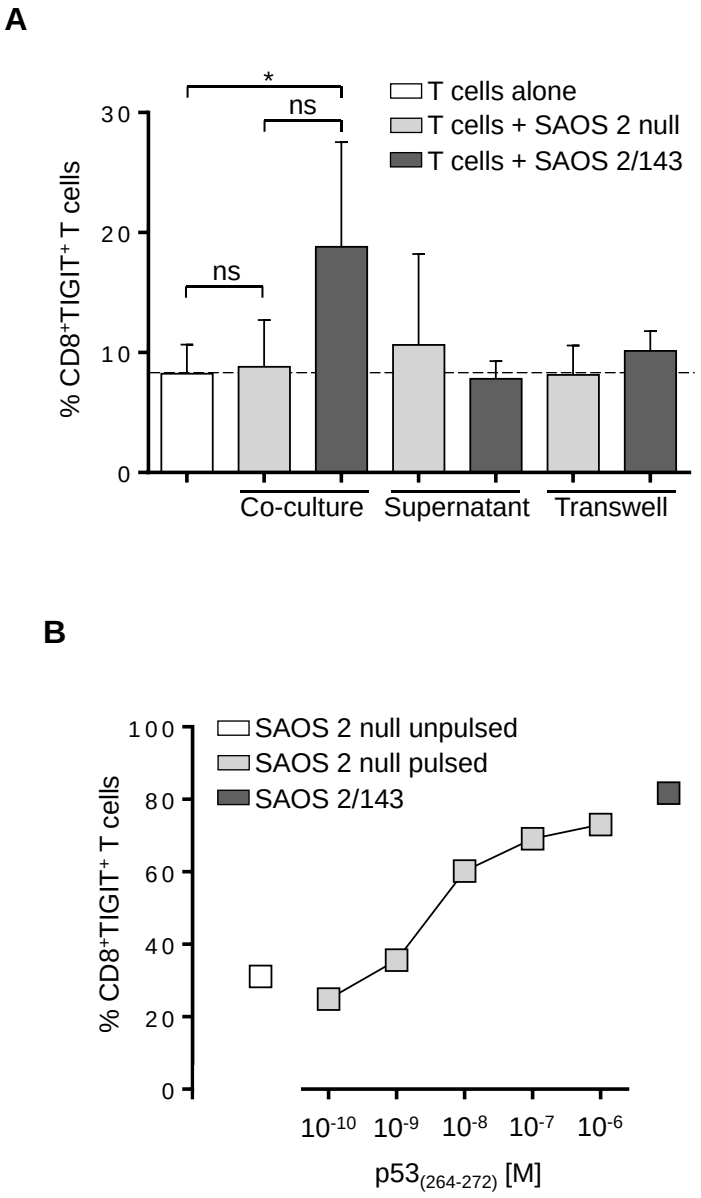

Figure 18: TIGIT upregulation is dependent on antigen-recognition
(**A**) Fraction of $CD8^+TIGIT^+$ T cells after 24h culture in medium alone, with SAOS 2 null or with SAOS 2/143 and in the corresponding supernatant or transwell culture (n=3 biological replicates). (**B**) TIGIT expression levels in $CD8^+$ T cells upon co-culture with SAOS 2/143 or SAOS 2 null pulsed with target antigen ($p53_{264-272}$ peptide). X-Axis indicates the concentration (in M) of p53 peptide (n=1 biological replicate). Statistical testing was performed with ANOVA followed by Tukey's multiple comparison test. Adjusted P values: *$p < 0.05$, **$p < 0.01$, ***$p < 0.001$, ns (not significant).

To assess the relevance of TIGIT/CD155 interaction in this model, healthy donor T cells were isolated and equipped with the scTCR without overexpression of a p53 isoform. After transduction, T cells were separated with immunomagnetic beads into low ($TIGIT^{low}$) and high ($TIGIT^{high}$) TIGIT expressing T cells. The procedure of magnetic separation seemed to moderately increase TIGIT expression in $TIGIT^{low}$ T cells (29.1 %), compared to untreated bulk T cells (14 %, Figure 19, A).

Nevertheless, TIGIT expression remained substantially lower compared to TIGIT^{high} T cells (98.9 %, Figure 19, A). In long-term colony-forming assays the cytolytic responses of both T cell groups were analyzed. In these assays, TIGIT^{high} cells exhibited an extenuated anti-tumor response. After co-culture with TIGIT^{high} cells, 32.17 % of target tumor cells remained viable, while TIGIT^{low} cells eradicated more tumor cells (6.41 % remaining viable tumor cells, Figure 19, B). TCR expression did not differ between TIGIT^{low} and TIGIT^{high} T cells (not shown). Importantly, the impaired cytotoxic capacity of TIGIT^{high} T cells could be partially restored by preventing TIGIT/CD155 interaction, using an anti-TIGIT blocking antibody (18.72 % vs. 32.17 % remaining viable tumor cells, Figure 19, B).

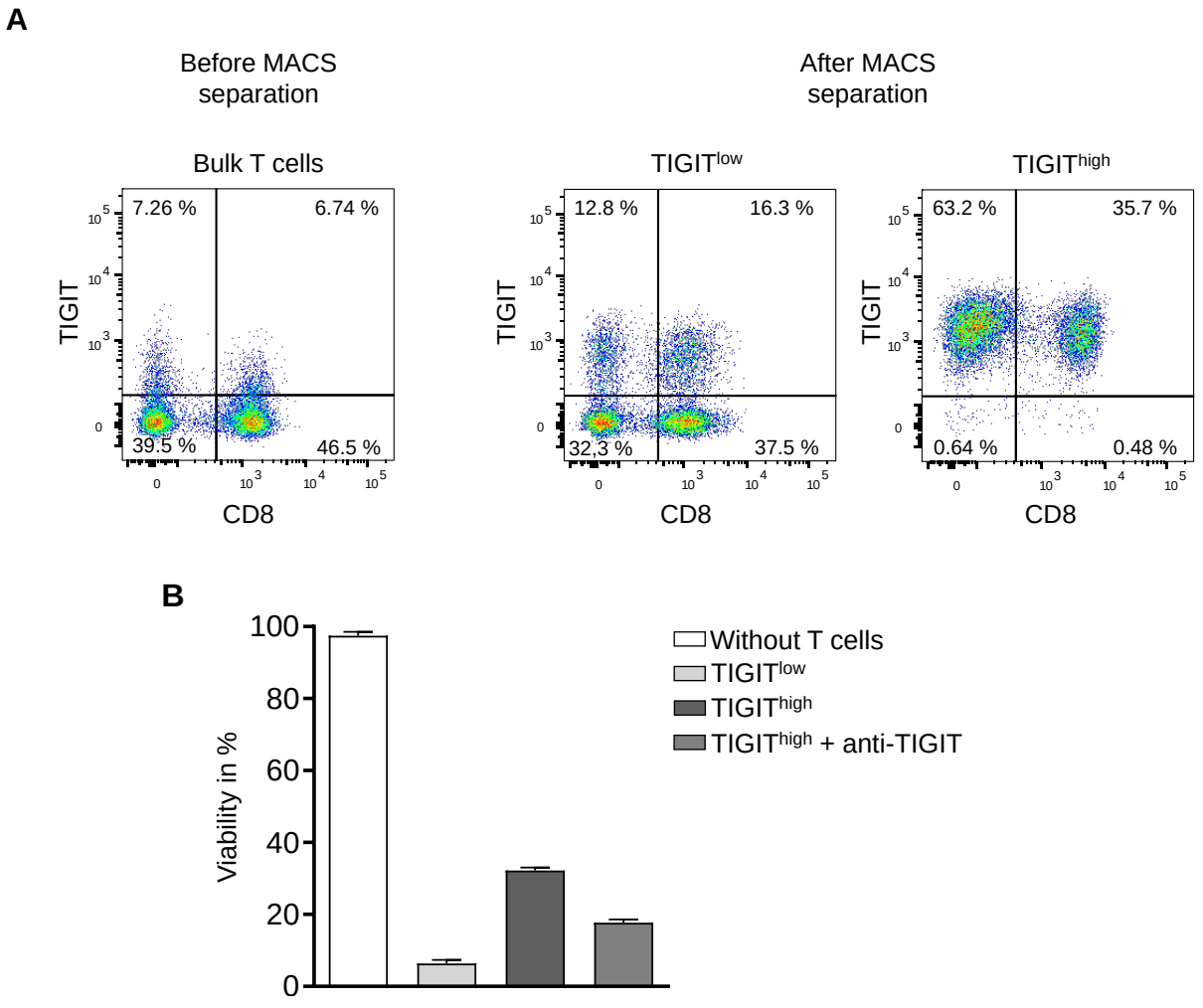

Figure 19: TIGIT negatively affects TCR-mediated anti-tumor immunity

(**A**) Representative flow cytometric measurement of CD8 and TIGIT expression before and after immunomagnetic (MACS) selection of TIGIT^{+} T cells (n≥3 biological replicates). (**B**) Quantitative data from a representative tumor colony-forming assay over 24h using TIGIT^{low} and TIGIT^{high} T cells (mainly CD8 T cells at the timepoint of the experiment, CD8 expression > 70 %). SAOS 2/143 served as target cells. An antibody against TIGIT (= anti-TIGIT) was used to block TIGIT and CD155 interaction. Y-Axis indicates the viability of tumor cells in percent. Values were normalized to control condition without T cells (n=3 biological replicates).

To further explore the mechanisms of TIGIT downregulation in Δ133p53α-modified T cells, the cells were treated with the autophagy inhibitor bafilomycin A1 which can partially restore Δ133p53α expression by preventing its autophagic degradation in $CD8^+CD28^-CD57^+$ T cells (9). Treatment with bafilomycin A1 induced an efficient reduction of TIGIT expression in control and Δ133p53α-transduced cells. Without treatment, 14.1 % of control and 6.38 % of Δ133p53α-modified T cells expressed TIGIT. After 24 hours of bafilomycin A1 treatment, the expression of TIGIT was reduced in both groups, with a residual expression of 0.5 % (Figure 20, A). To explore the downregulation of TIGIT transcripts, mRNA of both T cell groups (+/- bafilomycin A1) was isolated and expression was quantified by RT-qPCR. The results demonstrated a reduction of TIGIT mRNA expression in control and Δ133p53α-modified T cells by 90 % or more (control 0.1 and Δ133p53α 0.066 relative expression compared to control T cells without treatment, Figure 20, B). Furthermore, reduced TIGIT mRNA transcripts in Δ133p53α-transduced T cells (fold-change: 0.74, Figure 20, B) correlated with the reduced surface expression of TIGIT in these T cells (compare Figure 20, A and Figure 15, A) and suggests a regulation of TIGIT expression by Δ133p53α isoform on the RNA level.

A

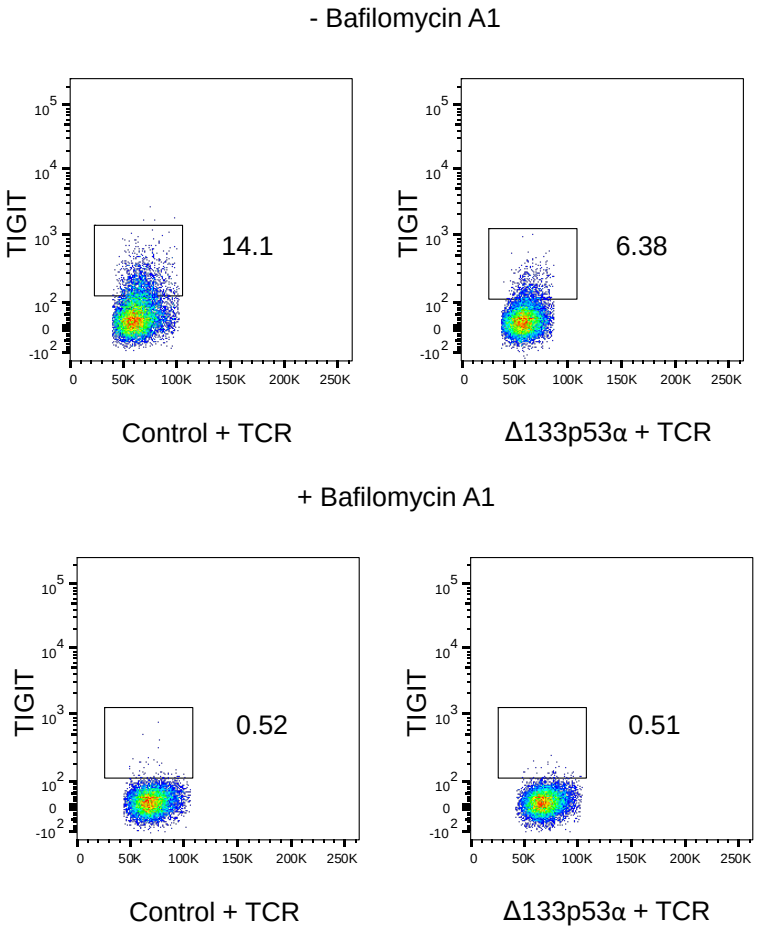

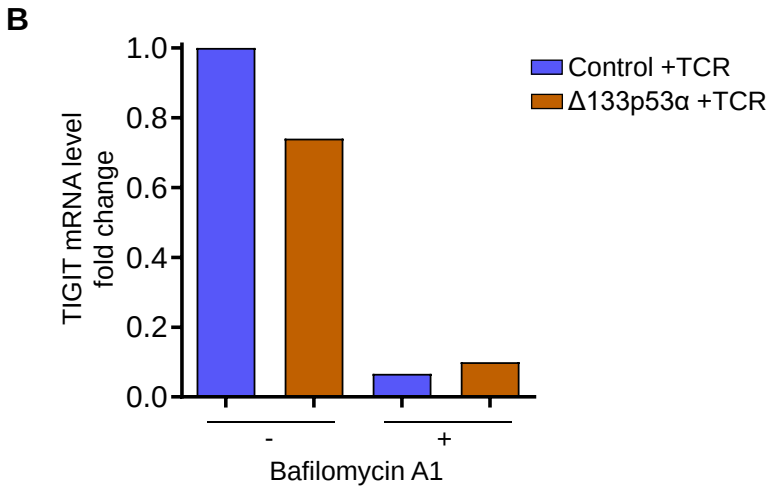

Figure 20: Bafilomycin A1 treatment reduces TIGIT expression at mRNA and protein levels
(**A**) Surface expression of TIGIT (top) and TIGIT mRNA levels (bottom) with or without bafilomycin A1 treatment for 24h. Protein levels were analyzed by flow cytometry. (**B**) mRNA transcripts were quantified and normalized to GAPDH by RT-qPCR. Representative data of n=3 (A) and n=1 (B) biological replicates.

5.4 Anti-tumor response of Δ133p53α-overexpressing T cells is enhanced in murine adoptive transfer model

Next, we tested if Δ133p53α-overexpression in tumor-antigen TCR$^+$ T cells also improves anti-tumor response *in vivo*. In a xenograft tumor model, immunodeficient NSG mice were subcutaneously injected in the right flank with SAOS 2/143 tumor cells. Seven days later, p53scTCR-equipped T cells co-transduced with Δ133p53α or mock vector were infused together with intraperitoneal injection of IL-2 for enhanced survival and proliferation (Figure 21, A). Tumor volumes were measured at least twice a week. Compared to the control group, tumor growth was delayed in a fraction of mice receiving TCR$^+$/Control and TCR$^+$/Δ133p53α-modified T cells (Figure 21, B). Importantly, long-term suppression of the tumor growth (beyond day 40) was observed in more animals receiving TCR$^+$/Δ133p53α-modified T cells (4/13), than mice receiving TCR$^+$/Control T cells (1/11, Figure 21, B). Experiments were terminated when the animals reached large tumors (≥ 1000 mm^3) or showed signs of GvHD. Accordingly, mice were sacrificed, and organs/serum were collected for analysis. Based on the time of each event of interest (= death/GvHD or tumor volume ≥ 1000 mm^3) survival curves were generated. Mice receiving T cells with TCR$^+$/Δ133p53α-modified T cells exhibited an improved median survival (45 day) compared to animals receiving TCR-transduced (37 days) and control (31 days) T cells (Figure 21, C).

A

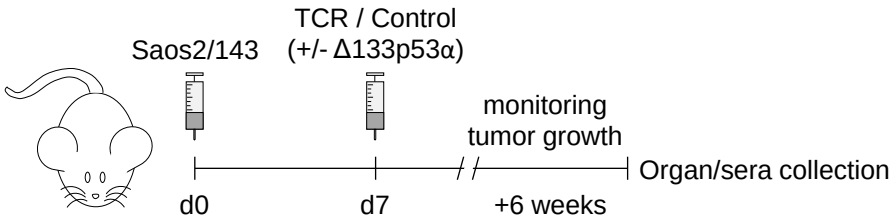
TCR / Control
Saos2/143
(+/- Δ133p53α)
monitoring
tumor growth
Organ/sera collection
d0
d7
+6 weeks

B

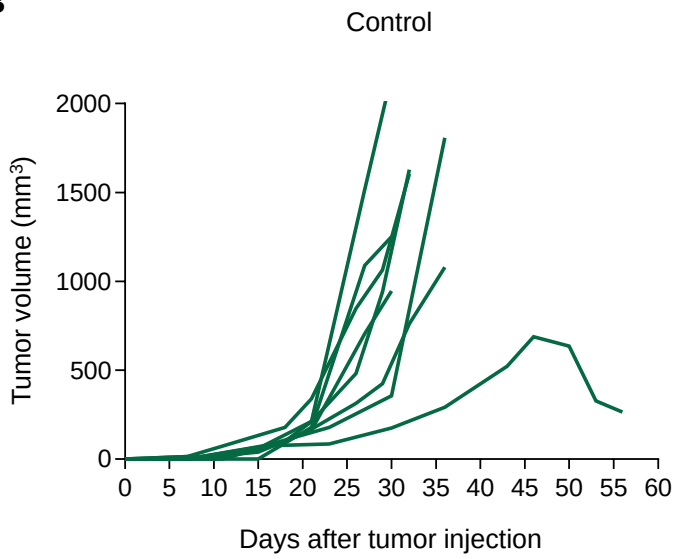
Control
Tumor volume (mm³)
2000
1500
1000
500
0
0 5 10 15 20 25 30 35 40 45 50 55 60
Days after tumor injection

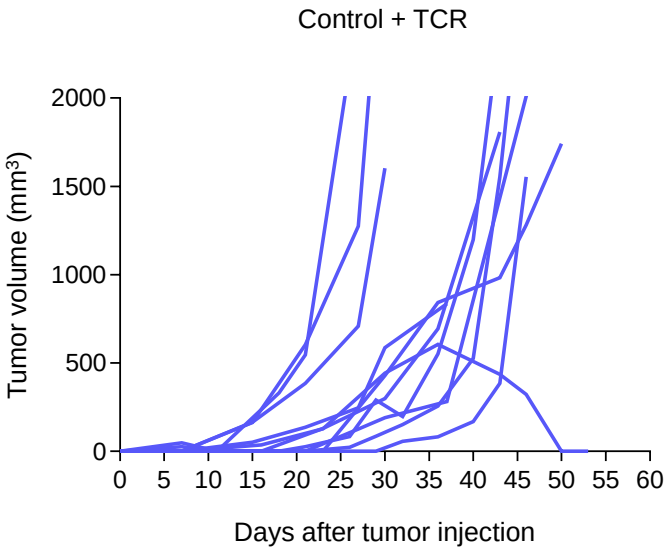
Control + TCR
Tumor volume (mm³)
2000
1500
1000
500
0
0 5 10 15 20 25 30 35 40 45 50 55 60
Days after tumor injection

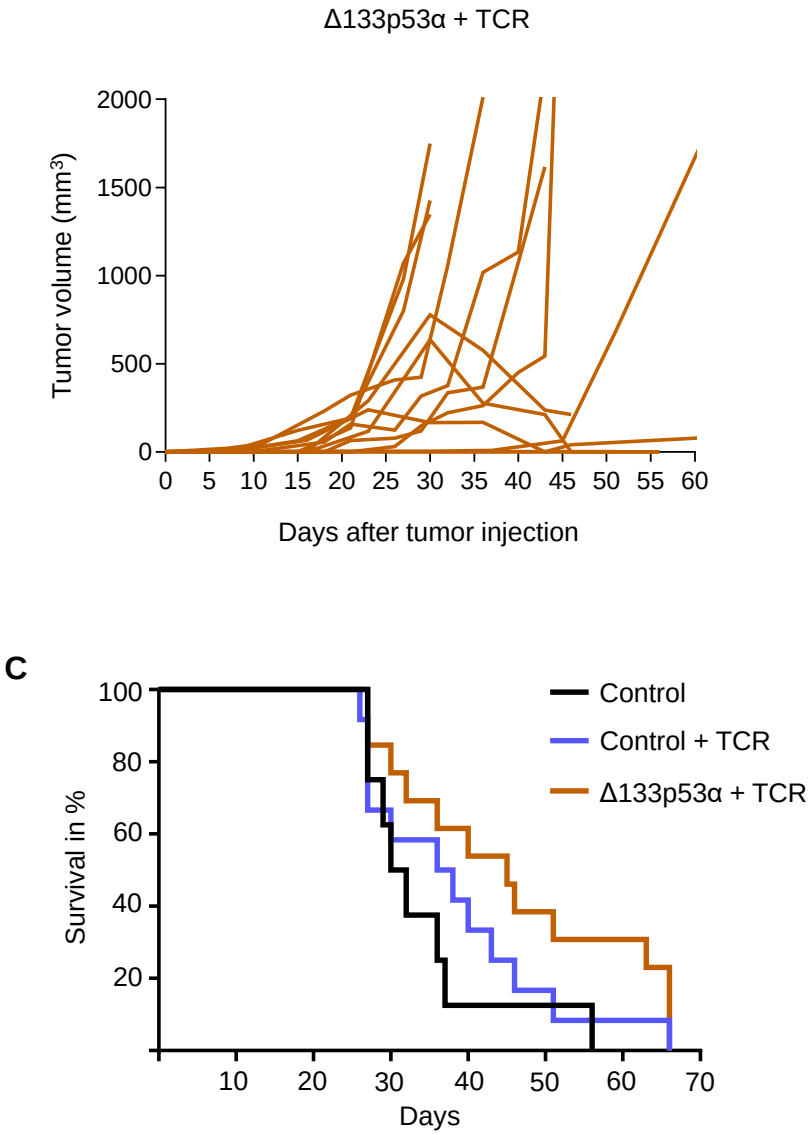

Figure 21: Superior anti-tumor response of TCR$^+$/Δ133p53α-overexpressing T cells in murine adoptive transfer model

(**A**) Schematic representation of a xenograft tumor model for adoptive T cell transfer using immunodeficient NOD-scid IL2rg^{null} (NSG) mice. SAOS 2/143 tumor cells were engrafted by subcutaneous injection at day 0. T cells from healthy donors were transduced with the scTCR and Δ133p53α (TCR$^+$/Δ133p53α) or control vector (TCR$^+$). Non-transduced T cells (Control) served as controls. T cells were infused together with IL-2 intraperitoneal at day 7. (**B**) Graphs represent tumor growth (volume) after injection of SAOS 2/143. (**C**) Survival curves of NSG mice after tumor injection. Mice bearing tumors ≥ 1000 mm^3 were sacrificed. Figure (**B**) and (**C**) show pooled data from n=3 independent experiments. Differences in survival between groups was tested by using the log-rank (Mantel-Cox) test resulting in p=0.4409 for Control vs. Control + TCR, p=0.0423 for Control vs. Δ133p53α + TCR and p=0.1842 for Control + TCR vs. Δ133p53α + TCR. Analysis includes 33 animals in total.

In most TCR-treated animals, anti-tumor response was not associated with any observable adverse effects. Only few animals which had received TCR$^+$/Δ133p53α T cells developed signs of GvHD including reduced activity, loss of fur, weight loss and eventually death (Figure 22, A). As we used a well-established and optimized

scTCR (119), which did not induce GvHD in previous experiments, TCR-mispairing is unlikely to be the cause of these adverse events. Affected mice were sacrificed and organs were examined regarding T cell infiltration. The spleen of animals treated with TCR$^+$/Δ133p53α-transduced cells exhibited splenomegaly with pronounced infiltration of mainly CD4$^+$ T cells (83.31 % CD4$^+$ vs. 12.92 % CD8$^+$ T cells). Interestingly, mice which received control T cells (with p53scTCR alone) showed less spleen infiltration of T cells with fewer CD4/Vβ3/TCR (1.71 % vs. 6.11 %) and fewer CD8/Vβ3/TCR (0.33 % vs. 0.52 %) expression (Figure 22, B).

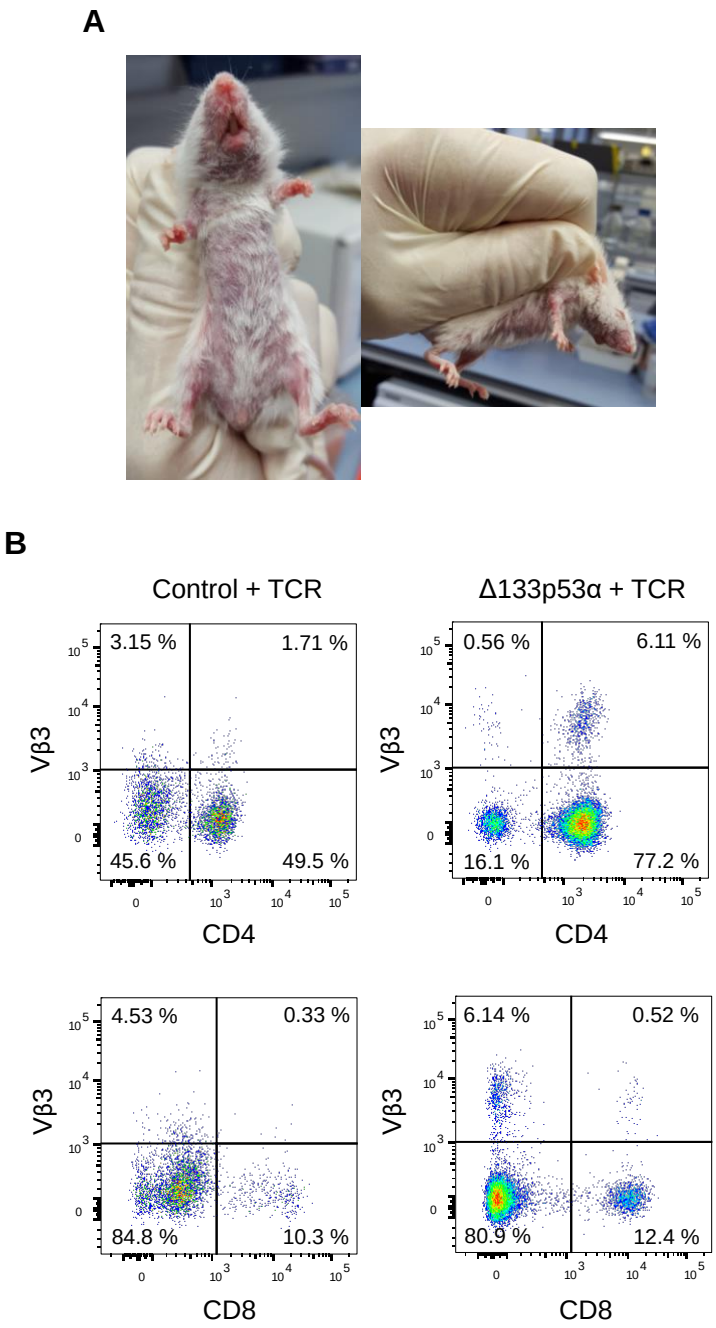

Figure 22: Anti-tumor responses may be associated with adverse events

(**A**) Exemplary pictures of one animal showing side effects (including reduced activity, loss of fur, closing of the eyelid and weight loss) after infusion of T cells. (**B**) Exemplary flow cytometric

measurement of CD8 and Vβ3 expression of spleen infiltrating TCR+/Δ133p53α T cells from one animal with observable side effects compared to one animal receiving TCR+/control T cells.

Recently published analyses of the same in vivo experiments additionally revealed an improved persistence of TCR+/Δ133p53α T cells in the peripheral blood (117). At day 7, a small fraction of CD8+ T cells could be detected in both, mice receiving TCR+/Δ133p53α and TCR+/control T cells. Over time, the frequency of control T cells declined substantially, while Δ133p53α-transduced T cells persisted in the peripheral blood until day 34 (117). Concomitantly, in sera of mice that developed GvHD, secreted levels of multiple cytokines and different chemokines were increased compared to mice receiving TCR+ T cells (Figure 23). Higher concentrations of inflammatory cytokines like IL17-A, IL-1β, TNF-β and IL-6, which heavily contributes to inflammatory processes like rheumatoid arthritis and cytokine release syndrome (CRS) after CAR-T cell therapy (124), were observed in the serum of GvHD-affected mice that received TCR+/Δ133p53α-transduced T cells (Figure 23, A). However, not all inflammatory cytokines were elevated compared to the control mice, for example MCP-1. On the other hand, cytokines like IL-23 were strikingly increased (Figure 23, A). Beside this increase in inflammatory cytokines, serum concentrations of effector cytokines like IFN-γ and TNF-α, as well as of stimulatory like IL-2, IL-15 and GM-CSF and regulatory cytokines were excessively elevated in these animals (IFN-γ > 50000 pg/ml, GM-CSF > 2000 pg/ml). In the serum of animals receiving control T cells with p53scTCR alone, only minor to moderate levels of these cytokines were detected (Figure 23, B-E).

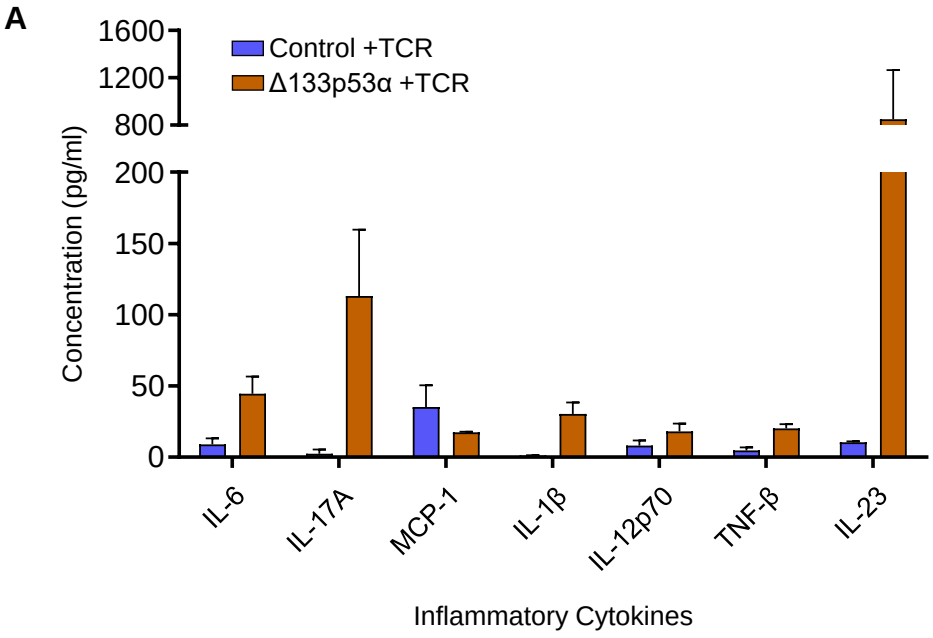

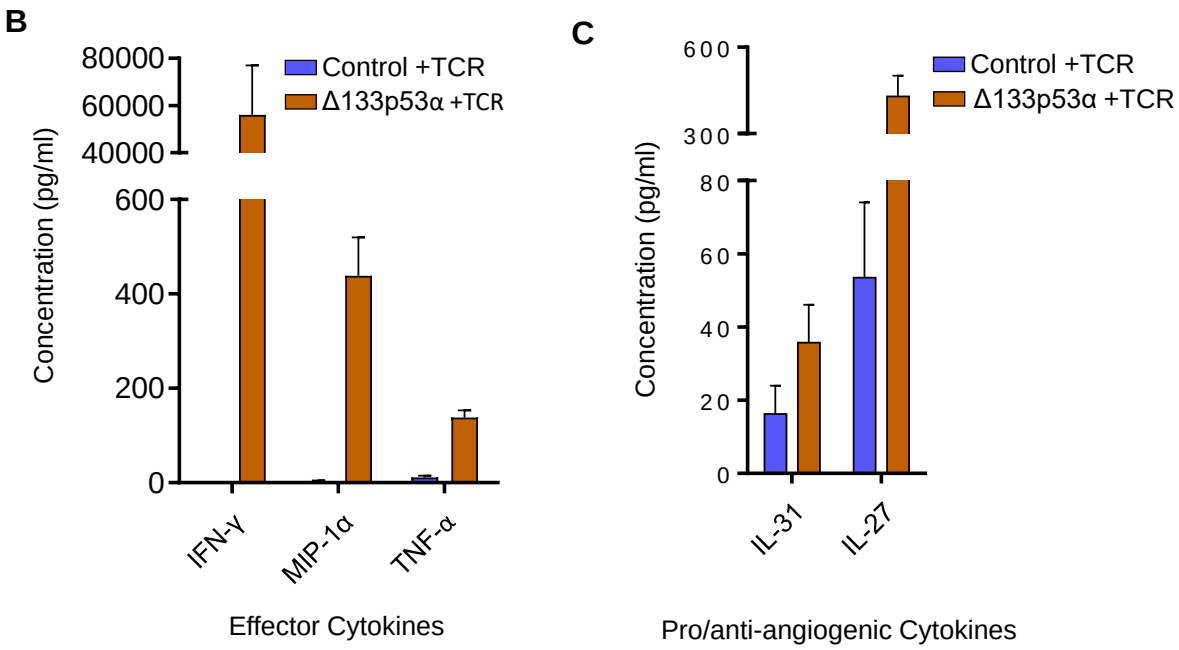
B
80000
60000
40000
600
400
200
0
Concentration (pg/ml)
Control +TCR
Δ133p53α +TCR
IFN-γ
MIP-1α
TNF-α
Effector Cytokines
C
600
300
80
60
40
20
0
Concentration (pg/ml)
Control +TCR
Δ133p53α +TCR
IL-31
IL-27
Pro/anti-angiogenic Cytokines

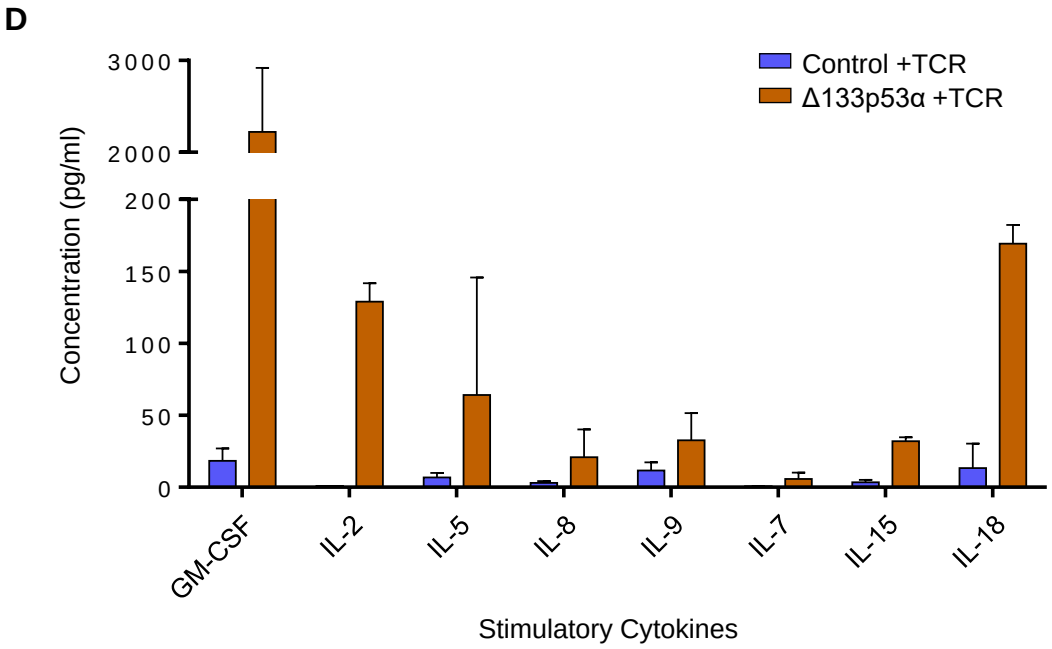
D
3000
2000
200
150
100
50
0
Concentration (pg/ml)
Control +TCR
Δ133p53α +TCR
GM-CSF
IL-2
IL-5
IL-8
IL-9
IL-7
IL-15
IL-18
Stimulatory Cytokines

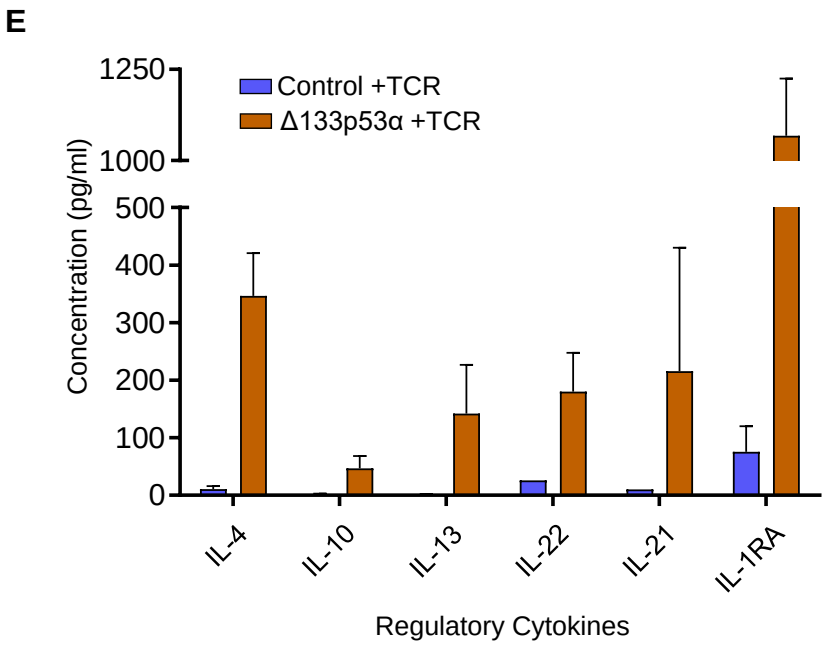

Figure 23: Adverse events are associated with elevated serum cytokine concentrations
Measurement of serum concentrations of inflammatory (**A**), effector (**B**), pro/anti-angiogenic (**C**), stimulatory (**D**) and regulatory (**E**) cytokines from one animal treated with TCR$^+$ T cells compared to one animal treated with TCR$^+$/Δ133p53α T cells. Serum from the peripheral blood was collected shortly before mice were sacrificed. Concentrations were determined by Multiplex Luminex Immunoassay (n=2 technical replicates).

To exclude a monoclonal expansion of TCR Vβ$^+$ cells, the TCR Vβ repertoire in spleen-infiltrating T cells was analyzed by flow cytometry. This analysis showed a distribution of polyclonal T cell populations, without the emergence of a monoclonal TCR Vβ cell population (Figure 24).

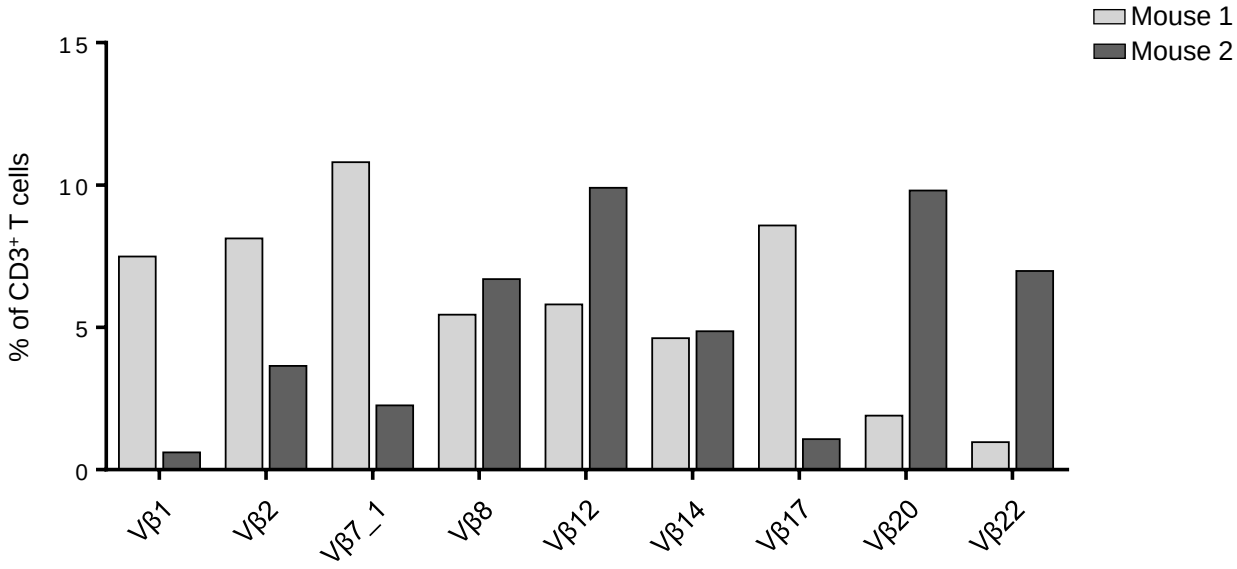

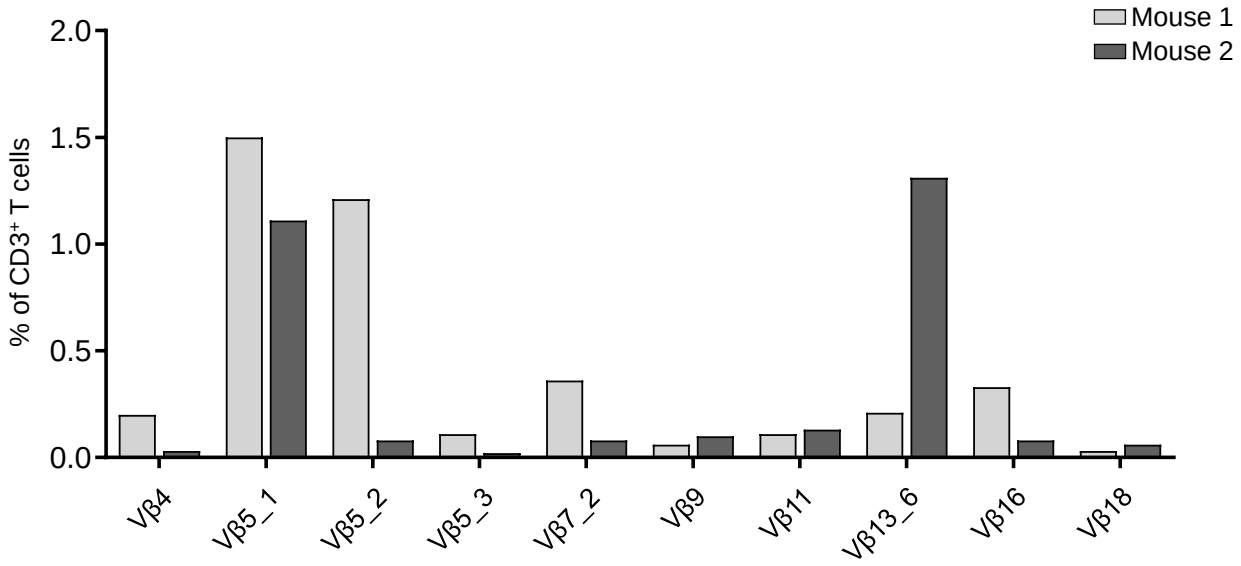

Figure 24: Distribution of TCR Vβ subfamilies among CD3$^+$ spleen-infiltrating T cells
TCR Vβ repertoire of spleen-infiltrating T cells from two mice treated with TCR$^+$/Δ133p53α cells (showing GvHD symptoms). Analysis was performed by flow cytometry using an antibody-panel against 19 different human TCR/Vβ chains.

5.5 Senescence in T cells from patients with multiple myeloma is associated with low Δ133p53α expression

T cell senescence occurs in elderly but healthy individuals, as well as in several human diseases, especially chronic viral infections and cancer (125). For example, in multiple myeloma, senescent T cells accumulate in the bone marrow (126). To further address the relevance of p53 isoform dysregulation in senescent T cells, the expression levels of Δ133p53α in T cells from myeloma patients were determined. T cells were collected from the peripheral blood of newly diagnosed and untreated patients. T cells from healthy donors were collected the same way and served as controls. First, different cell surface markers were analyzed by flow cytometry. The analysis showed that the subset of less differentiated CD28$^+$/CD57$^-$ was significantly reduced in CD8$^+$ T cell samples from myeloma patients (mean 38.68 %) compared to healthy donors (mean 58.86 %, p=0.0103, Figure 25, A). Concomitantly, the senescent-associated CD28$^-$/CD57$^+$ cells represented only a minor fraction of healthy donor CD8$^+$ T cell populations (mean 11.49 %), while this subset was considerably enriched in myeloma patients (mean 30.96 %, p=0.0012, Figure 25, A). Protein lysates of T cells from the same patients were used to determine Δ133p53α expression levels. In healthy donor (HD) T cells high expression levels of Δ133p53α could be confirmed, while minor or no expression was detected in patient samples

(MM, Figure 25, B). These results suggest that accumulation of $CD8^+/CD28^-/CD57^+$ in myeloma patients is associated with a strong downregulation of Δ133p53α expression.

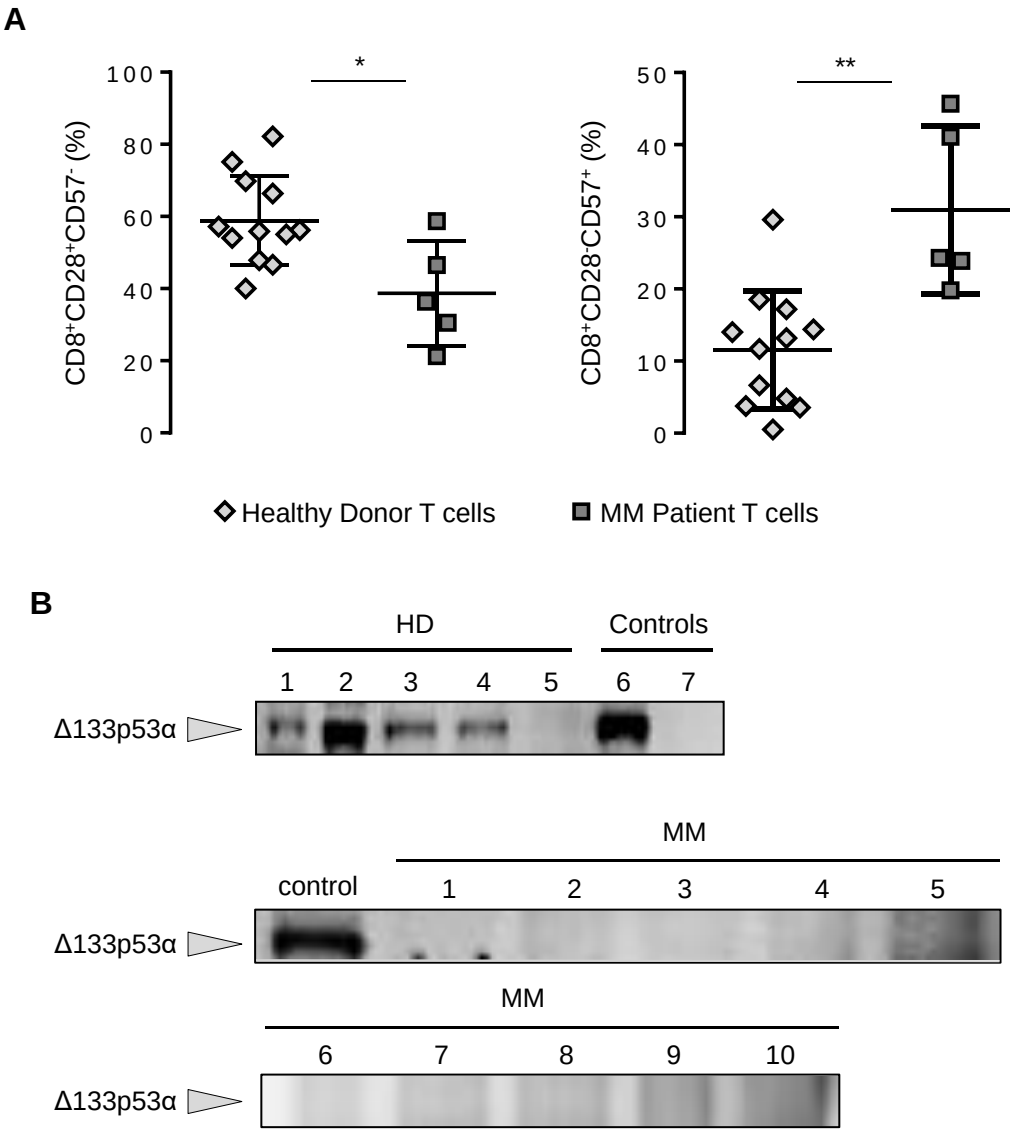

Figure 25: Senescent T cells accumulate in the peripheral blood of multiple myeloma patients

(**A**) Scatter plots showing the frequency and mean + standard deviation of $CD28^+CD57^-$ (left) and $CD28^-CD57^+$ of $CD8^+$ T cells (right) collected from the peripheral blood of untreated patients with newly diagnosed multiple myeloma (n=5 individual donors). Peripheral blood T cells from (n=12) healthy donors served as control. (**B**) Detection of Δ133p53α by western blot using protein lysate from myeloma patient (n=10) and healthy donor (n=5) peripheral blood T cells. Δ133p53α-transduced T cells were used as positive control and p53-null SAOS 2 cells were used as negative control (upper blot, lanes 6 and 7, respectively). Amount of protein of each sample from healthy donors and myeloma patients is listed below.

Sample (healthy donors)	Number	Amount of protein (µg)
KL3	1	60
HD53	2	100
HD55	3	43
HD56	4	36
HD57	5	30
Δ133p53α-transduced T cells (positive control)	6	60
SAOS 2 null (negative control)	7	20
Sample (myeloma patients)	Number	Amount of protein (µg)
Δ133p53α-transduced T cells (positive control)		60
P1	1	18
P2	2	47
P3	3	49
P4	4	60
P5	5	51
P37	6	60
P41	7	60
P46	8	32
20FN	9	60
O.K.	10	43

To test the cytolytic activity of the senescent T cells from myeloma patient, cells were expanded *in vitro* and transduced with the p53scTCR. As T cells from myeloma patients (compared to healthy donor T cells) showed increased levels of the inhibitory receptors TIGIT and PD-1 (117), one patient sample with high levels (P41) and one with low levels (P37) of $CD28^-/CD57^+$ cells were selected. Additionally, P37 T cells exhibited a low TIGIT expression (21% $CD8^+TIGIT^+$) compared to P41 T cells (77% $CD8^+TIGIT^+$). In short-term chromium release assays, cytolytic responses of $TIGIT^{high}$ T cells from patient P41 (25 % specific lysis at E:T=10:1) were markedly reduced compared to $TIGIT^{low}$ T cells from patient P37 (97 % specific lysis at E:T=10:1) or control T cells (75 % specific lysis at E:T=10:1) from a healthy donor at different E:T ratios (Figure 26, A). At an E:T ratio of 3:1 T cells from patient P41 hardly lysed any tumor cells (8 % specific lysis), while T cells from P37 (77 % specific lysis) and the control (49 % specific lysis) still showed an efficient response (Figure 26, A). In long-term tumor colony-forming assays, the impaired anti-tumor response of $TIGIT^{high}$ P41 T cells was observed as well. After 24 hours of co-culture with target tumor cells, the viability of remaining tumor colonies was still 98.7 %, while T cells from patient P37 reduced tumor cell viability to 15.87 % (Figure 26, B).

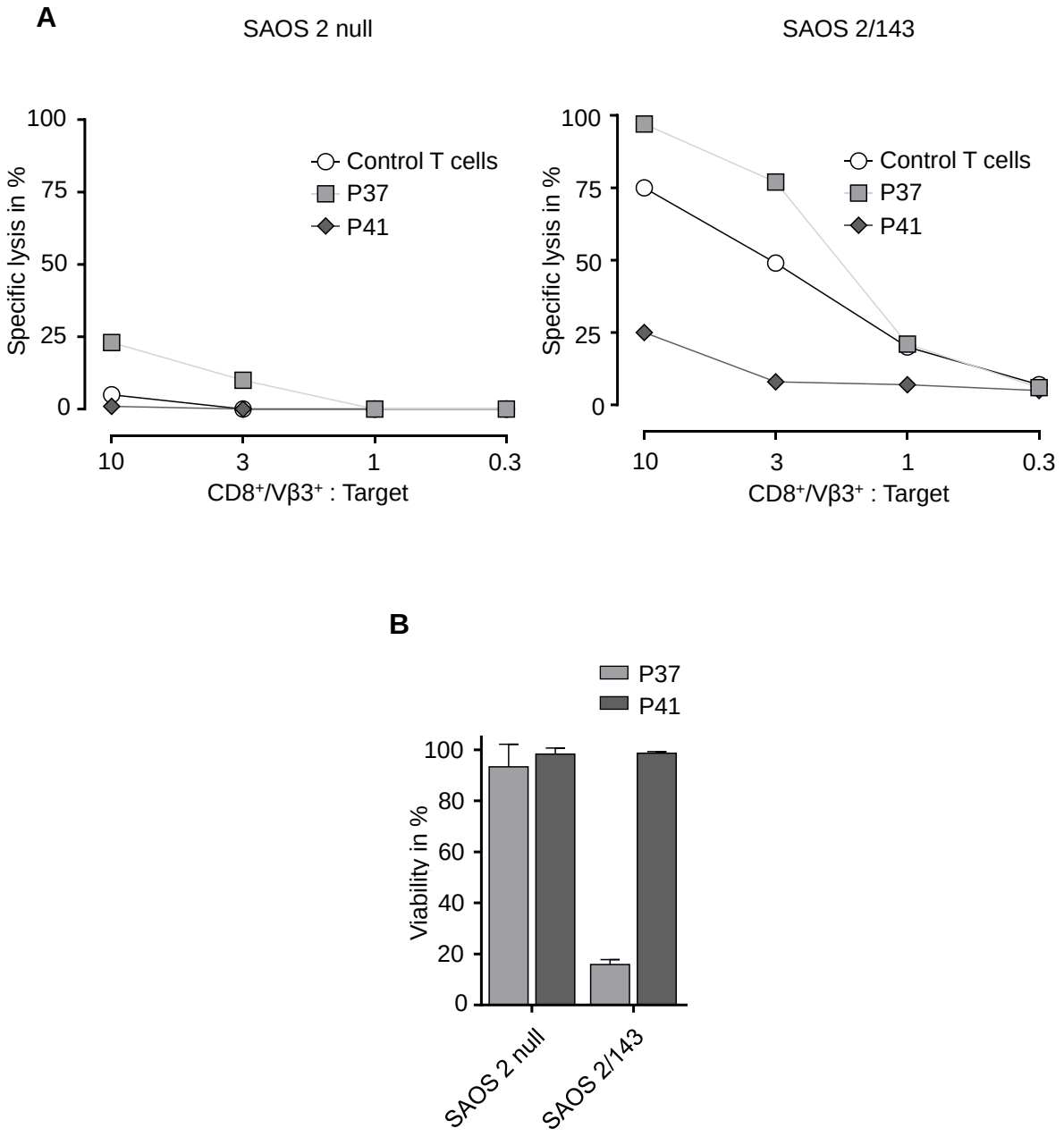

Figure 26: Myeloma patient T cells with senescent phenotype reveal impaired anti-tumor responses

(**A**) Short-term chromium release assay using p53scTCR-transduced T cells from two myeloma patient (P37 and P41) compared to p53 scTCR transduced T cells from one healthy donor (control). SAOS 2/143 was used as $p53^+$ target. SAOS 2 null (left) lacking the target antigen served as negative control target. (**B**) Tumor colony-forming assay comparing long-term killing capacity of P37 and P41 T cells at E:T=1:1 for 24 hours.

Next, myeloma patients with an enriched subset of $CD28^-/CD57^+$ cells were modified by overexpression of Δ133p53α in order to revert the senescent phenotype. T cells from two patients (M305 and M306) were isolated from the peripheral blood and genetically co-equipped with the p53scTCR and Δ133p53α. In both samples, CD45RA (29.8 % vs. 10.36 %) and CD62L (27.85 % vs. 9.74 %) were upregulated upon Δ133p53α overexpression compared to control T cells (mean values of T cells

from two different myeloma patients, Figure 27, A). These markers of rather less differentiated T cells were also increased in terms of MFI (CD45RA: 1739 in control vs. 3731 in Δ133p53α-modified T cells, CD62L: 859 in control vs. 1844 in Δ133p53α-modified T cells). Additionally, the high expression of TIGIT in myeloma patient T cells was reduced in terms of frequency (92.5 % in control vs. 76.9 % in Δ133p53α-transduced T cells) and MFI (4752 in control vs. 1803 in Δ133p53α-transduced T cells, Figure 27, A). Importantly, beside the upregulation of early differentiation markers, overexpression of Δ133p53α improved the cytolytic capacity of myeloma patient T cells at different effector to target ratios: for example 81 % specific lysis at E:T 10:1 compared to 50 % specific lysis in control T cells (Figure 27, B). At an E:T ratio of 3:1 Δ133p53α-transduced T cells still achieved a specific lysis of 68 %, while control T cells achieved 23 % (Figure 27, B).

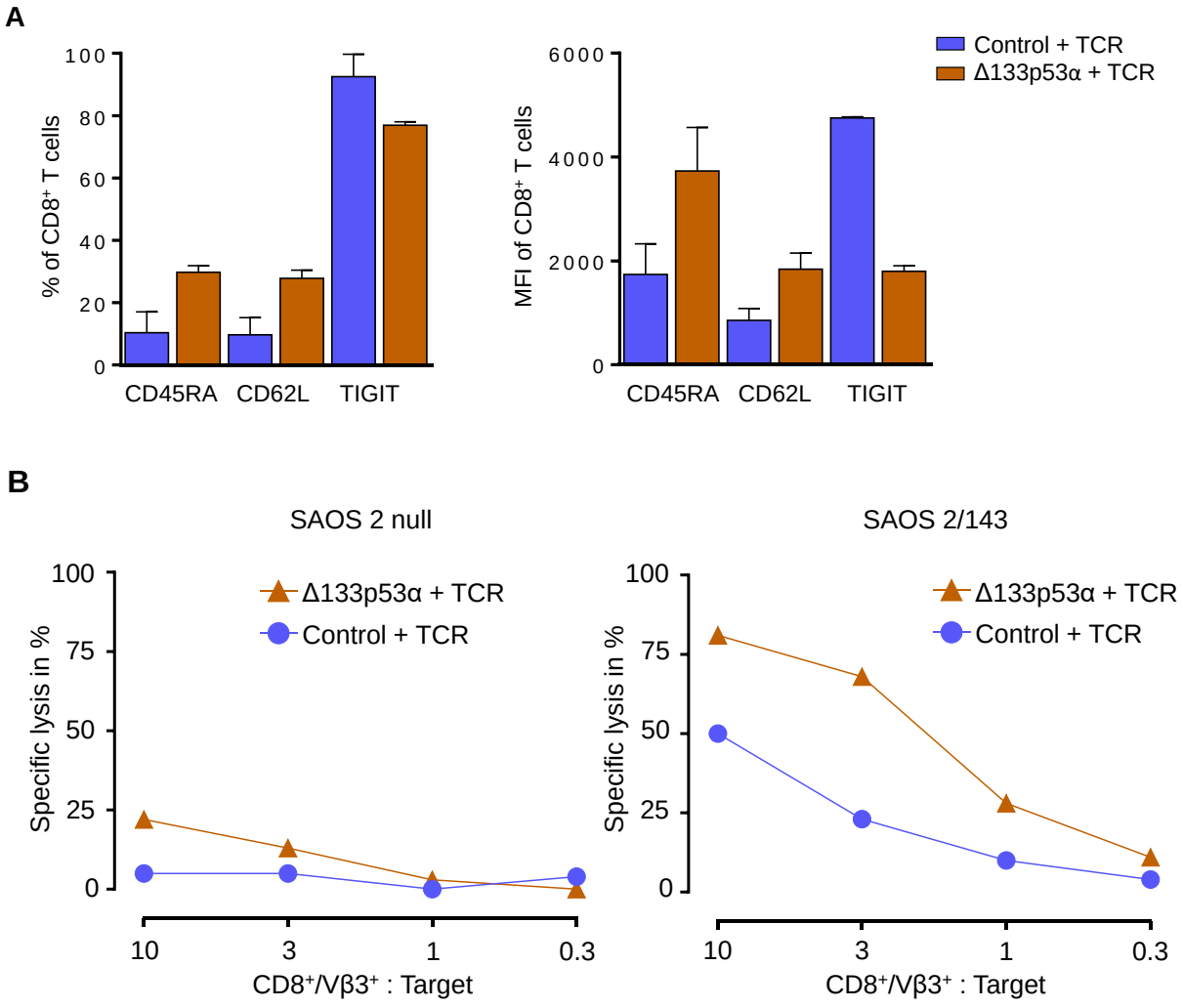

Figure 27: Δ133p53α-overexpression reverts the cellular phenotype in myeloma patient-derived T cells and improves their cytolytic capacity in vitro
(**A**) Bar graphs indicating the expression of CD45RA, CD62L and TIGIT in terms of percentage (left) and MFI (right) of CD8⁺ T cells. CD8⁺ T cells were collected from myeloma patients (MM305 and MM306) and transduced with Δ133p53α or empty vector (bars indicate mean values + standard

deviation of these 2 biological replicates). (**B**) Anti-tumor responses against SAOS 2/143 of p53scTCR^{+} myeloma patient (MM305) T cells with or without Δ133p53α-overexpression. Specific lysis was assessed by chromium-release assay at different E:T ratios. SAOS 2 served as negative control target. Representative of n=2 biological replicates.

6 Discussion

Adoptive transfer of TCR- or CAR-engineered T cells is a promising therapeutic approach for several cancer entities, with impressive clinical responses in some B cell malignancies. However, in a significant proportion of patients, infused T cells often fail to elicit an effective anti-tumor response (127, 128). In the TME, low nutrient availability, tumor-recruited immunosuppressive cells like MDSCs, CAFs and T_{regs} (129) and direct cell-cell interaction with tumor cells induce T cell exhaustion, anergy, terminal differentiation or senescence, features that are characterized by impaired cellular functions (130). Several studies provided growing evidence that T cell replicative potential and differentiation status are important factors that correlate with anti-tumor activity (63, 131-134). Interventions to prevent terminal differentiation and replicative senescence in T cells may therefore enhance anti-tumor responses upon adoptive T cell transfer in cancer patients. In human non-immune cells, the two p53 isoforms p53β and Δ133p53α have been reported to be critical in the regulation of cellular senescence (107). Few studies could demonstrate an association between the expression of different p53 isoforms in tumor cells and clinical prognosis in multiple myeloma, acute myeloid leukemia and breast cancer (106, 110, 113). Only one study to date has investigated the impact of p53 isoform expression on cellular senescence in non-modified, human $CD8^+$ T cells (9). However, it remains unknown how changes in p53 isoform expression influence the differentiation and function of tumor-antigen specific T cells, in particular in the context of a complex suppressive TME. To address this question, this study combined the retroviral introduction of a tumor-antigen specific TCR with overexpression of p53β or Δ133p53α in human T cells, with a particular focus on $CD8^+$ T cells subsets.

6.1 Modulation of T cell senescence by p53 isoforms *in vitro*

First, T cells were co-transduced with a tumor-antigen specific TCR and either p53β or Δ133p53α and characterized for their cellular phenotype and functional aspects. Overexpression of the introduced isoform was verified by western blot, and TCR expression was monitored by flow cytometry. Overexpression of p53β or Δ133p53α did not change the ratio of CD4/CD8 T cells nor influenced surface levels of the introduced TCR. This indicates that the effects observed in the following experiments were not influenced by altered CD4/CD8 or TCR expression. Surface receptors like

CD28 and CD57 were used to discriminate between naïve/less differentiated and senescent/late differentiated T cell subsets (135). While overexpression of p53β reduced the frequency of naïve $CD8^+CD28^+CD57^-$ T cells, transduction with Δ133p53α on the other hand led to an increase in $CD8^+CD28^+CD57^-$ cells and decrease of senescent-like $CD8^+CD28^-CD57^+$ T cells. Other receptors expressed by naïve T cells like CD27, CD62L and CCR7 were also slightly upregulated in Δ133p53α-modified cells. These findings indicate that Δ133p53α expression promotes phenotypes in antigen-specific T cells towards less differentiated cells, while p53β accelerates the onset of differentiation. For most surface markers analyzed, the reported differences between p53 isoform-modified and control T cells were statistically significant, even though fold changes were rather moderate. This might be explained by the fact that bulk T cell populations were used, which mainly included less differentiated $CD28^+CD57^-$ T cells and only a small fraction of late differentiated or senescent T cells. The effect of Δ133p53α-overexpression in an enriched senescent T cell population might have more impact on the phenotype, however transduction of only non-proliferative senescent T cells with retroviral transduction is not effective. To investigate this, other methods such as electroporation with Δ133p53α-mRNA need to be tested. It should also be noted that the changes in the cellular phenotype were observed early after transduction and may change during repetitive antigen-specific stimulation. There may also be differences between the phenotype of T cells cultured *in vitro* compared to freshly isolated cells (rather reflecting the *in vivo* phenotype). For example, T cells ultimately downregulate CD28 expression during the differentiation process *in vitro*, reflecting the phenotype observed in aging healthy individuals (*in vivo*). CD57 expression on the other hand is pronounced in senescent T cells *in vivo* but is hardly expressed on T cells after long-term *in vitro* culture (9). This contradictive phenotypic observation may be due to the proliferative arrest or due to increased apoptosis of $CD57^+$ T cells, finally leading to a loss of this population during *in vitro* culture. To determine the long-term effects of both isoforms *in vitro*, the proliferative capacity of p53 isoform-modified T cells was examined. T cells that overexpressed p53β failed to proliferate over a sustained period and rapidly reached cell cycle arrest, which is consistent with the observed reduction of $CD8^+CD28^+CD57^-$ T cell numbers. Transduction with Δ133p53α led to an enhanced proliferative capacity during chronic tumor antigen stimulation *in vitro*, reflecting its slight induction of a less differentiated cellular phenotype. These differences in the cellular phenotype and proliferative capacity

might be accompanied by metabolic changes, as T cells adapt their metabolism to the functional needs. Naïve T cells are characterized by a quiescent metabolic phenotype with low energy demand, mainly covered through oxidative phosphorylation and fatty acid oxidation (58, 136). Upon activation T cells undergo rapid proliferation with changes in cell size and function, resulting in the engagement of aerobic glycolysis to cover the increased energetic demands (136). In recently published experiments, we observed in polyclonal stimulated Δ133p53α-modified $CD8^+$ T cells a slight reduction of extracellular acidification rate (ECAR, indicating reduced glycolytic activity), as well as oxygen consumption rate (OCR, indicating reduced mitochondrial respiration) early after transduction (117, 137). The rather quiescent metabolic state of these T cells correlates with the cellular phenotype changes and might contribute to the enhanced long-term proliferation. However, further experiments are needed to evaluate the effects of Δ133p53α on the glycolytic and mitochondrial activity. Monitoring the metabolic phenotype during different time points of *in vitro* culture and under several stress conditions like hypoxia, glucose deprivation and in tumor condition medium, combined with the analysis of other mitochondrial (mass, shape, membrane potential) and glycolytic (glucose uptake, receptors, and enzymes) parameters would provide a deeper characterization of the metabolic changes induced by Δ133p53α. Together with transcriptomic analysis, this might facilitate the discovery of potential mechanisms of action. Beside a less differentiated cellular and more quiescent metabolic phenotype, the rate of apoptosis is another important factor that may influence the overall long-term expansion of T cells. At the end of an immune response, expanded effector T cells are typically cleared via apoptosis (138). Also, senescent T cells are prone to apoptosis-induced cell death *in vitro* (139, 140). We therefore analyzed apoptosis in p53β- and Δ133p53α-transduced T cells. Overexpression of p53β resulted in increased rates of apoptosis compared to control T cells, while Δ133p53α-overexpression was associated with reduce apoptotic cell death (117).

Taken together, these experiments suggest that both isoforms are involved and have opposite effects in the regulation of cellular senescence in tumor-antigen specific T cells. Overexpression of p53β mainly accelerates the differentiation of $CD8^+$ T cells, finally leading to a premature cell cycle arrest, while overexpression of Δ133p53α is associated with increased proliferative capacity and less differentiated phenotypes. These observations are in line with previously reported findings in

human fibroblasts (107), human T cells (9) and (for Δ133p53α) even in zebrafish, which naturally express a Δ133p53α-like isoform (141). Several studies proposed that both isoforms, at least partially, regulate senescence through interaction with p53FL. It was reported that p53β can cooperate with p53FL, while Δ133p53α has a dominant-negative effect on p53FL activity (142-144). The interaction with p53FL and with each other may be crucial for the activity of p53 isoforms on cellular functions. Although protein expression of p53FL seems to be unaffected by Δ133p53α- and p53β-overexpression, it has already been reported that Δ133p53α is able to prevent the p53FL-mediated downregulation of CD28 in $CD8^+$ T cells (9). This indicates that effects of Δ133p53α are at least partially mediated through modulation of p53FL function. Only few other mechanisms of action that are not related to p53FL have been described as well (discussed in chapter 6.4). In T cells, mechanisms of action are less well-studied so far.

The observation that Δ133p53α promoted a less differentiated phenotype in $CD8^+$ T cells could be exploited for translational application in T cell-based cancer immunotherapy, as it has been demonstrated that transfer of naïve rather than central memory T cells generated superior anti-tumor responses *in vivo* (14). Retrospective analysis from clinical trials also showed that application of less differentiated T cells was associated with improved *in vivo* persistence and anti-tumor responses of infused T cells (4, 145). Therefore, a major objective of this study was to investigate the effects of Δ133p53α not only on the cellular phenotype but on effector functions of T cells in a cancer immunotherapy model. The capacity of transduced T cells to recognize, secret effector molecules and eliminate target tumor cells was the main functional readout. In long-term killing assays using a human osteosarcoma cell line as target tumor model, p53β-modified T cells exhibited a severely impaired anti-tumor activity. In sharp contrast, overexpression of Δ133p53α led to an improved long-term cytolytic response compared to control T cells. These cytotoxicity assays were performed at the late timepoints of *in vitro* culture when control T cells already exhibited a reduction of proliferation. Therefore Δ133p53α-transduced T cells had a proliferative advantage, which might substantially impact the cytotoxic capacity of the T cells in these experiments. In short-term killing assays early after transduction, anti-tumor responses were not improved by overexpression of Δ133p53α (data not shown). To better understand the effects of Δ133p53α on effector T cell functions, additional parameters including degranulation and cytokine

secretion were evaluated. These experiments revealed that although non-modified control cells hardly proliferated, the cells maintained their capacity to degranulate and secrete major cytokines. However, it could be demonstrated for the first time that Δ133p53α-modified T cells released more lytic effector molecules and higher concentrations of pro-inflammatory and effector cytokines after activation by the target antigen *in vitro* as well as in preclinical *in vivo* tumor model. Besides the enhanced proliferation of Δ133p53α-transduced T cells, this presumably contributed to the improved anti-tumor activity observed in the cytotoxic assays but might also contribute to adverse effects like CRS. Under resting conditions only few cytokines (most prominent IL-2) were secreted at higher concentrations by Δ133p53α-overexpressing T cells. In this setting, concentrations of inflammatory cytokines like IL-6 (data not shown) and IL-1β were not elevated or even lower compared to control T cells. Part of these inflammatory cytokines (including IL-1β and IL-6) belong to the so-called senescence-associated secretory phenotype (SASP) that is a key feature of senescent cells and has detrimental effects on the surrounding tissue microenvironment (146). Whether the secretion of SASP factors is reduced in Δ133p53α-overexpressing tumor-antigen specific T cells (under resting conditions) needs to be further investigated. However, one study already demonstrated that high levels of SASP factors are expressed by senescent ($CD28^{-}CD57^{+}$) T cells and could be reduced in this polyclonal population by reconstitution of Δ133p53α expression (9).

Another aspect which could impact effector functions in the context of tumor-specific cytotoxicity is the expression of inhibitory molecules like PD-1 and TIGIT. These inhibitory molecules, which are expressed by T cells and other immune cells (including NK cells), function as so-called inhibitory immune checkpoints that can restrain immune responses (147). Tumor cells can utilize these receptors by expression of the corresponding ligands (PD-L1 and CD155, respectively). Blocking the interaction of ligands and receptors using specific inhibitors (called immune checkpoint inhibitors) has been shown to boost anti-tumor responses of T cells and are well-established therapies for several cancer entities like renal cell carcinoma or Hodgkin's lymphoma (147, 148). Interestingly, overexpression of Δ133p53α reduced the expression of different immune checkpoint molecules (CD160, TIGIT and to a lesser extent PD-1). To address the inhibitory potential of these molecules on the cytolytic activity of tumor antigen TCR-specific T cells, we used as a tumor model a

target tumor cell line that expresses high levels of the corresponding ligands (CD155 and PD-L1). Further experiments demonstrated that interaction of TIGIT and its ligand CD155 severely impairs tumor eradication in this model. We demonstrated that cell-cell contact, and antigen-dependent activation were required to induce upregulation of TIGIT expression in T cells. Interaction with tumor cells that do not express the target antigen and cell free tumor-conditioned medium did not significantly increase TIGIT expression. Moreover, T cells with high TIGIT expression hardly lysed CD155-expressing target tumor cells. Preventing TIGIT-CD155 interaction with a monoclonal anti-TIGIT blocking antibody restored the anti-tumor responses *in vitro*. Additionally, preclinical studies and clinical data have highlighted the relevance of targeting TIGIT for anti-tumor responses of T cells (149, 150). This illustrates the potential benefit of inhibitory receptor downregulation by Δ133p53α.

6.2 *In vivo* studies of Δ133p53α-overexpression in antigen-specific T cells

Overall, our *in vitro* data indicate that overexpression of Δ133p53α promotes a less differentiated phenotype in $CD8^+$ T cells and is associated with enhanced effector functions and improved anti-tumor cytotoxicity. In a next step, the efficacy of Δ133p53α-transduced T cell was evaluated *in vivo*. Sufficient T cell proliferation is pivotal for clinical efficacy of adoptive T cell therapy, which was demonstrated by studies in mice and humans. Infused T cells must not only reach and recognize their targets but need to expand significantly upon activation (64). Clinical trials in melanoma patients for example reported a correlation between telomere length of infused T cells and anti-tumor efficacy (15, 64). The finite lifespan of T cells due to replicative senescence therefore limits the efficiency of adoptive T cell transfer, a process that may be slowed down by modulation of Δ133p53α. The effects of Δ133p53α overexpression in human T cells were tested in an adoptive T cell transfer approach using a xenograft mouse model of osteosarcoma. In this model, mice receiving Δ133p53α-transduced T cells exhibited a slight survival advantage. In these mice, infused $CD4^+$ and $CD8^+$ T cells also persisted longer in the peripheral blood after transfer (117). However, this enhanced persistence and anti-tumor activity, resulted in severe side effects in some mice, characterized by a loss of fur, reduced mobility, weight loss and eventually death. Similar symptoms are also observed in murine models of graft versus host disease (GvHD) (151) and cytokine release syndrome (CRS) (152). Mice suffering from these adverse effects had also a massive

infiltration of T cells (mainly $CD4^+$ subset) in the spleen. To test if the adverse effects have led to mono- or oligoclonal proliferation of alloreactive T cells, the TCR expression pattern was analyzed. Analysis of the TCR repertoire however revealed a polyclonal T cell response. In further experiments, serum of the affected mice was collected to measure concentrations of different cytokines. Remarkably, the adverse events were associated with excessive amounts of cytokines secreted by the infused T cells. Especially the increased levels of inflammatory cytokines like IL-6 are commonly observed in CRS after CAR-T cell therapy (153). Similar observations of hyperinflammation were made in a murine model of Δ133p53α (154). As mice naturally lack a human Δ133p53-equivalent isoform (155), the authors generated a mouse expressing an isoform, which lacks the first 122 amino acids (Δ122p53) and mimics the functions of Δ133p53 proteins. These mice developed different inflammatory pathologies, lymphocyte aggregations and high serum concentrations of pro-inflammatory cytokines. Pro-proliferative and anti-apoptotic proteins were upregulated in PBMCs isolated from Δ122p53 mice (154). These findings show similarities between the Δ133p53α and Δ122p53 proteins, however Δ122p53 encodes for two different proteins. Due to alternative splicing, Δ122p53 can generate Δ122p53α and Δ122p53AS (an equivalent to Δ133p53β), therefore the observed effects could be induced by one or both proteins (154, 156). To overcome these and other potential adverse events, safety approaches may be necessary. Interleukin-induced hyperinflammation could be addressed by monoclonal antibodies like Tocilizumab, a humanized antibody against the IL-6 receptor (157). Excessive proliferation, oncogenic events as well as off-target toxicities could be terminated by applying an inducible caspase 9 “safety switch” system (10).

6.3 Δ133p53α in cancer patient derived senescent T cells

After testing adoptive transfer of Δ133p53α-modified T cells in this xenograft tumor model, we evaluated if the approach of modulating p53 isoform expression is applicable to regulate T cell differentiation and function in cancer patient derived T cells. A study could already demonstrate that non-proliferative $CD8^+CD28^-CD57^+$ T cells accumulate in the peripheral blood of healthy individuals as a function of age (9). These terminally differentiated T cells have an increased expression of p53β and a reduced expression of Δ133p53α protein. In the same study, the authors isolated

$CD8^+CD28^-CD57^+$ T cells from lung cancer tissue and observed elevated levels of p53β and low levels of Δ133p53α isoform (9).

Terminally differentiated and senescent T cells accumulate also in the peripheral blood of patients suffering from other malignancies such as multiple myeloma (5). Therefore, we collected PBMCs isolated from healthy donors which contained low or moderate numbers of $CD8^+CD28^-CD57^+$ T cells and compared them with PBMCs collected from newly diagnosed (without treatment) myeloma patients, which revealed increased numbers of this T cell subset. The patient-derived T cells (mainly late differentiated $CD28^-CD57^+$ subset) harbored very low to no Δ133p53α expression at the protein level, while T cells from healthy individuals (mainly early differentiated $CD28^+CD57^-$ subset) mostly showed a strong expression of this isoform. This supports the idea that p53 isoforms are not only involved in the "natural" process of senescence in the context of aging but also contribute to senescence in pathologic conditions like cancer. However, it should be considered that the sample size was rather small (10 patients and 5 healthy donors), and patient/control samples were not matched for influencing factors like donor age and gender. The age of patients and healthy donors was not compared, as this information was not available. We cannot exclude that the (presumably old) age of myeloma patients might have contributed to the high frequency of senescent T cells and isoform expression. In future studies, a detailed comparison of more and age matched samples would be helpful. Also, bone marrow samples could provide more insight into T cell senescence in myeloma patients as the micromilieu of malignant and bystander cells might induce or at least favor the onset of T cell senescence.

Another approach to investigate the relevance of manipulating Δ133p53α expression in patient samples was to restore Δ133p53α protein levels by retroviral transduction. Experiments conducted in this regard have largely reflected the observations we have made in healthy donor T cells. The relatively low expression of T cell markers associated with early differentiation state like CD45RA and CD62L in myeloma patient T cells could be increased upon transduction with Δ133p53α. Concomitantly, high expression of TIGIT in non-modified myeloma patient T cells decreased upon transduction. This partial "rejuvenation" of late differentiated/senescent T cells from cancer patients might also improve T cell functions and could offer a significant improvement for autologous T cell-based immunotherapies. Indeed, the myeloma

patient-derived T cells acquired a superior cytotoxic capacity after overexpression of Δ133p53α, further supporting the feasibility of (at least partially) reverting senescence-induced T cell dysfunction by modulation of p53 isoform expression.

6.4 Δ133p53α isoform's mechanism of action

Taken together, the experiments performed in this study indicate that overexpression of Δ133p53α is associated with delayed onset of cellular senescence and can revert senescence in dysfunctional $CD8^+$ T cells from cancer patients. However, the exact mechanisms that lead to the improved anti-tumor cytotoxicity of Δ133p53α-modified T cells remain unclear. Therefore, it would be important to identify pathways or single factors that are directly regulated by Δ133p53α in further studies. Several studies suggested that Δ133p53α regulates the expression of p53 target genes through a dominant-negative effect on p53FL (103, 107), which may explain the delay of cellular senescence. Δ133p53α isoform lacks the transactivation as well as a part of the DNA-binding domain, but contains the C-terminal oligomerization domain of p53FL (103) and was shown to form hetero-oligomers with p53FL (158). Subsequent studies have shown that overexpression of Δ133p53α reduces expression of p53 target genes like $p21^{WAF1/CIP1}$ (143), confirming previously reported findings (107). The protein p21 is a strong cyclin-dependent kinase inhibitor (CDKI) and suppresses cell cycle progression through inhibition of cyclin/cdk2 complexes (159-161). In recently published experiments, we could demonstrate the downregulation of p21 upon Δ133p53α-overexpression in human T cells (117). Repression of this p53FL-induced cell cycle inhibitor illustrates one aspect of the enhanced proliferative capacity associated with Δ133p53α overexpression. Another main regulator of p53 function is the ubiquitin E3-ligase MDM2 that was shown to interact with p53 isoforms (162). MDM2 promotes the ubiquitin-dependent degradation of p53FL (163). Later it was demonstrated that MDM2 can promote ubiquitination and degradation of only one isoform (p53β), while other isoforms are not degraded via this interaction. On the other hand, it can mediate NEDDylation of p53β, protecting it from proteasome degradation (162). Although MDM2 did not promote degradation of p53 isoforms other than p53β, all isoforms bind to MDM2 including Δ133p53α that showed a weak but consistent interaction (162). As we could demonstrate, Δ133p53α overexpression in T cells is also associated with reduced expression with MDM2 (117), while expression of p53FL remains unchanged (9). Whether Δ133p53α

interacts with other molecules or can function as a p53-independent transcription factor by direct binding to specific DNA regions remains to be determined. However, we conducted first experiments to evaluate possible changes in Δ133p53α-induced histone modifications (117). Changes in active (H3K4me3) or repressive (H3K9me3) histone marks could influence the gene expression (164) and contribute to the effects of Δ133p53α overexpression. Although our results showed no significant differences in H3K9me3a, a slight increase in H3K4me3 was observed, potentially leading to an increased number of active genes and subsequent transcription in Δ133p53α-transduced T cells (117).

It is reasonable to consider that p53 isoforms do not act as single factors, but rather regulate different cellular processes by interacting with each other and with p53FL. ~~Name~~, one of the leaders in the field of p53 isoforms, described p53 as “an ensemble of different oligomers, each composed of distinct p53 protein isoforms”, with each oligomer having “a different intrinsic transcriptional activity and promoter specificity” (cited from (165)). The subtle coordinated activities of p53 isoform oligomers therefore define the p53-mediated cell-response (102, 165). Another important aspect is that functions of p53 isoforms are cell-type specific (102), and most studies were performed with non-immune cells or even non-human cells. Further studies are needed to confirm mechanisms of p53 isoform function in T cells and other immune cells. In general, it is challenging to attribute a specific function to a single isoform. Thus, considering the cellular context and co-expression of other isoforms seems pivotal for p53 isoform functions. Furthermore, Δ133p53α-mRNA transcription is regulated by epigenetic events (103) as well as by p53α and p63/p73 family members via transactivation of the internal promotor (142, 166). For example, one study identified that Δ133p53α and the p53 related protein p73 form complexes that promote DNA double strand break repair mechanisms after γ-irradiation in tumor cell lines (167). This cooperation with p73 might also contribute to an enhanced proliferative capacity but needs to be demonstrated in T cells. At a functional level, total Δ133p53 mRNA expression is increased in different human cancers and is associated with disease progression (142), raising the question of oncogenic properties of this isoforms. In this regard, promotion of malignant tumor formation would make Δ133p53α an inappropriate target for genetic manipulation in T cell-based adoptive therapy. However, studies to date in normal human cells have not reported oncogenic nor mutagenic properties of Δ133p53α (142). Two studies

reported that Δ133p53α-overexpression was not only enhancing generation of induced pluripotent stem cells (iPSCs) from differentiated cells, but even reduced chromosomal aberrations in these cells (168, 169). During the DNA-damage response, a well-known source of cellular senescence (170), Δ133p53α is involved in the promotion of the DNA double-strand break repair via upregulation of different repair genes (171). Finally, *in vitro* findings of our study indicate that Δ133p53α-overexpression prolongs the life span of normal human T cells and restores proliferation of terminal differentiated T cells without inducing malignant transformation in the modified cells.

6.5 Conclusion

Improving the “fitness” and functionality of tumor antigen receptor-engineered T cells is pivotal for effective T cell-based cancer immunotherapy. Several studies identified Δ133p53α as a naturally expressed isoform which is involved in the regulation of proliferation, differentiation, and senescence in different human cells and suggested its modulation as a presumably safe method for preventing premature proliferation arrest (9, 107, 143). The findings of this thesis further support the role of Δ133p53α as a key regulator of T cell “fitness” and functional properties. Δ133p53α-transduced T cells acquired a long-term proliferative capacity, increased secretion of cytokines and effector molecules, as well as a superior tumor-specific cytotoxicity. Of course, repeating experiments with more biological replicates, ideally with mainly senescent T cells, could further increase the evidence of this hypothesis. Additionally, follow up experiments are needed for deeper characterization of p53 isoform functions in T cells and the mechanisms of action that mediate Δ133p53α functions. The observed effects may also be enhanced by combination with for example optimized stimulation via Interleukin-15 (172) or checkpoint-blockade (173). Safety issues may be addressed by application of suicide genes (10) or targeting Δ133p53α-expression with small-molecule compounds (174). Overall, the data presented in this thesis work offer a novel, feasible and promising approach to improve T cell functionality for cell-based cancer immunotherapy and potentially broad application beyond.

7 Reference List

1. Sung H, Ferlay J, Siegel RL, Laversanne M, Soerjomataram I, Jemal A, Bray F. Global Cancer Statistics 2020: GLOBOCAN Estimates of Incidence and Mortality Worldwide for 36 Cancers in 185 Countries. CA Cancer J Clin. 2021;71(3):209-249 10.3322/caac.21660.
2. Restifo NP, Dudley ME, Rosenberg SA. Adoptive immunotherapy for cancer: harnessing the T cell response. Nat Rev Immunol. 2012;12(4):269-281 10.1038/nri3191.
3. Pitt JM, Marabelle A, Eggermont A, Soria JC, Kroemer G, Zitvogel L. Targeting the tumor microenvironment: removing obstruction to anticancer immune responses and immunotherapy. Ann Oncol. 2016;27(8):1482-1492 10.1093/annonc/mdw168.
4. Klebanoff CA, Gattinoni L, Restifo NP. Sorting through subsets: which T-cell populations mediate highly effective adoptive immunotherapy? J Immunother. 2012;35(9):651-660 10.1097/CJI.0b013e31827806e6.
5. Suen H, Brown R, Yang S, Weatherburn C, Ho PJ, Woodland N, Nassif N, Barbaro P, Bryant C, Hart D, Gibson J, Joshua D. Multiple myeloma causes clonal T-cell immunosenescence: identification of potential novel targets for promoting tumour immunity and implications for checkpoint blockade. Leukemia. 2016;30(8):1716-1724 10.1038/leu.2016.84.
6. Effros RB, Dagarag M, Spaulding C, Man J. The role of CD8+ T-cell replicative senescence in human aging. Immunol Rev. 2005;205:147-157 10.1111/j.0105-2896.2005.00259.x.
7. Courtois-Cox S, Jones SL, Cichowski K. Many roads lead to oncogene-induced senescence. Oncogene. 2008;27(20):2801-2809 10.1038/sj.onc.1210950.
8. Levine AJ. p53, the cellular gatekeeper for growth and division. Cell. 1997;88(3):323-331 10.1016/s0092-8674(00)81871-1.
9. Mondal AM, Horikawa I, Pine SR, Fujita K, Morgan KM, Vera E, Mazur SJ, Appella E, Vojtesek B, Blasco MA, Lane DP, Harris CC. p53 isoforms regulate aging- and tumor-associated replicative senescence in T lymphocytes. J Clin Invest. 2013;123(12):5247-5257 10.1172/JCI70355.
10. Di Stasi A, Tey SK, Dotti G, Fujita Y, Kennedy-Nasser A, Martinez C, Straathof K, Liu E, Durett AG, Grilley B, Liu H, Cruz CR, Savoldo B, Gee AP, Schindler J, Krance RA, Heslop HE, Spencer DM, Rooney CM, Brenner MK. Inducible apoptosis as a safety switch for adoptive cell therapy. N Engl J Med. 2011;365(18):1673-1683 10.1056/NEJMoa1106152.
11. Sudhakar A. History of Cancer, Ancient and Modern Treatment Methods. J Cancer Sci Ther. 2009;1(2):1-4 10.4172/1948-5956.100000e2.
12. Hanahan D, Weinberg RA. Hallmarks of Cancer: The Next Generation. Cell. 2011;144(5):646-674 10.1016/j.cell.2011.02.013.
13. Gattinoni L, Klebanoff CA, Palmer DC, Wrzesinski C, Kerstann K, Yu Z, Finkelstein SE, Theoret MR, Rosenberg SA, Restifo NP. Acquisition of full effector function in vitro paradoxically impairs the in vivo antitumor efficacy of adoptively transferred CD8+ T cells. J Clin Invest. 2005;115(6):1616-1626 10.1172/JCI24480.
14. Hinrichs CS, Borman ZA, Cassard L, Gattinoni L, Spolski R, Yu Z, Sanchez-Perez L, Muranski P, Kern SJ, Logun C, Palmer DC, Ji Y, Reger RN, Leonard WJ, Danner RL, Rosenberg SA, Restifo NP. Adoptively transferred effector cells derived from naive rather than central memory CD8+ T cells mediate superior antitumor immunity. Proc Natl Acad Sci U S A. 2009;106(41):17469-17474 10.1073/pnas.0907448106.
15. Zhou J, Shen X, Huang J, Hodes RJ, Rosenberg SA, Robbins PF. Telomere length of transferred lymphocytes correlates with in vivo persistence and tumor regression in melanoma patients receiving cell transfer therapy. J Immunol. 2005;175(10):7046-7052
16. June CH. Principles of adoptive T cell cancer therapy. J Clin Invest. 2007;117(5):1204-1212 10.1172/jci31446.
17. Lane D, Levine A. p53 Research: the past thirty years and the next thirty years. Cold Spring Harb Perspect Biol. 2010;2(12):a000893 10.1101/cshperspect.a000893.

18. Lizee G, Overwijk WW, Radvanyi L, Gao J, Sharma P, Hwu P. Harnessing the power of the immune system to target cancer. Annu Rev Med. 2013;64:71-90 10.1146/annurev-med-112311-083918.
19. Ehrlich P. Ueber den jetzigen Stand der Karzinomforschung1908.
20. Dunn GP, Bruce AT, Ikeda H, Old LJ, Schreiber RD. Cancer immunoediting: from immunosurveillance to tumor escape. Nat Immunol. 2002;3:991 10.1038/ni1102-991.
21. Burnet M. Cancer: a biological approach. III. Viruses associated with neoplastic conditions. IV. Practical applications. Br Med J. 1957;1(5023):841-847
22. Burnet FM. The concept of immunological surveillance. Prog Exp Tumor Res. 1970;13:1-27
23. Burnet M. Immunological factors in the process of carcinogenesis. Br Med Bull. 1964;20:154-158
24. Shinkai Y, Rathbun G, Lam KP, Oltz EM, Stewart V, Mendelsohn M, Charron J, Datta M, Young F, Stall AM, et al. RAG-2-deficient mice lack mature lymphocytes owing to inability to initiate V(D)J rearrangement. Cell. 1992;68(5):855-867
25. Shankaran V, Ikeda H, Bruce AT, White JM, Swanson PE, Old LJ, Schreiber RD. IFNgamma and lymphocytes prevent primary tumour development and shape tumour immunogenicity. Nature. 2001;410(6832):1107-1111 10.1038/35074122.
26. Birkeland SA, Storm HH, Lamm LU, Barlow L, Blohme I, Forsberg B, Eklund B, Fjeldborg O, Friedberg M, Frodin L, et al. Cancer risk after renal transplantation in the Nordic countries, 1964-1986. Int J Cancer. 1995;60(2):183-189
27. Clark WH, Jr., Elder DE, Guerry Dt, Braitman LE, Trock BJ, Schultz D, Synnestvedt M, Halpern AC. Model predicting survival in stage I melanoma based on tumor progression. J Natl Cancer Inst. 1989;81(24):1893-1904
28. Clemente CG, Mihm Jr. MC, Bufalino R, Zurrida S, Collini P, Cascinelli N. Prognostic value of tumor infiltrating lymphocytes in the vertical growth phase of primary cutaneous melanoma. Cancer. 1996;77(7):1303-1310 doi:10.1002/(SICI)1097-0142(19960401)77:7<1303::AID-CNCR12>3.0.CO;2-5.
29. Sato E, Olson SH, Ahn J, Bundy B, Nishikawa H, Qian F, Jungbluth AA, Frosina D, Gnjatic S, Ambrosone C, Kepner J, Odunsi T, Ritter G, Lele S, Chen YT, Ohtani H, Old LJ, Odunsi K. Intraepithelial CD8+ tumor-infiltrating lymphocytes and a high CD8+/regulatory T cell ratio are associated with favorable prognosis in ovarian cancer. Proc Natl Acad Sci U S A. 2005;102(51):18538-18543 10.1073/pnas.0509182102.
30. Rodriguez Perez A, Campillo-Davo D, Van Tendeloo VFI, Benitez-Ribas D. Cellular immunotherapy: a clinical state-of-the-art of a new paradigm for cancer treatment. Clin Transl Oncol. 2020;22(11):1923-1937 10.1007/s12094-020-02344-4.
31. Rosenberg SA, Packard BS, Aebersold PM, Solomon D, Topalian SL, Toy ST, Simon P, Lotze MT, Yang JC, Seipp CA, et al. Use of tumor-infiltrating lymphocytes and interleukin-2 in the immunotherapy of patients with metastatic melanoma. A preliminary report. N Engl J Med. 1988;319(25):1676-1680 10.1056/nejm198812223192527.
32. Duong CP, Yong CS, Kershaw MH, Slaney CY, Darcy PK. Cancer immunotherapy utilizing gene-modified T cells: From the bench to the clinic. Mol Immunol. 2015;67(2 Pt A):46-57 10.1016/j.molimm.2014.12.009.
33. Topalian SL, Solomon D, Avis FP, Chang AE, Freerksen DL, Linehan WM, Lotze MT, Robertson CN, Seipp CA, Simon P, et al. Immunotherapy of patients with advanced cancer using tumor-infiltrating lymphocytes and recombinant interleukin-2: a pilot study. J Clin Oncol. 1988;6(5):839-853 10.1200/jco.1988.6.5.839.
34. Rosenberg SA, Aebersold P, Cornetta K, Kasid A, Morgan RA, Moen R, Karson EM, Lotze MT, Yang JC, Topalian SL, Merino MJ, Culver K, Miller AD, Blaese RM, Anderson WF. Gene Transfer into Humans — Immunotherapy of Patients with Advanced Melanoma, Using Tumor-Infiltrating Lymphocytes Modified by Retroviral Gene Transduction. N Engl J Med. 1990;323(9):570-578 10.1056/nejm199008303230904.
35. Walia V, Mu EW, Lin JC, Samuels Y. Delving into somatic variation in sporadic melanoma. Pigment cell & melanoma research. 2012;25(2):155-170 10.1111/j.1755-148X.2012.00976.x.

36. Spear TT, Evavold BD, Baker BM, Nishimura MI. Understanding TCR affinity, antigen specificity, and cross-reactivity to improve TCR gene-modified T cells for cancer immunotherapy. Cancer Immunol Immunother. 2019;68(11):1881-1889 10.1007/s00262-019-02401-0.
37. Kuball J, Schmitz FW, Voss RH, Ferreira EA, Engel R, Guillaume P, Strand S, Romero P, Huber C, Sherman LA, Theobald M. Cooperation of human tumor-reactive CD4+ and CD8+ T cells after redirection of their specificity by a high-affinity p53A2.1-specific TCR. Immunity. 2005;22(1):117-129 10.1016/j.immuni.2004.12.005.
38. Theobald M, Biggs J, Dittmer D, Levine AJ, Sherman LA. Targeting p53 as a general tumor antigen. Proc Natl Acad Sci U S A. 1995;92(26):11993-11997 10.1073/pnas.92.26.11993.
39. Stanislawski T, Voss RH, Lotz C, Sadovnikova E, Willemsen RA, Kuball J, Ruppert T, Bolhuis RL, Melief CJ, Huber C, Stauss HJ, Theobald M. Circumventing tolerance to a human MDM2-derived tumor antigen by TCR gene transfer. Nat Immunol. 2001;2(10):962-970 10.1038/ni1001-962.
40. Johnson LA, Morgan RA, Dudley ME, Cassard L, Yang JC, Hughes MS, Kammula US, Royal RE, Sherry RM, Wunderlich JR, Lee CC, Restifo NP, Schwarz SL, Cogdill AP, Bishop RJ, Kim H, Brewer CC, Rudy SF, VanWaes C, Davis JL, Mathur A, Ripley RT, Nathan DA, Laurencot CM, Rosenberg SA. Gene therapy with human and mouse T-cell receptors mediates cancer regression and targets normal tissues expressing cognate antigen. Blood. 2009;114(3):535-546 10.1182/blood-2009-03-211714.
41. Morgan RA, Dudley ME, Wunderlich JR, Hughes MS, Yang JC, Sherry RM, Royal RE, Topalian SL, Kammula US, Restifo NP, Zheng Z, Nahvi A, de Vries CR, Rogers-Freezer LJ, Mavroukakis SA, Rosenberg SA. Cancer regression in patients after transfer of genetically engineered lymphocytes. Science. 2006;314(5796):126-129 10.1126/science.1129003.
42. Met O, Jensen KM, Chamberlain CA, Donia M, Svane IM. Principles of adoptive T cell therapy in cancer. Semin Immunopathol. 2019;41(1):49-58 10.1007/s00281-018-0703-z.
43. Svane I, Donia M, Met Ö. Adoptive T Cell Therapy in: Haanen JBAG, Califano R, Lugowska I, Garassino MC (eds). ESMO handbook of immuno-oncology. Lugano: ESMO Press, 2018. Reprinted with permission from the European Society for Medical Oncology; ©; 2018. p. 15–22.
44. Bendle GM, Linnemann C, Hooijkaas AI, Bies L, de Witte MA, Jorritsma A, Kaiser AD, Pouw N, Debets R, Kieback E, Uckert W, Song JY, Haanen JB, Schumacher TN. Lethal graft-versus-host disease in mouse models of T cell receptor gene therapy. Nat Med. 2010;16(5):565-570, 561p following 570 10.1038/nm.2128.
45. Bubenik J. MHC class I down-regulation: tumour escape from immune surveillance? (review). Int J Oncol. 2004;25(2):487-491
46. June CH, O'Connor RS, Kawalekar OU, Ghassemi S, Milone MC. CAR T cell immunotherapy for human cancer. Science. 2018;359(6382):1361-1365 10.1126/science.aar6711.
47. Gross G, Gorochov G, Waks T, Eshhar Z. Generation of effector T cells expressing chimeric T cell receptor with antibody type-specificity. Transplant Proc. 1989;21(1 Pt 1):127-130
48. Courtney AH, Lo WL, Weiss A. TCR Signaling: Mechanisms of Initiation and Propagation. Trends Biochem Sci. 2018;43(2):108-123 10.1016/j.tibs.2017.11.008.
49. Chen L, Flies DB. Molecular mechanisms of T cell co-stimulation and co-inhibition. Nat Rev Immunol. 2013;13(4):227-242 10.1038/nri3405.
50. Brentjens RJ, Davila ML, Riviere I, Park J, Wang X, Cowell LG, Bartido S, Stefanski J, Taylor C, Olszewska M, Borquez-Ojeda O, Qu J, Wasielewska T, He Q, Bernal Y, Rijo IV, Hedvat C, Kobos R, Curran K, Steinherz P, Jurcic J, Rosenblat T, Maslak P, Frattini M, Sadelain M. CD19-targeted T cells rapidly induce molecular remissions in adults with chemotherapy-refractory acute lymphoblastic leukemia. Sci Transl Med. 2013;5(177):177ra138 10.1126/scitranslmed.3005930.
51. Kochenderfer JN, Wilson WH, Janik JE, Dudley ME, Stetler-Stevenson M, Feldman SA, Maric I, Raffeld M, Nathan DA, Lanier BJ, Morgan RA, Rosenberg SA. Eradication of B-lineage cells and

regression of lymphoma in a patient treated with autologous T cells genetically engineered to recognize CD19. Blood. 2010;116(20):4099-4102 10.1182/blood-2010-04-281931.
52. Porter DL, Levine BL, Kalos M, Bagg A, June CH. Chimeric antigen receptor-modified T cells in chronic lymphoid leukemia. N Engl J Med. 2011;365(8):725-733 10.1056/NEJMoa1103849.
53. Lee DW, Kochenderfer JN, Stetler-Stevenson M, Cui YK, Delbrook C, Feldman SA, Fry TJ, Orentas R, Sabatino M, Shah NN, Steinberg SM, Stroncek D, Tschernia N, Yuan C, Zhang H, Zhang L, Rosenberg SA, Wayne AS, Mackall CL. T cells expressing CD19 chimeric antigen receptors for acute lymphoblastic leukaemia in children and young adults: a phase 1 dose-escalation trial. Lancet. 2015;385(9967):517-528 10.1016/s0140-6736(14)61403-3.
54. Grupp SA, Kalos M, Barrett D, Aplenc R, Porter DL, Rheingold SR, Teachey DT, Chew A, Hauck B, Wright JF, Milone MC, Levine BL, June CH. Chimeric antigen receptor-modified T cells for acute lymphoid leukemia. N Engl J Med. 2013;368(16):1509-1518 10.1056/NEJMoa1215134.
55. Beatty GL, Gladney WL. Immune escape mechanisms as a guide for cancer immunotherapy. Clin Cancer Res. 2015;21(4):687-692 10.1158/1078-0432.CCR-14-1860.
56. Hanahan D, Coussens LM. Accessories to the crime: functions of cells recruited to the tumor microenvironment. Cancer Cell. 2012;21(3):309-322 10.1016/j.ccr.2012.02.022.
57. Gajewski TF, Schreiber H, Fu YX. Innate and adaptive immune cells in the tumor microenvironment. Nat Immunol. 2013;14(10):1014-1022 10.1038/ni.2703.
58. Buck MD, O'Sullivan D, Pearce EL. T cell metabolism drives immunity. J Exp Med. 2015;212(9):1345-1360 10.1084/jem.20151159.
59. Thommen DS, Schumacher TN. T Cell Dysfunction in Cancer. Cancer Cell. 2018;33(4):547-562 10.1016/j.ccell.2018.03.012.
60. Westendorf AM, Skibbe K, Adamczyk A, Buer J, Geffers R, Hansen W, Pastille E, Jendrossek V. Hypoxia Enhances Immunosuppression by Inhibiting CD4+ Effector T Cell Function and Promoting Treg Activity. Cell Physiol Biochem. 2017;41(4):1271-1284 10.1159/000464429.
61. Scharping NE, Delgoffe GM. Tumor Microenvironment Metabolism: A New Checkpoint for Anti-Tumor Immunity. Vaccines (Basel). 2016;4(4) 10.3390/vaccines4040046.
62. Kato Y, Ozawa S, Miyamoto C, Maehata Y, Suzuki A, Maeda T, Baba Y. Acidic extracellular microenvironment and cancer. Cancer Cell Int. 2013;13(1):89 10.1186/1475-2867-13-89.
63. Kishton RJ, Sukumar M, Restifo NP. Metabolic Regulation of T Cell Longevity and Function in Tumor Immunotherapy. Cell Metab. 2017;26(1):94-109 10.1016/j.cmet.2017.06.016.
64. Lim WA, June CH. The Principles of Engineering Immune Cells to Treat Cancer. Cell. 2017;168(4):724-740 10.1016/j.cell.2017.01.016.
65. Porter DL, Hwang WT, Frey NV, Lacey SF, Shaw PA, Loren AW, Bagg A, Marcucci KT, Shen A, Gonzalez V, Ambrose D, Grupp SA, Chew A, Zheng Z, Milone MC, Levine BL, Melenhorst JJ, June CH. Chimeric antigen receptor T cells persist and induce sustained remissions in relapsed refractory chronic lymphocytic leukemia. Sci Transl Med. 2015;7(303):303ra139 10.1126/scitranslmed.aac5415.
66. Schwartz RH. T cell anergy. Annu Rev Immunol. 2003;21:305-334 10.1146/annurev.immunol.21.120601.141110.
67. Fourcade J, Sun Z, Pagliano O, Guillaume P, Luescher IF, Sander C, Kirkwood JM, Olive D, Kuchroo V, Zarour HM. CD8(+) T cells specific for tumor antigens can be rendered dysfunctional by the tumor microenvironment through upregulation of the inhibitory receptors BTLA and PD-1. Cancer Res. 2012;72(4):887-896 10.1158/0008-5472.CAN-11-2637.
68. Woo SR, Turnis ME, Goldberg MV, Bankoti J, Selby M, Nirschl CJ, Bettini ML, Gravano DM, Vogel P, Liu CL, Tangsombatvisit S, Grosso JF, Netto G, Smeltzer MP, Chaux A, Utz PJ, Workman CJ, Pardoll DM, Korman AJ, Drake CG, Vignali DA. Immune inhibitory molecules LAG-3 and PD-1 synergistically regulate T-cell function to promote tumoral immune escape. Cancer Res. 2012;72(4):917-927 10.1158/0008-5472.CAN-11-1620.
69. Larkin J, Chiarion-Sileni V, Gonzalez R, Grob JJ, Cowey CL, Lao CD, Schadendorf D, Dummer R, Smylie M, Rutkowski P, Ferrucci PF, Hill A, Wagstaff J, Carlino MS, Haanen JB, Maio M, Marquez-Rodas I, McArthur GA, Ascierto PA, Long GV, Callahan MK, Postow MA, Grossmann K, Sznol M, Dreno B, Bastholt L, Yang A, Rollin LM, Horak C, Hodi FS, Wolchok JD. Combined

Nivolumab and Ipilimumab or Monotherapy in Untreated Melanoma. N Engl J Med. 2015;373(1):23-34 10.1056/NEJMoa1504030.
70. Song Y, Wang B, Song R, Hao Y, Wang D, Li Y, Jiang Y, Xu L, Ma Y, Zheng H, Kong Y, Zeng H. T-cell Immunoglobulin and ITIM Domain Contributes to CD8(+) T-cell Immunosenescence. Aging Cell. 2018;17(2) 10.1111/acel.12716.
71. AdvanTIG-202: Anti-PD-1 Monoclonal Antibody Tislelizumab (BGB-A317) Combined With or Without Anti-TIGIT Monoclonal Antibody Ociperlimab (BGB-A1217) in Participants With Previously Treated Recurrent or Metastatic Cervical Cancer. https://ClinicalTrials.gov/show/NCT04693234.
72. A Study to Assess the Safety and Efficacy of AZD2936 in Participants With Advanced or Metastatic Non-small Cell Lung Cancer (NSCLC). https://ClinicalTrials.gov/show/NCT04995523.
73. Zimberelimab (AB122) With TIGIT Inhibitor Domvanalimab (AB154) in PD-1 Relapsed/Refractory Melanoma. https://ClinicalTrials.gov/show/NCT05130177.
74. Immuno-Oncology Drugs Elotuzumab, Anti-LAG-3 and Anti-TIGIT. https://ClinicalTrials.gov/show/NCT04150965.
75. Montes CL, Chapoval AI, Nelson J, Orhue V, Zhang X, Schulze DH, Strome SE, Gastman BR. Tumor-induced senescent T cells with suppressor function: a potential form of tumor immune evasion. Cancer Res. 2008;68(3):870-879 10.1158/0008-5472.Can-07-2282.
76. Tsukishiro T, Donnenberg AD, Whiteside TL. Rapid turnover of the CD8(+)CD28(-) T-cell subset of effector cells in the circulation of patients with head and neck cancer. Cancer Immunol Immunother. 2003;52(10):599-607 10.1007/s00262-003-0395-6.
77. Ye J, Peng G. Controlling T cell senescence in the tumor microenvironment for tumor immunotherapy. Oncoimmunology. 2015;4(3):e994398 10.4161/2162402x.2014.994398.
78. Pawelec G. Hallmarks of human "immunosenescence": adaptation or dysregulation? Immun Ageing. 2012;9(1):15 10.1186/1742-4933-9-15.
79. Grubeck-Loebenstein B, Della Bella S, Iorio AM, Michel JP, Pawelec G, Solana R. Immunosenescence and vaccine failure in the elderly. Aging Clin Exp Res. 2009;21(3):201-209
80. Ginaldi L, Loreto MF, Corsi MP, Modesti M, De Martinis M. Immunosenescence and infectious diseases. Microbes and infection. 2001;3(10):851-857
81. Moreira A, Gross S, Kirchberger MC, Erdmann M, Schuler G, Heinzerling L. Senescence markers: Predictive for response to checkpoint inhibitors. Int J Cancer. 2019;144(5):1147-1150 10.1002/ijc.31763.
82. Huff WX, Kwon JH, Henriquez M, Fetcko K, Dey M. The Evolving Role of CD8(+)CD28(-) Immunosenescent T Cells in Cancer Immunology. Int J Mol Sci. 2019;20(11) 10.3390/ijms20112810.
83. Akbar AN, Henson SM, Lanna A. Senescence of T Lymphocytes: Implications for Enhancing Human Immunity. Trends Immunol. 2016;37(12):866-876 10.1016/j.it.2016.09.002.
84. Hayflick L, Moorhead PS. The serial cultivation of human diploid cell strains. Exp Cell Res. 1961;25:585-621
85. Shay JW, Wright WE. Hayflick, his limit, and cellular ageing. Nat Rev Mol Cell Biol. 2000;1(1):72-76 10.1038/35036093.
86. Harley CB, Vaziri H, Counter CM, Allsopp RC. The telomere hypothesis of cellular aging. Exp Gerontol. 1992;27(4):375-382 10.1016/0531-5565(92)90068-b.
87. Collado M, Blasco MA, Serrano M. Cellular senescence in cancer and aging. Cell. 2007;130(2):223-233 10.1016/j.cell.2007.07.003.
88. Childs BG, Durik M, Baker DJ, van Deursen JM. Cellular senescence in aging and age-related disease: from mechanisms to therapy. Nat Med. 2015;21(12):1424-1435 10.1038/nm.4000.
89. Bartkova J, Rezaei N, Liontos M, Karakaidos P, Kletsas D, Issaeva N, Vassiliou LV, Kolettas E, Niforou K, Zoumpourlis VC, Takaoka M, Nakagawa H, Tort F, Fugger K, Johansson F, Sehested M, Andersen CL, Dyrskjot L, Orntoft T, Lukas J, Kittas C, Helleday T, Halazonetis TD, Bartek J, Gorgoulis VG. Oncogene-induced senescence is part of the tumorigenesis barrier imposed by DNA damage checkpoints. Nature. 2006;444(7119):633-637 10.1038/nature05268.

90. Henson SM, Lanna A, Riddell NE, Franzese O, Macaulay R, Griffiths SJ, Puleston DJ, Watson AS, Simon AK, Tooze SA, Akbar AN. p38 signaling inhibits mTORC1-independent autophagy in senescent human CD8(+) T cells. J Clin Invest. 2014;124(9):4004-4016 10.1172/JCI75051.
91. Momand J, Zambetti GP, Olson DC, George D, Levine AJ. The mdm-2 oncogene product forms a complex with the p53 protein and inhibits p53-mediated transactivation. Cell. 1992;69(7):1237-1245 10.1016/0092-8674(92)90644-r.
92. Vogelstein B, Lane D, Levine AJ. Surfing the p53 network. Nature. 2000;408(6810):307-310 10.1038/35042675.
93. Ou HL, Schumacher B. DNA damage responses and p53 in the aging process. Blood. 2018;131(5):488-495 10.1182/blood-2017-07-746396.
94. Shiloh Y. ATM and related protein kinases: safeguarding genome integrity. Nat Rev Cancer. 2003;3(3):155-168 10.1038/nrc1011.
95. Rufini A, Tucci P, Celardo I, Melino G. Senescence and aging: the critical roles of p53. Oncogene. 2013;32(43):5129-5143 10.1038/onc.2012.640.
96. Lane DP. Cancer. p53, guardian of the genome. Nature. 1992;358(6381):15-16 10.1038/358015a0.
97. Karimian A, Ahmadi Y, Yousefi B. Multiple functions of p21 in cell cycle, apoptosis and transcriptional regulation after DNA damage. DNA Repair (Amst). 2016;42:63-71 10.1016/j.dnarep.2016.04.008.
98. Kastan MB, Zhan Q, el-Deiry WS, Carrier F, Jacks T, Walsh WV, Plunkett BS, Vogelstein B, Fornace AJ, Jr. A mammalian cell cycle checkpoint pathway utilizing p53 and GADD45 is defective in ataxia-telangiectasia. Cell. 1992;71(4):587-597 10.1016/0092-8674(92)90593-2.
99. Shaw P, Bovey R, Tardy S, Sahli R, Sordat B, Costa J. Induction of apoptosis by wild-type p53 in a human colon tumor-derived cell line. Proc Natl Acad Sci U S A. 1992;89(10):4495-4499 10.1073/pnas.89.10.4495.
100. Gottlieb E, Vousden KH. p53 regulation of metabolic pathways. Cold Spring Harb Perspect Biol. 2010;2(4):a001040 10.1101/cshperspect.a001040.
101. Hu W. The role of p53 gene family in reproduction. Cold Spring Harb Perspect Biol. 2009;1(6):a001073 10.1101/cshperspect.a001073.
102. Joruiz SM, Bourdon JC. p53 Isoforms: Key Regulators of the Cell Fate Decision. Cold Spring Harb Perspect Med. 2016;6(8) 10.1101/cshperspect.a026039.
103. Bourdon JC, Fernandes K, Murray-Zmijewski F, Liu G, Diot A, Xirodimas DP, Saville MK, Lane DP. p53 isoforms can regulate p53 transcriptional activity. Genes Dev. 2005;19(18):2122-2137 10.1101/gad.1339905.
104. Kastenhuber ER, Lowe SW. Putting p53 in Context. Cell. 2017;170(6):1062-1078 10.1016/j.cell.2017.08.028.
105. Anensen N, Oyan AM, Bourdon JC, Kalland KH, Bruserud O, Gjertsen BT. A distinct p53 protein isoform signature reflects the onset of induction chemotherapy for acute myeloid leukemia. Clin Cancer Res. 2006;12(13):3985-3992 10.1158/1078-0432.CCR-05-1970.
106. Rojas EA, Corchete LA, De Ramon C, Krzeminski P, Quwaider D, Garcia-Sanz R, Martinez-Lopez J, Oriol A, Rosinol L, Blade J, Lahuerta JJ, San Miguel JF, Gonzalez M, Mateos MV, Bourdon JC, Misiewicz-Krzeminska I, Gutierrez NC. Expression of p53 protein isoforms predicts survival in patients with multiple myeloma. Am J Hematol. 2022;97(6):700-710 10.1002/ajh.26507.
107. Fujita K, Mondal AM, Horikawa I, Nguyen GH, Kumamoto K, Sohn JJ, Bowman ED, Mathe EA, Schetter AJ, Pine SR, Ji H, Vojtesek B, Bourdon JC, Lane DP, Harris CC. p53 isoforms Delta133p53 and p53beta are endogenous regulators of replicative cellular senescence. Nat Cell Biol. 2009;11(9):1135-1142 10.1038/ncb1928.
108. Bourdon JC, Khoury MP, Diot A, Baker L, Fernandes K, Aoubala M, Quinlan P, Purdie CA, Jordan LB, Prats AC, Lane DP, Thompson AM. p53 mutant breast cancer patients expressing p53gamma have as good a prognosis as wild-type p53 breast cancer patients. Breast Cancer Res. 2011;13(1):R7 10.1186/bcr2811.

109. Takahashi R, Giannini C, Sarkaria JN, Schroeder M, Rogers J, Mastroeni D, Scrable H. p53 isoform profiling in glioblastoma and injured brain. Oncogene. 2013;32(26):3165-3174 10.1038/onc.2012.322.
110. Anensen N, Hjelle SM, Van Belle W, Haaland I, Silden E, Bourdon JC, Hovland R, Tasken K, Knappskog S, Lonning PE, Bruserud O, Gjertsen BT. Correlation analysis of p53 protein isoforms with NPM1/FLT3 mutations and therapy response in acute myeloid leukemia. Oncogene. 2012;31(12):1533-1545 10.1038/onc.2011.348.
111. Nutthasirikul N, Limpaiboon T, Leelayuwat C, Patrakitkomjorn S, Jearanaikoon P. Ratio disruption of the 133p53 and TAp53 isoform equilibrium correlates with poor clinical outcome in intrahepatic cholangiocarcinoma. Int J Oncol. 2013;42(4):1181-1188 10.3892/ijo.2013.1818.
112. Hofstetter G, Berger A, Schuster E, Wolf A, Hager G, Vergote I, Cadron I, Sehouli J, Braicu EI, Mahner S, Speiser P, Marth C, Zeimet AG, Ulmer H, Zeillinger R, Concin N. Delta133p53 is an independent prognostic marker in p53 mutant advanced serous ovarian cancer. Br J Cancer. 2011;105(10):1593-1599 10.1038/bjc.2011.433.
113. Avery-Kiejda KA, Morten B, Wong-Brown MW, Mathe A, Scott RJ. The relative mRNA expression of p53 isoforms in breast cancer is associated with clinical features and outcome. Carcinogenesis. 2014;35(3):586-596 10.1093/carcin/bgt411.
114. Khoury MP, Bourdon JC. The isoforms of the p53 protein. Cold Spring Harb Perspect Biol. 2010;2(3):a000927 10.1101/cshperspect.a000927.
115. Kuball J, Schuler M, Antunes Ferreira E, Herr W, Neumann M, Obenauer-Kutner L, Westreich L, Huber C, Wolfel T, Theobald M. Generating p53-specific cytotoxic T lymphocytes by recombinant adenoviral vector-based vaccination in mice, but not man. Gene Ther. 2002;9(13):833-843 10.1038/sj.gt.3301709.
116. Amann E. Characterization of a murine TCR specific for HLA-A2.1 restricted non-mutated MDM2 peptide for cancer immunotherapy. Thesis published by Johannes Gutenberg-Universität Mainz. 2018 http://doi.org/10.25358/openscience-2633.
117. Legscha KJ, Antunes Ferreira E, Chamoun A, Lang A, Awwad MHS, Ton G, Galetzka D, Guezguez B, Hundemer M, Bourdon JC, Munder M, Theobald M, Echchannaoui H. Delta133p53alpha enhances metabolic and cellular fitness of TCR-engineered T cells and promotes superior antitumor immunity. J Immunother Cancer. 2021;9(6) 10.1136/jitc-2020-001846.
118. Awwad MHS, Mahmoud A, Bruns H, Echchannaoui H, Kriegsmann K, Lutz R, Raab MS, Bertsch U, Munder M, Jauch A, Weisel K, Maier B, Weinhold N, Salwender HJ, Eckstein V, Hanel M, Fenk R, Durig J, Brors B, Benner A, Muller-Tidow C, Goldschmidt H, Hundemer M. Selective elimination of immunosuppressive T cells in patients with multiple myeloma. Leukemia. 2021;35(9):2602-2615 10.1038/s41375-021-01172-x.
119. Echchannaoui H, Petschenka J, Ferreira EA, Hauptrock B, Lotz-Jenne C, Voss RH, Theobald M. A Potent Tumor-Reactive p53-Specific Single-Chain TCR without On- or Off-Target Autoimmunity In Vivo. Mol Ther. 2019;27(1):261-271 10.1016/j.ymthe.2018.11.006.
120. Weijtens ME, Willemsen RA, Hart EH, Bolhuis RL. A retroviral vector system 'STITCH' in combination with an optimized single chain antibody chimeric receptor gene structure allows efficient gene transduction and expression in human T lymphocytes. Gene Ther. 1998;5(9):1195-1203 10.1038/sj.gt.3300696.
121. Soneoka Y, Cannon PM, Ramsdale EE, Griffiths JC, Romano G, Kingsman SM, Kingsman AJ. A transient three-plasmid expression system for the production of high titer retroviral vectors. Nucleic Acids Res. 1995;23(4):628-633 10.1093/nar/23.4.628.
122. Ren H, Cao K, Wang M. A Correlation Between Differentiation Phenotypes of Infused T Cells and Anti-Cancer Immunotherapy. Front Immunol. 2021;12:745109 10.3389/fimmu.2021.745109.
123. Marin-Acevedo JA, Dholaria B, Soyano AE, Knutson KL, Chumsri S, Lou Y. Next generation of immune checkpoint therapy in cancer: new developments and challenges. J Hematol Oncol. 2018;11(1):39 10.1186/s13045-018-0582-8.

124. Kishimoto T. IL-6: from arthritis to CAR-T-cell therapy and COVID-19. Int Immunol. 2021;33(10):515-519 10.1093/intimm/dxab011.
125. Xu W, Larbi A. Markers of T Cell Senescence in Humans. Int J Mol Sci. 2017;18(8) 10.3390/ijms18081742.
126. Joshua D, Suen H, Brown R, Bryant C, Ho PJ, Hart D, Gibson J. The T Cell in Myeloma. Clin Lymphoma Myeloma Leuk. 2016;16(10):537-542 10.1016/j.clml.2016.08.003.
127. Louis CU, Savoldo B, Dotti G, Pule M, Yvon E, Myers GD, Rossig C, Russell HV, Diouf O, Liu E, Liu H, Wu MF, Gee AP, Mei Z, Rooney CM, Heslop HE, Brenner MK. Antitumor activity and long-term fate of chimeric antigen receptor-positive T cells in patients with neuroblastoma. Blood. 2011;118(23):6050-6056 10.1182/blood-2011-05-354449.
128. Janelle V, Delisle JS. T-Cell Dysfunction as a Limitation of Adoptive Immunotherapy: Current Concepts and Mitigation Strategies. Cancers (Basel). 2021;13(4) 10.3390/cancers13040598.
129. Haist M, Stege H, Grabbe S, Bros M. The Functional Crosstalk between Myeloid-Derived Suppressor Cells and Regulatory T Cells within the Immunosuppressive Tumor Microenvironment. Cancers (Basel). 2021;13(2) 10.3390/cancers13020210.
130. Baruch EN, Berg AL, Besser MJ, Schachter J, Markel G. Adoptive T Cell Therapy: An Overview of Obstacles and Opportunities. Cancer. 2017;123:2154-2162 10.1002/cncr.30491.
131. Klebanoff CA, Gattinoni L, Torabi-Parizi P, Kerstann K, Cardones AR, Finkelstein SE, Palmer DC, Antony PA, Hwang ST, Rosenberg SA, Waldmann TA, Restifo NP. Central memory self/tumor-reactive CD8(+) T cells confer superior antitumor immunity compared with effector memory T cells. Proc Natl Acad Sci U S A. 2005;102(27):9571-9576 10.1073/pnas.0503726102.
132. Rosenberg SA, Yang JC, Sherry RM, Kammula US, Hughes MS, Phan GQ, Citrin DE, Restifo NP, Robbins PF, Wunderlich JR, Morton KE, Laurencot CM, Steinberg SM, White DE, Dudley ME. Durable complete responses in heavily pretreated patients with metastatic melanoma using T-cell transfer immunotherapy. Clin Cancer Res. 2011;17(13):4550-4557 10.1158/1078-0432.CCR-11-0116.
133. Sabatino M, Hu J, Sommariva M, Gautam S, Fellowes V, Hocker JD, Dougherty S, Qin H, Klebanoff CA, Fry TJ, Gress RE, Kochenderfer JN, Stroncek DF, Ji Y, Gattinoni L. Generation of clinical-grade CD19-specific CAR-modified CD8+ memory stem cells for the treatment of human B-cell malignancies. Blood. 2016;128(4):519-528 10.1182/blood-2015-11-683847.
134. Deng Q, Han G, Puebla-Osorio N, Ma MCJ, Strati P, Chasen B, Dai E, Dang M, Jain N, Yang H, Wang Y, Zhang S, Wang R, Chen R, Showell J, Ghosh S, Patchva S, Zhang Q, Sun R, Hagemeister F, Fayad L, Samaniego F, Lee HC, Nastoupil LJ, Fowler N, Eric Davis R, Westin J, Neelapu SS, Wang L, Green MR. Characteristics of anti-CD19 CAR T cell infusion products associated with efficacy and toxicity in patients with large B cell lymphomas. Nat Med. 2020;26(12):1878-1887 10.1038/s41591-020-1061-7.
135. Pangrazzi L, Reidla J, Carmona Arana JA, Naismith E, Miggitsch C, Meryk A, Keller M, Krause AAN, Melzer FL, Trieb K, Schirmer M, Grubeck-Loebenstein B, Weinberger B. CD28 and CD57 define four populations with distinct phenotypic properties within human CD8(+) T cells. Eur J Immunol. 2020;50(3):363-379 10.1002/eji.201948362.
136. Wang R, Dillon CP, Shi LZ, Milasta S, Carter R, Finkelstein D, McCormick LL, Fitzgerald P, Chi H, Munger J, Green DR. The transcription factor Myc controls metabolic reprogramming upon T lymphocyte activation. Immunity. 2011;35(6):871-882 10.1016/j.immuni.2011.09.021.
137. Souza Gondim de Oliveria L. Analysis of the metabolism of tumor-antigen specific CD8+ T cells overexpressing the Delta133p53alpha isoform [Bachelor]: Johannes-Gutenberg University Mainz; 2018.
138. Zhang N, Hartig H, Dzhagalov I, Draper D, He YW. The role of apoptosis in the development and function of T lymphocytes. Cell Res. 2005;15(10):749-769 10.1038/sj.cr.7290345.
139. Plunkett FJ, Franzese O, Finney HM, Fletcher JM, Belaramani LL, Salmon M, Dokal I, Webster D, Lawson AD, Akbar AN. The loss of telomerase activity in highly differentiated CD8+CD28-CD27- T cells is associated with decreased Akt (Ser473) phosphorylation. J Immunol. 2007;178(12):7710-7719 10.4049/jimmunol.178.12.7710.

140. Di Mitri D, Azevedo RI, Henson SM, Libri V, Riddell NE, Macaulay R, Kipling D, Soares MV, Battistini L, Akbar AN. Reversible senescence in human CD4+CD45RA+CD27- memory T cells. J Immunol. 2011;187(5):2093-2100 10.4049/jimmunol.1100978.
141. Davidson WR, Kari C, Ren Q, Daroczi B, Dicker AP, Rodeck U. Differential regulation of p53 function by the N-terminal DeltaNp53 and Delta113p53 isoforms in zebrafish embryos. BMC Dev Biol. 2010;10:102 10.1186/1471-213X-10-102.
142. Joruiz SM, Beck JA, Horikawa I, Harris CC. The Delta133p53 Isoforms, Tuners of the p53 Pathway. Cancers (Basel). 2020;12(11) 10.3390/cancers12113422.
143. von Muhlinen N, Horikawa I, Alam F, Isogaya K, Lissa D, Vojtesek B, Lane DP, Harris CC. p53 isoforms regulate premature aging in human cells. Oncogene. 2018;37(18):2379-2393 10.1038/s41388-017-0101-3.
144. Horikawa I, Fujita K, Jenkins LM, Hiyoshi Y, Mondal AM, Vojtesek B, Lane DP, Appella E, Harris CC. Autophagic degradation of the inhibitory p53 isoform Delta133p53alpha as a regulatory mechanism for p53-mediated senescence. Nat Commun. 2014;5:4706 10.1038/ncomms5706.
145. Li Y, Wu D, Yang X, Zhou S. Immunotherapeutic Potential of T Memory Stem Cells. Front Oncol. 2021;11:723888 10.3389/fonc.2021.723888.
146. Coppe JP, Desprez PY, Krtolica A, Campisi J. The senescence-associated secretory phenotype: the dark side of tumor suppression. Annu Rev Pathol. 2010;5:99-118 10.1146/annurev-pathol-121808-102144.
147. Li X, Shao C, Shi Y, Han W. Lessons learned from the blockade of immune checkpoints in cancer immunotherapy. J Hematol Oncol. 2018;11(1):31 10.1186/s13045-018-0578-4.
148. Sharma P, Allison JP. The future of immune checkpoint therapy. Science. 2015;348(6230):56-61 10.1126/science.aaa8172.
149. Guillerey C, Harjunpaa H, Carrie N, Kassem S, Teo T, Miles K, Krumeich S, Weulersse M, Cuisinier M, Stannard K, Yu Y, Minnie SA, Hill GR, Dougall WC, Avet-Loiseau H, Teng MWL, Nakamura K, Martinet L, Smyth MJ. TIGIT immune checkpoint blockade restores CD8(+) T-cell immunity against multiple myeloma. Blood. 2018;132(16):1689-1694 10.1182/blood-2018-01-825265.
150. Harjunpaa H, Guillerey C. TIGIT as an emerging immune checkpoint. Clin Exp Immunol. 2020;200(2):108-119 10.1111/cei.13407.
151. Schroeder MA, DiPersio JF. Mouse models of graft-versus-host disease: advances and limitations. Dis Model Mech. 2011;4(3):318-333 10.1242/dmm.006668.
152. Weissmuller S, Kronhart S, Kreuz D, Schnierle B, Kalinke U, Kirberg J, Hanschmann KM, Waibler Z. TGN1412 Induces Lymphopenia and Human Cytokine Release in a Humanized Mouse Model. PLoS One. 2016;11(3):e0149093 10.1371/journal.pone.0149093.
153. Frey N, Porter D. Cytokine Release Syndrome with Chimeric Antigen Receptor T Cell Therapy. Biol Blood Marrow Transplant. 2019;25(4):e123-e127 10.1016/j.bbmt.2018.12.756.
154. Slatter TL, Hung N, Campbell H, Rubio C, Mehta R, Renshaw P, Williams G, Wilson M, Engelmann A, Jeffs A, Royds JA, Baird MA, Braithwaite AW. Hyperproliferation, cancer, and inflammation in mice expressing a Delta133p53-like isoform. Blood. 2011;117(19):5166-5177 10.1182/blood-2010-11-321851.
155. Marcel V, Dichtel-Danjoy ML, Sagne C, Hafsi H, Ma D, Ortiz-Cuaran S, Olivier M, Hall J, Mollereau B, Hainaut P, Bourdon JC. Biological functions of p53 isoforms through evolution: lessons from animal and cellular models. Cell Death Differ. 2011;18(12):1815-1824 10.1038/cdd.2011.120.
156. Kazantseva M, Mehta S, Eiholzer RA, Hung N, Wiles A, Slatter TL, Braithwaite AW. A mouse model of the Delta133p53 isoform: roles in cancer progression and inflammation. Mamm Genome. 2018;29(11-12):831-842 10.1007/s00335-018-9758-3.
157. Le RQ, Li L, Yuan W, Shord SS, Nie L, Habtemariam BA, Przepiorka D, Farrell AT, Pazdur R. FDA Approval Summary: Tocilizumab for Treatment of Chimeric Antigen Receptor T Cell-Induced Severe or Life-Threatening Cytokine Release Syndrome. Oncologist. 2018;23(8):943-947 10.1634/theoncologist.2018-0028.

158. Oh L, Hainaut P, Blanchet S, Ariffin H. Expression of p53 N-terminal isoforms in B-cell precursor acute lymphoblastic leukemia and its correlation with clinicopathological profiles. BMC Cancer. 2020;20(1):110 10.1186/s12885-020-6599-8.
159. Gartel AL, Serfas MS, Tyner AL. p21--negative regulator of the cell cycle. Proc Soc Exp Biol Med. 1996;213(2):138-149 10.3181/00379727-213-44046.
160. Brugarolas J, Moberg K, Boyd SD, Taya Y, Jacks T, Lees JA. Inhibition of cyclin-dependent kinase 2 by p21 is necessary for retinoblastoma protein-mediated G1 arrest after gamma-irradiation. Proc Natl Acad Sci U S A. 1999;96(3):1002-1007 10.1073/pnas.96.3.1002.
161. Gartel AL, Radhakrishnan SK. Lost in transcription: p21 repression, mechanisms, and consequences. Cancer Res. 2005;65(10):3980-3985 10.1158/0008-5472.CAN-04-3995.
162. Camus S, Menendez S, Fernandes K, Kua N, Liu G, Xirodimas DP, Lane DP, Bourdon JC. The p53 isoforms are differentially modified by Mdm2. Cell Cycle. 2012;11(8):1646-1655 10.4161/cc.20119.
163. Honda R, Tanaka H, Yasuda H. Oncoprotein MDM2 is a ubiquitin ligase E3 for tumor suppressor p53. FEBS Lett. 1997;420(1):25-27 10.1016/s0014-5793(97)01480-4.
164. Zhang T, Cooper S, Brockdorff N. The interplay of histone modifications - writers that read. EMBO Rep. 2015;16(11):1467-1481 10.15252/embr.201540945.
165. Bourdon JC. p53 isoforms change p53 paradigm. Mol Cell Oncol. 2014;1(4):e969136 10.4161/23723548.2014.969136.
166. Marcel V, Petit I, Murray-Zmijewski F, Goullet de Rugy T, Fernandes K, Meuray V, Diot A, Lane DP, Aberdam D, Bourdon JC. Diverse p63 and p73 isoforms regulate Delta133p53 expression through modulation of the internal TP53 promoter activity. Cell Death Differ. 2012;19(5):816-826 10.1038/cdd.2011.152.
167. Gong H, Zhang Y, Jiang K, Ye S, Chen S, Zhang Q, Peng J, Chen J. p73 coordinates with Delta133p53 to promote DNA double-strand break repair. Cell Death Differ. 2018;25(6):1063-1079 10.1038/s41418-018-0085-8.
168. Horikawa I, Park KY, Isogaya K, Hiyoshi Y, Li H, Anami K, Robles AI, Mondal AM, Fujita K, Serrano M, Harris CC. Delta133p53 represses p53-inducible senescence genes and enhances the generation of human induced pluripotent stem cells. Cell Death Differ. 2017;24(6):1017-1028 10.1038/cdd.2017.48.
169. Gong L, Pan X, Chen H, Rao L, Zeng Y, Hang H, Peng J, Xiao L, Chen J. p53 isoform Delta133p53 promotes efficiency of induced pluripotent stem cells and ensures genomic integrity during reprogramming. Sci Rep. 2016;6:37281 10.1038/srep37281.
170. d'Adda di Fagagna F. Living on a break: cellular senescence as a DNA-damage response. Nat Rev Cancer. 2008;8(7):512-522 10.1038/nrc2440.
171. Gong L, Gong H, Pan X, Chang C, Ou Z, Ye S, Yin L, Yang L, Tao T, Zhang Z, Liu C, Lane DP, Peng J, Chen J. p53 isoform Delta113p53/Delta133p53 promotes DNA double-strand break repair to protect cell from death and senescence in response to DNA damage. Cell Res. 2015;25(3):351-369 10.1038/cr.2015.22.
172. Hurton LV, Singh H, Najjar AM, Switzer KC, Mi T, Maiti S, Olivares S, Rabinovich B, Huls H, Forget MA, Datar V, Kebriaei P, Lee DA, Champlin RE, Cooper LJ. Tethered IL-15 augments antitumor activity and promotes a stem-cell memory subset in tumor-specific T cells. Proc Natl Acad Sci U S A. 2016;113(48):E7788-E7797 10.1073/pnas.1610544113.
173. Martinez M, Kim S, St Jean N, O'Brien S, Lian L, Sun J, Verona RI, Moon E. Addition of anti-TIM3 or anti-TIGIT Antibodies to anti-PD1 Blockade Augments Human T cell Adoptive Cell Transfer. Oncoimmunology. 2021;10(1):1873607 10.1080/2162402X.2021.1873607.
174. Lissa D, Ungerleider K, Horikawa I, Dranachak P, Oliphan E, Beck J, Jo S, Inglese J, Harris CC. Targeting Delta133p53 isoform with small-molecule compounds to modulate cellular senescence. AACR Special Conference on Advancing Precision Medicine Drug Development: Incorporation of Real-World Data and Other Novel Strategies; January 9-12; San Diego, CA2020.

8 Supplements

Vector maps

pBu_IRES_puro:

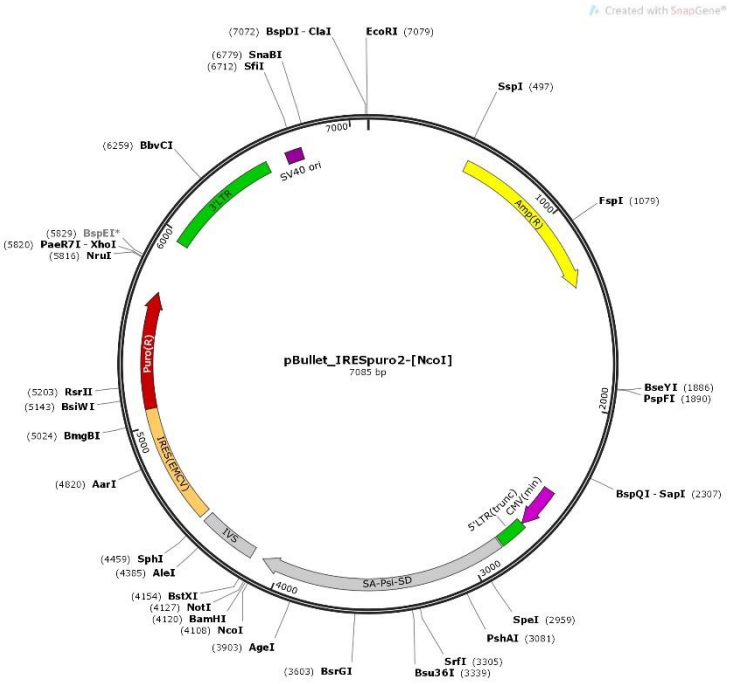

pMx_IRES_puro:

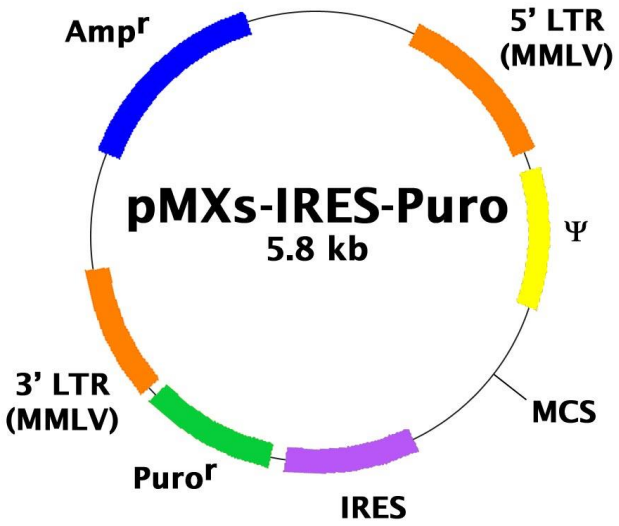

pMx_IRES_neo:

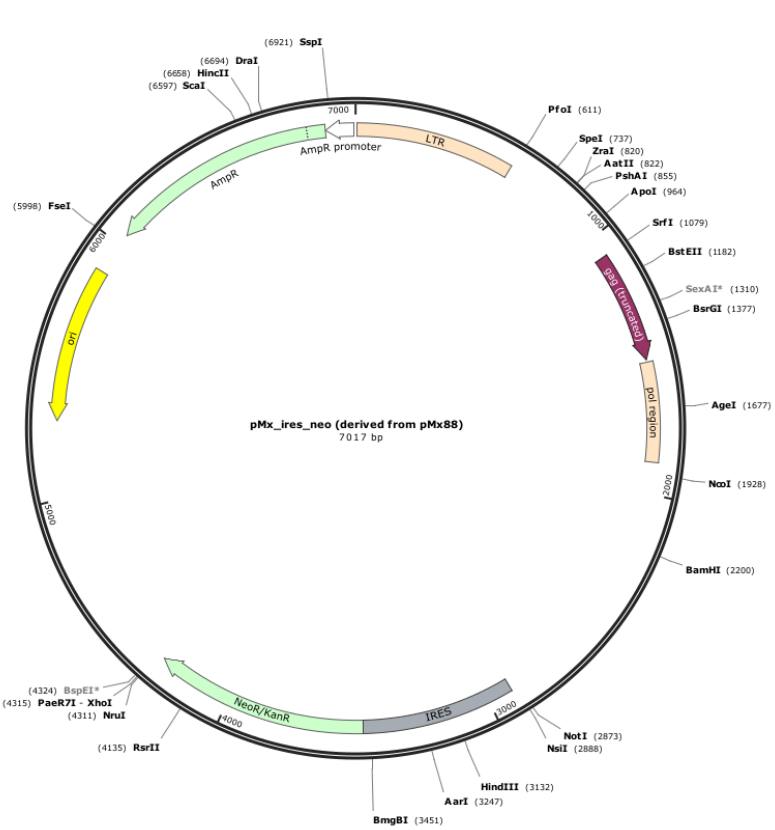
Created with SnapGene®
(6921) SspI
(6694) DraI
(6658) HincII
(6597) ScaI
7000
PfoI (611)
SpeI (737)
ZraI (820)
AatII (822)
PshAI (855)
ApoI (964)
1000
SrfI (1079)
BstEII (1182)
SexAI* (1310)
BsrGI (1377)
LTR
AmpR promoter
AmpR
(5998) FseI
6000
ori
gag (truncated)
pol region
AgeI (1677)
pMx_ires_neo (derived from pMx88)
7017 bp
2000
NcoI (1928)
5000
BamHI (2200)
(4324) BspEI*
(4315) PaeR7I - XhoI
(4311) NruI
NeoR/KanR
IRES
3000
4000
NotI (2873)
NsiI (2888)
(4135) RsrII
HindIII (3132)
AarI (3247)
BmgBI (3451)

Acknowledgment

I would like to express my gratitude to my primary supervisors Univ. Prof. Dr. Matthias Theobald and Dr. Hakim Echchannaoui for the opportunity to complete my doctoral thesis on this exciting project. Especially, I would like to thank Dr. Hakim Echchannaoui for his instructive and dedicated teaching and supervision throughout the thesis. I am deeply grateful for the teaching and assistance by Edite Antunes. The lively discussion and assistance by all members of AG Theobald/Echchannaoui/~~Name~~ was greatly appreciated.

I wish to extend my thanks to my family and close friends for their strong and consistent support.